COMPARATIVE ANALYSIS OF HIGH VOLTAGE ALTERNATING CURRENT & HIGH VOLTAGE DIRECT CURRENT OFFSHORE COLLECTION GRID SYSTEMS

By

CALEB JORDACHE PILLAY

Student No: 21133160

A dissertation submitted in fulfilment of the requirements for the Master of Engineering Degree in the Department of Electrical Power Engineering, Faculty of Engineering and the Built Environment

Durban University of Technology

Supervisor: Dr Kabeya Musasa

Co-Supervisor: Dr. Innocent E. Davidson

October, 2021

As the candidate's supervisor, I agree to the submission of this dissertation

Dr. M. Kabeya _____

NAME OF SUPERVISOR SIGNATURE

Prof I.E. Davidson _____

NAME OF CO-SUPERVISOR SIGNATURE

DECLARATION

I hereby declare that this dissertation is my work, and each text has been correctly referenced or cited. Moreover, this work has not been previously published in portion or whole for another degree at any other University.

This research was duly supervised by Dr. Kabeya Musasa and Prof Innocent E. Davidson at the Durban University of Technology.

Submitted by:

……..18/10/2020……

Caleb Pillay Date

Student Number: 21133160

Approved for Final Submission by:

….....19/11/2021…….

Supervisor: Dr Kabeya Musasa Date

……. …….

Co-Supervisor: Prof Innocent E. Davidson Date

ACKNOWLEDGEMENTS

My sincere gratitude and appreciation go to my supervisor, Dr. K. Musasa for his invaluable support and guidance throughout this study. Without his patience, guidance, knowledge, and encouragement, I would not have made headway in this project.

To Prenushka Ayar, I am eternally grateful for the love and support you have shown me through this project. Without your constant support and motivation, it would not have been possible to complete this dissertation.

Lastly, I am immensely grateful to my parents for the love, prayers, and support they have shown throughout this project as well as in the years leading up to this point. Your constant sacrifice and encouragement have made this possible.

ABSTRACT

An increase in industries as well as the world's population, is causing a strain on the electricity supply. This coupled with the fact that fossil fuel supplies are decreasing, is leading the world to new, greener methods of electrical energy generation. Offshore wind farms are being developed far offshore and solar farms are being developed in remote locations with intense sunlight. This allows for the optimal operation of these systems. HVAC collection systems for offshore wind farms have traditionally been used but imposes limitations on the transmission distance. Exuberant amounts of capital are required for greater distances. HVDC systems have started to be recognised as a viable method of transmitting this electrical energy at a much lower cost on longer distances. This study shows a comparative performance and cost evaluation of both HVAC and HVDC collection systems for offshore wind farms. It evaluates the efficiency of the wind farm based on system losses, determines the advantages, disadvantages, and cost implications of each system, and determines the best type of technology to be used in offshore applications. The study looks at a case of a 40 MW wind farm at a distance of 120 km offshore. A simulation is developed for each system using MATLAB simulation software to determine the performance of each system during normal operation and fault conditions. From these simulations, it was found that HVDC collection systems have much higher efficiency when compared to HVAC systems and perform better under both normal operation and fault conditions. HVDC systems also have a lower cost once the break-even distance point is passed. From the study, it is found that HVDC collection systems are much better suited to allow offshore wind farms to have a high efficiency as well as be located further offshore to allow for maximum wind usage. The technology can be used for other long-distance transmission systems and incorporated for other renewable energy generation systems.

TABLE OF CONTENTS

LIST OF FIGURES

LIST OF TABLES

NOMENCLATURE

A	Swept area of the turbine blade
C_p	Power coefficient of the turbine
Hz	Hertz
I_d	Diode current
I_{gd}	Grid current in d axis
I_{gq}	Grid current in q axis
I_L	Current across the inductor
I_{sd}	Stator current in d axis
I_{sq}	Stator current in q axis
kW	Kilowatt
L_{ir}	Rotor self-inductance
L_{is}	Stator self-inductance
L_m	Mutual inductance
L_r	Rotor inductance
L_s	Stator inductance
L_{sd}	Stator direct inductance
L_{sq}	Stator quadrature inductance
L_T	Total inductance
L_{Tr}	Inductance of the transformer
MW	Megawatt
n	Number of degree of saturation
N_p	Number of the generator pole pairs
P	Rated power of the system
P_m	Mechanical power output of the turbine
P_s	Active power generated by the generator
R_{shunt}	Shunt resistance
q	Charge of the electron
Q	Quality factor
Q_f	Reactive power of the filter
Q_s	Reactive power generated by the generator
R	Radius of the wind blade
R_m	Small torque sensing resistor

R_r	Rotor resistance
R_s	Stator resistance
R_T	Total resistance
R_x	Transmission cable
S	Slip
T_e	Electromagnetic torque
T_g	Generator torque
T_m	Mechanical torque
T_t	Aerodynamic torque
U_P	Instantaneous voltage
V	Air velocity
V_{gd}	Grid voltage in d axis
V_{gq}	Grid voltage in q axis
V_{rq}	Rotor voltage in q axis
V_{rd}	Rotor voltage in d axis
V_{sd}	Stator voltage d axis
V_{sq}	Stator voltage in q axis
W	Empirical Weibull scale factor
ω_t	Turbine speed
ω_g	Generator speed
φ_{sd}	Stator flux in d axis
φ_{sq}	Stator flux in q axis
φ_{rd}	Rotor flux in d axis
φ_{rq}	Rotor flux in q axis
ω_r	Angular velocity of the rotor
ω_s	Angular velocity of the stator
β	Pitch angle
ψ	Angle at which the filter is energized
φ	Angular displacement between voltage and current
ω_e	Synchronous angular speed
λ	Flux linkage
σ	Dispersion coefficient of the generator
ρ	Density of the air

ACRONYMS

AC	Alternating current
CB	Circuit Breaker
CPU	Central processing unit
DC	Direct current
DFIG	Doubly-fed induction generator
DG	Distributed generation
FACTS	Flexible AC transmission systems
GSC	Grid side converter
HAWT	Horizontal axis wind turbine
HV	High voltage
HVDC-LCC	High Voltage Direct Current Line Commutated Converter
HVDC-VSC	High Voltage Direct Current Voltage Source Converter
IEEE	Institute of Electrical and Electronics Engineers
IGBT	Insulated-gate bipolar transistor
LV	Low Voltage
MPPT	Maximum power point tracking
MV	Medium voltage
PCC	Point of common coupling
PMSG	Permanent magnet synchronous generator
PU	Per unit
PWM	Pulse width modulation
RSC	Rotor side converter
SCIG	Squirrel cage induction generator
SSC	Stator side converter
STATCOM	Static synchronous compensator
WECU	Wind energy conversion unit
WRIG	Wound-rotor induction generator
WTG	Wind turbine generator
WTT	Wind turbine transformer

CHAPTER 1: INTRODUCTION

1.1 Background and motivation

In today's society, industries and residential areas depend on electrical energy every day. These consumers require a constant supply of energy, free of harmonic distortion, voltage fluctuations, and frequency variations. Coal-fired power generation supplies approximately 41% of the world's electricity [1] and in South Africa, it is as high as 90% of the country's energy supply [2].

Due to the decreasing supply of fossil fuels and the ever-increasing need for electrical energy, new sustainable approaches need to be taken for electricity generation, such as wind, solar, hydro, etc. These electrical energy generation systems are being established in outlying regions and even at sea to generate the maximum amount of renewable energy possible. These energy sources need to be incorporated into the power grid to ease the system strain. When these energy sources are incorporated into the power grid, they are continuously being connected and disconnected from the power grid in response to customer demand.

However, before connecting any energy source into power grids they must meet certain requirements (i.e. the standard grid code requirements) [3]. For example, in the South African grid code, it is stipulated that: "power producer and end-use customers shall take all reasonable steps to ensure that the power factor at the point of supply is at all times 0.9 lagging or higher (i.e. the limit on reactive power absorbed from the utility grid)." This requirement applies to the end-users at each point of supply. A leading power factor (or reactive power injected into the power grid) shall not be accepted unless specified in a contractual agreement with the system operator [4]. From the international standard grid code: the frequency variation is limited to 0.5 Hz, the voltage variation is limited to 0.1 per unit or 10%. Furthermore, the generator and grid voltage are required to be in phase, with a total power factor limited to about 1% [5]. Consequently, the integration of these sources of energy to the power grid would require transmission systems that would optimally comply with the standard grid code, while being cost-effective. Different methods used for transmission of this electrical energy need to be researched to determine the best-suited transmission system for these systems.

Although there are various renewable generation technologies, the generation of electrical power through wind energy is becoming an increasingly important topic. For instance, by 2018, the worldwide wind power cumulative capacity has increased to 600 GW [6]. The international energy agency predicts that wind capacity will reach 1000 GW by 2025 [7]. Offshore wind technology is a comparatively new concept but as technology develops, its cost decreases. Due to this reduction in cost and the benefits of wind farm technology, growth is expected in the near future.

Offshore wind farms are increasing in popularity as there are fewer site restrictions at sea and strong and constant wind speeds are experienced. This will enable the production of high-power outputs. As these offshore wind farms are at sea, the technical challenge is to have strong structural stability and be compact to withstand high wind speeds.

Currently, all existing wind farms comprise of an internal AC collection grid and either an AC or DC transmission system that links it to the utility grid. Only a few theoretical and small-scale models of wind farms that use DC collection grids are available. Therefore, a suitable practical configuration does not presently exist. Technically, an offshore wind power plant with an internal AC collection grid is designed with a combination of AC wind energy conversion units (WECUs). The WECU comprises of a wind turbine, a generator, and a power transformer. In wind farms with DC collection grids, power converters or rectifiers replace the need for a power transformer. These rectifiers are required in each WECU for the AC to DC signal transformation. These power converters also assist in power conditioning to allow for control of the speed, voltage, and torque as well as power compensation to improve the stability of the voltage; and power filtering to provide high power quality.

The size and weight largely impact the development of offshore equipment. Power converters help to reduce the size of the offshore wind farm structure by using a smaller number of magnetic components as compared to power transformers, therefore the weight and size of the WECU are reduced. DC control and protection devices are still being researched and therefore currently make AC collections grids the only viable option.

This issue has been resolved and may not pose a problem for the DC collection grids in the future. This study investigates the technical advantages of wind farms with a DC collection grid over the traditional wind farm with an AC collection grid.

1.2 Problem Statement

The use of HVAC collection grids for offshore wind farms presents a problem with the efficiency and cost of the system over longer distances. HVAC systems create a higher loss and nullify the advantages of higher wind speeds experience further offshore. The problem of this dissertation is addressed by the following research questions:

- What is the efficiency of the AC and DC collection grid systems?
- What are the advantages, disadvantages, and cost implications of each system?
- What is the best technology-based on cost and efficiency?

1.3 Aims and objectives

The aim and objectives of this project are to compare the use of HVAC and HVDC collection grids with offshore wind farms. This determines the best system to be used when developing an offshore wind farm by looking at their efficiency as well as their performance during fault conditions. Based on the research questions the desired objectives would be to:

- Evaluate the efficiency of the wind farm based on system losses.
- Determine the advantages, disadvantages, and cost implications of each system.
- Determine the best type of technology to be selected to enable efficiency and cost-effectiveness.

1.4 Contribution

The research detailed in this dissertation explores the evaluation of HVAC and HVDC collection grids for offshore wind farms. The main contribution of this work is found in Chapter 5, where the evaluation of these collection grids is analysed. This allows an insight into the performance, cost, and efficiency of HVAC and HVDC collection grids.

Contributions from this work have been reported and published in the following proceedings:

- C.J. Pillay, M. Kabeya and I.E. Davidson, “Transmission systems: HVAC vs HVDC”, In Proceedings of the International Conference on Industrial Engineering

and Operations Management (IEOM), August 10 – 14, 2020, Detroit, Michigan, USA.

1.5 Limitations

The research in this dissertation explores is limited to HVAC and HVDC collection grids and transmission for offshore wind farms. The research focuses on the research questions listed above and does not look at factors outside the aims of the dissertation.

1.6 Dissertation outline

The presented dissertation consists of six main chapters, a brief description of the contents as contained in each chapter is given as follows:

Chapter one presents the introduction of the dissertation. This includes the motivation, aims and objectives, research questions, and contribution of the study.

Chapter two presents the literature review. It explains HVDC and HVAC wind farm systems. It looks into the components of a wind farm, the comparison between types of wind farms, transmission systems used, and the economic details of each wind farm system.

Chapter three presents a theoretical background of wind farm collection grids that utilize HVAC and HVDC. This chapter looks at HVAC grid topologies and typical wind conversion units. This chapter looks at the design model, topologies, and delivery systems for HVDC grids.

Chapter four presents the system modelling and simulations conducted to compare each system. This includes the simulation of the systems using MATLAB.

Chapter five looks at the comparative analysis between HVAC and HVDC collection grids. The results obtained in chapter four are discussed here and explained.

Chapter six provides a summary of the entire dissertation and also shows recommendations for future work.

CHAPTER 2: LITERATURE REVIEW

2.1 Introduction

This chapter focuses on offshore wind farms and the technology used on these wind farms. HVAC and HVDC collection grids are discussed and a comparison of different HVDC technologies is carried out. It also gives a theoretical understanding of the technology used in each type of collection grid, configurations of wind energy conversion units and discusses the transmission systems for HVAC and HVDC. The economic aspects of each system are shown and methods for calculating cost models of all equipment are detailed. Collection grids for HVAC and HVDC are compared based on currently published literature and for the intention of this dissertation, importance is given to advantages that improve efficiency and cost of offshore wind farms as well as transmission of energy to the grid.

2.2 Off-shore wind farms

A wind farm is a group of wind turbines in the same location employed to produce electrical power by converting mechanical energy to electrical energy. Wind farms differ in size ranging from two turbines to several hundred wind turbines covering a large area. These wind farms can be either onshore or offshore. Offshore wind farms are constructed at sea, to harvest maximum wind energy and in turn, generate electricity. The generation of electricity is higher at offshore locations than on land due to the higher wind speeds. Offshore wind farm energy generation costs have always exceeded onshore wind generation, however, currently, these costs are decreasing [8]. This price reduction is making it more reasonable to allow for offshore wind farms. Typically, wind turbines are located in fairly shallow water and have foundations on the sea bed. Wind farms with floating platforms are in the early stages of development as of 2020, allowing for these wind farms to be moved to deeper waters.

Typical offshore wind farms are composed of a group of WECUs. Each WECU comprises of a wind turbine composed of its mechanical parts such as a power transformer and generator including power electronics circuits. These WECUs are most commonly configured in radial or parallel, both series-parallel, loop or series, and star interconnections. [9-11].

The power produced by the WECU's is collected by an AC collection grid and transmitted via submarine cables to the onshore grid. This power can be transmitted by either HVAC or HVDC transmission. As most offshore wind farms are a relatively long distance away from shore, HVDC is generally used to alleviate losses for this transmission [12].

A typical AC wind farm configuration with an HVDC transmission system requires a power transformer, to step up the voltage, and a rectifier, to convert this voltage to DC so it can be transmitted to shore. The power transformer and rectifier stations are installed on an offshore platform. An HVDC-inverter platform is used to convert the power back to HVAC for transmission and distribution onshore. Using an AC collection grid and HVDC transmission requires the wind farm to have three platforms. Although it uses three platforms converting to HVDC for the transmission has its advantages.

Offshore wind farms with HVDC collection are very similar to traditional offshore wind farms. The components are the same except for the replacement of the power transformer, by a converter. AC collection grids were preferred over DC collection grids due to technology for control and protection devices, being in their infancy [13, 14]

However, with recent improvements in technology, efficient control and protection devices for the DC collection grids are available at lower costs [15-21]. This technology may make the use of DC collection grids more feasible than AC collection grids. The main difference between the AC and DC collection grids is the use of the power transformer in the WECU. In a DC collection grid, the transformer is replaced by rectifiers which, for the same power rating, are significantly smaller. This allows the system to become more compact [22].

Without the need for a power transformer, the system only requires two platforms, one for the rectifier and the other for the inverter. This will reduce the cost of the system and still allow for good control and stability of the system. Only small-scale DC collection grid prototypes exist thus far and there are no full-scale operational wind farms.

2.3 Wind farm technology

Renewable energy generation systems, such as WECU's, need to be incorporated into the existing electrical grid. The power generated by these WECUs must be transmitted to the onshore power network. To do this there are three main sections that the WECU system

can be divided into; Generation, Collection, and Transmission, each with its technical aspects. There are different methods for the collection and transmission of this power.

2.3.1 Collection systems

Collection systems can include wind turbine and generators configurations, platform size, wind-power plant layout, and cables and power electronics converters design. The different methods or technologies for this each have their advantages and disadvantages.

2.3.1.1 Wind turbines

A wind turbine consists of several components to allow the conversion of mechanical-to-electrical energy. A sectioned view of a typical wind turbine is shown in Figure 2-1. Although there are several alternatives to this component layout, the figure depicts a common wind turbine and aids in locating and describing the different components.

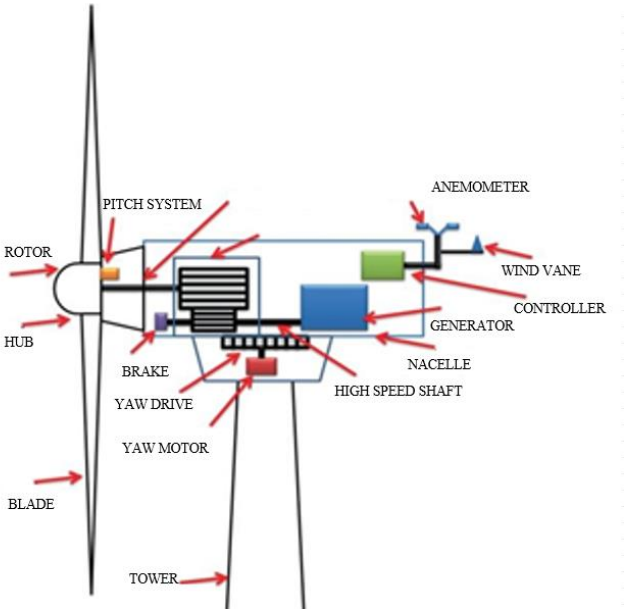

Figure 2- 1: Wind Turbine Components

Figure 2-2 shows that the wind turbine works by its rotor blades being turned by wind energy. The turbine blades are used to convert wind energy to mechanical energy and are mounted on the rotor hub. The rotor hub is installed on the main shaft, known as the low-speed shaft. The gearbox is used to transfer the mechanical energy to a high-speed shaft and to the generator, which converts the mechanical energy into electrical energy.

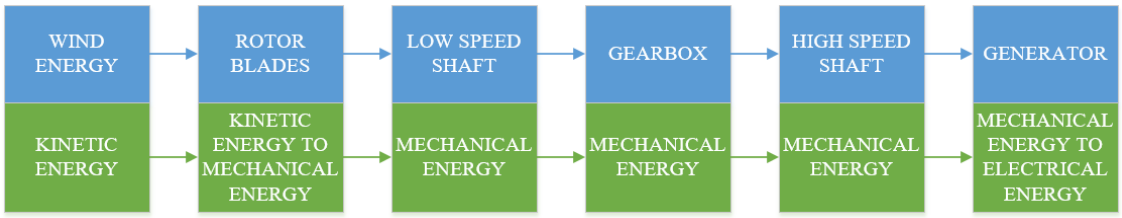

Figure 2- 2: Wind Turbine Energy Conversion

The generated power is then sent to the power transformer which steps up the voltage for transmission. Based on the transmission distance, the power is then sent to a rectifier to convert the AC power to DC to be transmitted to shore.

2.3.1.2 Turbine blade

One of the most distinctive features of a turbine is the blades, they are also responsible for carrying out the task of transforming the wind energy into mechanical energy. Most commonly a turbine will have three curved shaped blades to harness maximum wind energy without strain on the tower and blades.

As the blades are curved, a difference in wind speed is created above (V_{w1}) and below (V_{w2}) the blade. According to Bernoulli's principle, air speed and pressure are inversely proportional, therefore the pressure at the top of the blade (P_{w1}) is lower than the pressure at the bottom of the blade (P_{w2}) resulting in the lift force of the blade (F_w). The rotational movement of the turbine is created by torque from the turbine shaft. The power of an air mass flowing at speed (V_w) through an area can be calculated by:

$$P_w = \frac{1}{2}\rho A V_w^3 \tag{2-1}$$

where ρ is the air density in kg/m^3, A is the sweep area in m^2, and V_w is the wind speed in m/s. The wind power captured by the blade and converted into mechanical power can be calculated by:

$$P_M = \frac{1}{2}\rho A V_w^3 C_p \tag{2-2}$$

where, C_p is the power coefficient of the blade. This coefficient has a theoretical maximum value of 0.59 according to the Betz limit.

Equation (2-2) shows that wind speed and power are directly proportional. Locating wind farms in areas of higher wind speeds is the only way to allow for maximum power generation. Offshore wind farms utilize this technique as the wind speeds are steadier and higher than on land. The wind power can be increased eight times by doubling the wind speed, this is due to the wind power being a cubic function of speed.

2.3.1.3 Gearbox

A standard generator, at 50Hz, operates at a rated speed of 1000 or 1500 rpm based on the number of poles. This is much higher than an average wind turbine can produce, which is normally between 6-20rpm. A gearbox is used to connect the low-speed rotor to the high-speed generator with a gear ratio (Υ_{gb}). Equation 2-3 can be used to determine the gearbox ratio.

$$\Upsilon_{gb} = \frac{n_m}{n_M} = \frac{(1-s)\times 60\times f_s}{P\times n_M} \tag{2-3}$$

where n_m and n_M are the generator and turbine rated speeds in rpm respectively, s is the rated slip, f_s is the rated stator frequency in Hz, and P is the number of pole pairs of the generator.

2.3.1.4 Generators

For mechanical energy to be converted to electrical energy, the use of a generator is required. Over the years, different types of generators have been tried and tested in WECU's. These range from the squirrel cage induction generator (SCIG), doubly fed induction generator (DFIG), wound rotor synchronous generator (WRSG), and permanent magnet synchronous generator (PMSG), all with various power ratings [23].

2.3.1.4.1 Doubly-Fed Induction Generator

In wind energy production today, the DFIG is currently the main player. This workhorse is popular as it can produce maximum energy from variable wind speeds using its interface controls [24]. The DFIG offers the advantage of speed control with reduced losses [25].

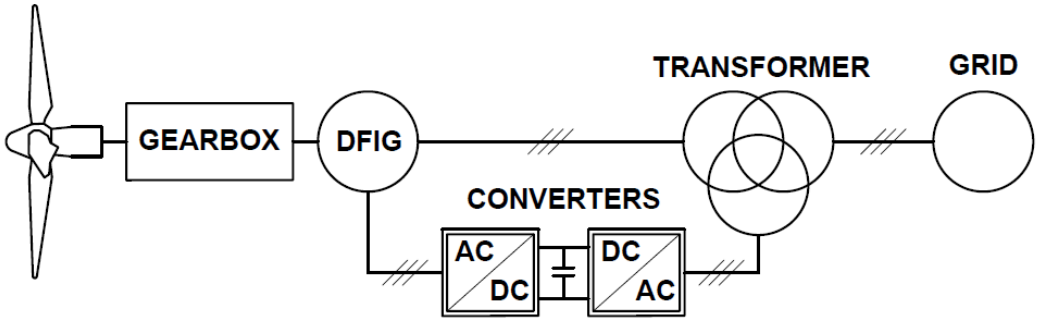

Figure 2- 3: Doubly Fed Induction Generator SLD

Figure 2-3 shows a single-line drawing of a doubly-fed induction generator. The generator's stator is connected directly to the grid, while its rotor is connected through a power converter system [26]. The generator operates within 30% of the synchronous speed. This compensates for different wind speeds and enables control of the active power on the generator side and reactive power control on the grid side. The power converter is cost-effective and requires less space [27].

2.3.1.4.2 Squirrel Cage Induction Generator

The SCIG, shown in Figure 2-4, is relatively low in cost and maintenance [24]. SCIGs are used for traditional direct grid connections as they are robust and simple to use. These turbines are currently available today and operate at a constant speed [28]. Two-speed SCIGs are also available, which utilizes a tapped stator winding to allow two-speed operation. SCIGs are also used in applications with variable-speed systems. The largest offshore wind energy systems using SCIGs are around 3.5 MW capacity [29].

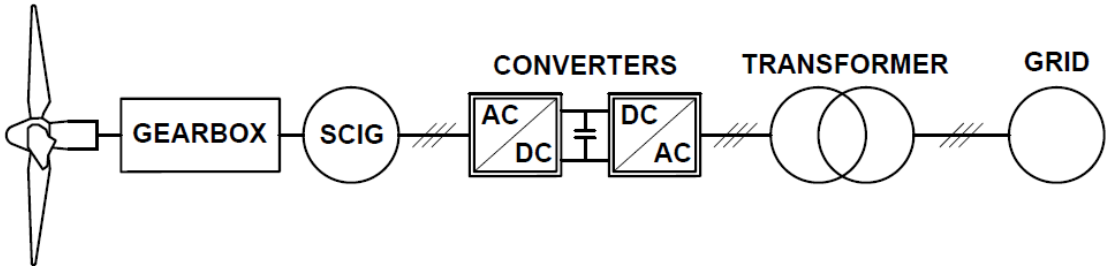

Figure 2- 4 : Squirrel Cage Induction Generator SLD

2.3.1.4.3 Synchronous Generator

The most popular synchronous generators used in wind farms are split into two types; Permanent Magnet Synchronous Generators (PMSGs) and Wound Rotor Synchronous Generators (WRSGs). The SLD for these generators are shown in Figure 2-5. They are well suited for systems up to 7.5 MW [29].

The stator windings of the WRSG are directly linked to the grid which limits the rotational speed by the frequency of the supply grid. Slip rings and brushes are used to excite the rotor windings. Synchronous generators do not require additional reactive power compensation systems as compared to induction generators. Another advantage is that it does not require a gearbox[30].

As the excitation of the permanent magnet generator is provided without any energy supply its efficiency is higher than that of the induction generator [31]. However, the drawback of these generators is the costly materials they are made from which are hard to work with during manufacture. For excitation of PMSG, the use of a power converter is required. This assists to adjust the generation voltage and frequency to the transmission voltage and frequency respectively. The benefit of generating power at any speed comes with the additional expense. The magnetic materials of PMSGs are sensitive to temperature and require the rotor temperature to be monitored and a cooling system to be in place [29-31].

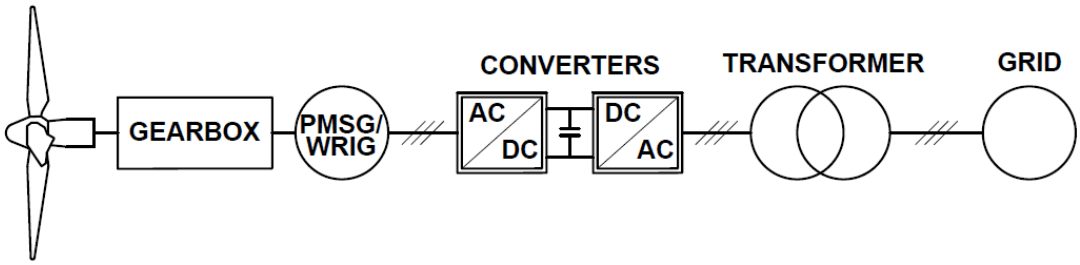

Figure 2- 5 : Synchronous Generator SLD

2.3.1.5 Towers

Wind speeds increase as the altitude increases, to take advantage of this fact, wind turbines are erected on towers typically 100m or higher [32]. The tower is used to support the nacelle and the turbine rotor as well as provide elevation for improved wind conditions. Power cables connecting the generator to the transformer are housed in the tower [33]. In order to reduce the weight and size of the nacelle, the power converters are

sometimes located at the base of the tower. Towers are constructed of steel and concrete with a concrete base and steel upper section. To avoid turbulence the tower is required to be at least 25 to 30 m high [34].

2.3.1.6 Transformers

Each turbine in a wind farm is equipped with a step-up transformer, which steps up the output voltage of the turbine generator to a medium voltage distribution level used by the collector system. However, these transformers are considered to be one of the sensitive and weak components in a wind farm. Usually, shell transformers are used for this application but intermittency of wind power imposes some demanding specifications. To ensure the future dependability of these transformers, requirements such as switching and transient over-voltages, voltage and loading variations, harmonics as well as loss evaluation need to be incorporated [35].

2.3.1.7 Power converters

One of the main components for a DC collection grid is the power converters at the base of each WT tower. These converters are used to step up the generator output voltage, from 690 V up to 40 kV. There are two main converter types as well as two main configurations type that are generally used. The power converter also performs functions such as power conditioning, rectification, and filtering.

2.3.1.7.1 Line Commutated Converter (HVDC-LCC)

Line Commutated Converters shown in Figure 2-6A use thyristor-based technology. A thyristor is a solid-state semiconductor device that incorporates four layers of P-type and N-type materials. The thyristors conduct when a current trigger is applied to the gate, making it a bi-stable switch. For commutation to occur, the converters require a high synchronous voltage source. This makes black start operations near impossible [36]. The LCC operates at the highest voltage and power rating level compared to other HVDC converter technologies [37]. The firing angle on both the rectifier and inverter side is regulated to allow for good power control. The output current is kept constant due to the unidirectional flow of DC received by the AC network. Power reversal is carried out by

inverting the DC voltage polarity but keeping the current direction constant, this method allows for fast reversal. This technology is reliable and operates with minimal maintenance thus making it the most popular among HVDC schemes [38].

2.3.1.7.2 Voltage Source Converter (HVDC-VSC)

Figure 2-6B shows the use of insulated-gate bipolar transistor (IGBT) technology in voltage source converters. Black-start capabilities are possible with the VSC as it creates its AC voltage and can be switched on or off at any time [39]. Pulse width modulation (PWM) is used to operate the converters at a high frequency, this allows for constant voltage during the adjustment of the amplitude and phase angle [40]. VSC has the ability to control its active and reactive power allowing for a high degree of flexibility making it useful in urban power networks [41]. Low device rating, high power losses, and high dielectric stress affect the capacity limits of VSC-HVDC as compared to LCC. VSC technology utilizes PWM techniques to control the switching frequency of the IGBT, and reduction of the generated harmonic distortion. The overall efficiency of VSC is very low when compared to LCC converters due to high switching losses in the IGBTs. [42].

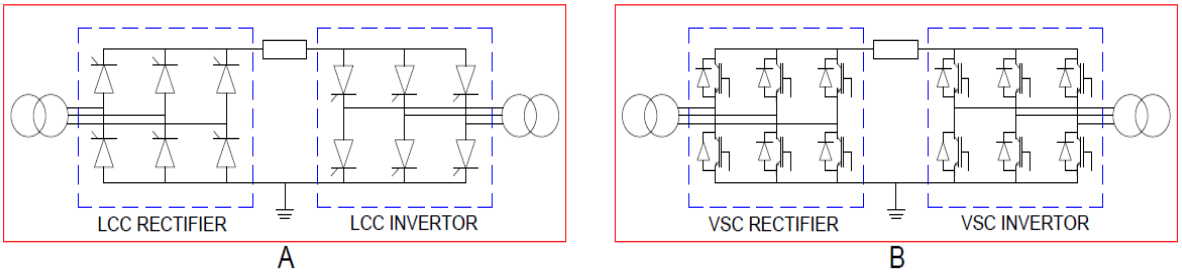

Figure 2- 6: LCC and VSC Converter Schematics

2.3.2 Comparison between HVDC-LCC and HVDC-VSC

Industrial HVDC schemes in operation today utilize HVDC-LCC systems, which use thyristors technology [43]. The thyristors delayed firing makes the voltage lead the current, therefore the reactive power is absorbed by the HVDC LCC link. HVDC LCC is especially feasible for long-distance transmission of large amounts of electric power at very high voltages.

A major advantage of VSC schemes is the IGBT technology it is comprised of, which are independent of the zero crossings of the current and the operation of the surrounding AC grid. The reactive power is also controlled independently without the use of reactive compensation. This makes VSC favourable over LCC due to the level of power controllability. VSC also limits inverter commutation failures and reduces the injection of harmonic currents into the system [44]. The major drawback of VSC is the power losses due to switching operations. This is a major factor in bulk power transmission, making HVDC VSC less economical [45]. Overall, VSC has an approximate loss of 1.6 – 1.8 %, while LCC has losses of 0.8% [46].

2.3.3 WECU Configuration types

WECU's connections are classified as either connected in a ring or radial configurations, although there are other configurations mentioned, these are a variation or modification of the ring or radial configurations.

2.3.3.1 Shunt / Radial Configurations

Low cable costs and simplistic control schemes have made radial feeders popular for wind farms. The radial configuration, however, has low reliability. For example, the function of the wind farm may be inhibited due to a cable fault. Each chain of parallel-connected WECUs is exposed to the same terminal DC voltage. Each chain can generate a total current $i_{dc}(t)$, given by Equation (2-4), where $i_{do}(t)$ is the total current output of each WECU; and k represents the total number of WECUs on each chain. The WECU's are connected to an offshore platform via a DC cable. If n is the total wind farm chains, Equation (2-5) can be used to determine the output current collected from the wind farm.

$$i_{dc}(t) = \sum_{k=1}^{k} i_{do(k)}(t) \tag{2-4}$$

$$i_{DC}(t) = \sum_{n=1}^{n} i_{dc(n)}(t) \tag{2-5}$$

As seen from Equation (2-4), the parallel-connected WECU's in each chain build up the current magnitude of the system but operate at the same terminal voltage. To allow for the transmission of the generated power, the use of an HVDC-offshore platform is essential. The platform will allow the voltage to be stepped up for transmission. The

output terminals of each WECU in the system are connected to an MV link and have a high voltage-boost ratio. Due to this fact, all WECUs on a wind farm with radial feeder topology must incorporate power converters with a high boost ratio and that can support a medium-voltage level.

2.3.3.2 Series / Ring Configurations

Ring feeds offer high reliability compared to radial systems. One of the disadvantages of the ring feeder configuration is that the converters must be able to operate at a high voltage. This is due to the fact that if one WECU fails, leading to a loss of output power, the other WECUs must compensate.

For the ring feed topology, the series-connected WECUs in each chain build up a voltage $V_{dc}(t)$ across the DC collector as given by Equation (2-6), where $V_{do}(t)$ is the output voltage of each WECU; and k represents the total number of WECUs in the series-connected circuit.

$$V_{dc}(t) = \sum_{k=1}^{k} V_{do(k)}(t) \tag{2-6}$$

By increasing k the voltage can be high enough to avoid the use of an HVDC platform for this topology, according to Equation (2-6). The ring feeder has a simple configuration that is cost-effective for offshore DC collection systems.

2.3.4 DC collection grid protection and control

Some of the factors hindering the implementation of DC collection grids in offshore wind farms include; the lack of feasible protection systems, standards, and guidelines [47].

Maintaining a DC-link voltage with minimum variation is one of the most important factors for incorporating a wind farm with a DC collection grid into the current energy grid. A DC voltage variation out of the allowable range can cause the DC collection system to fail. Various protection and control methods such as; the use of solid-state protection devices, energy storage systems (ESS), and power electronic converters can offer greater flexibility [48-51].

2.3.4.1 Protection devices

The key design criteria for a Protection Device (PD) include reliability, speed, economics, and low complexity [49, 52]. Conventional AC systems have protective devices such as circuit breakers which will detach equipment from the system. By causing the interruption at zero crossing, arcs are minimized and the possibility of interruptions is reduced [53]. DC systems on the other hand cannot rely on this method as there is no sinusoidal wave form. To overcome this problem, the PD has to operate almost instantaneously to disconnect the system before it can reach the full fault level [54].

HVDC grids can expect three types of faults to occur. A fault on the AC side of the power converter station can occur which can be single- or multi-phase. This can lead to generation losses or grid loading. For an HVDC system to be successful, it is required to stop a fault from being transmitted from one AC system to another.

The next fault that can be experienced is on the DC side of the power converter. These are complex fault types to handle as compared to AC faults. During a DC fault, due to the low impedance characteristic of DC cables, the direct bus voltages in the HVDC grid are significantly reduced, nearly stopping the power flow.

Finally, the power converter itself can experience a fault, which can disconnect a section of the HVDC grid. The world's first HVDC breaker has been launched by ABB and is a promising device for HVDC grid protection [55].

2.3.4.2 Energy Storage System

A typical model of an energy storage system is a battery or capacitor [56]. An ESS aims to sustain a continuous DC-link voltage between the utility grid and wind farm by regulating the power exchange. The utility AC grid voltage at the infinite busbar (VR) and the voltage at the point of common coupling (PCC) (V_{pcc}) can be expressed in terms of V_{dc} and D, where V_{dc} is the DC-grid voltage and D is the converter duty ratio. $P_{pcc(w)}$ is the total real power and $Q_{pcc(w)}$ is the reactive power. $P_{pcc(w)} = P_{dc(w)} - R_{dc} I_{dc}^2$, with $P_{dc(w)}$ as the total real power output of the wind farm; R_{dc} is the resistance of the DC transmission line; and I_{dc} is the DC transmission line current. Equation (2-7) shows the difference in voltage between the utility grid and the wind farm.

$$V_{pcc} - V_R = \Delta V_{RS} = Z_g \times \left(\frac{P_{dc(w)} - jQ_{pcc(w)}}{V_{pcc}} \right) \tag{2-7}$$

The voltage difference ΔV_{RS} is related to the short-circuit impedance of the utility grid and the real power output of the wind farm. From Equation (2-7) the variations of the output power of the wind farm will result in the variations in the output voltage of the wind farm. If Z_g, the impedance, is small, then ΔV_{RS} will be small resulting in a strong grid and vice versa. For example, looking at Equation (2-8), where $P_{dc(w)}$ is the real power of the wind farm, P_d is the real power of each WECU and $P_{dc(g)}$ is the total real power required by the load, then the voltage across the DC collector will either increase or decrease with variations in $P_{dc(g)}$ or $P_{dc(w)}$.

$$P_{dc(w)} = \sum_k P_{dc(k)} \tag{2-8}$$

For the collection system to be stable and ignoring transmission losses $P_{dc(w)}$ must be equal to $P_{dc(g)}$ in every instant. During normal operation or if $P_{dc(w)} \simeq P_{dc(g)}$, the ESS will remain at standby mode, while during variations, the ESS regulates the DC-Link voltage by charging or discharging. Under the low wind and high demand conditions, the ESS must switch to discharging mode to maintain the stability of the system, while under high wind and low load conditions it must switch to charging mode.

2.3.4.3 Bidirectional DC-DC converter

The bi-directional DC-DC converter allows for power flow between the ESS and DC collection grid. Power fluctuations are absorbed by the ESS which improves the DC collection system properties. Figure 2-7 shows a bidirectional DC-DC converter for high-power applications [57].

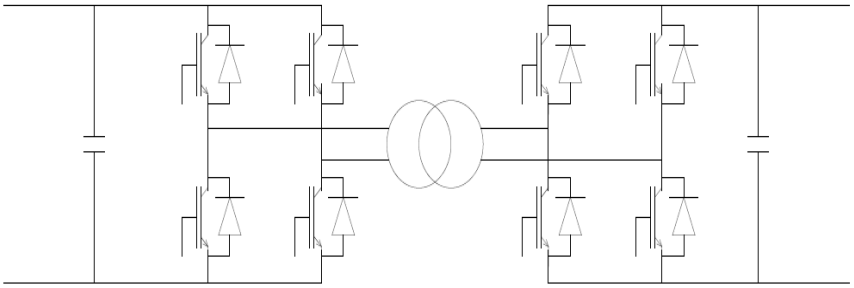

Figure 2- 7: Bi-Directional DC/DC Converter

2.4 Transmission systems

Without the use of additional compensation, the offshore wind farm is required to be in close proximity to the power grid, due to cable charging currents causing distance limitations. Using this compensation requires additional platforms, which increase the cost of the system.

2.4.1 HVAC Systems

The production of reactive power while transmitting HVAC is a major challenge. It is possible to use HVAC for short-distance transmission. Flexible Alternating Current Transmission Systems (FACTS) have been used to enhance the performance of long-distance AC transmission [58]. However, lately, the technology has been extended to devices, which can also control power flow. The operation of FACTS can be explained by Figure 2-8. Power transmitted in the system depends on the voltages at each end of the interconnection, as well as the impedance and the difference in angle between both systems. Different FACTS devices can actively influence these parameters and control the power flow through the interconnection [59].

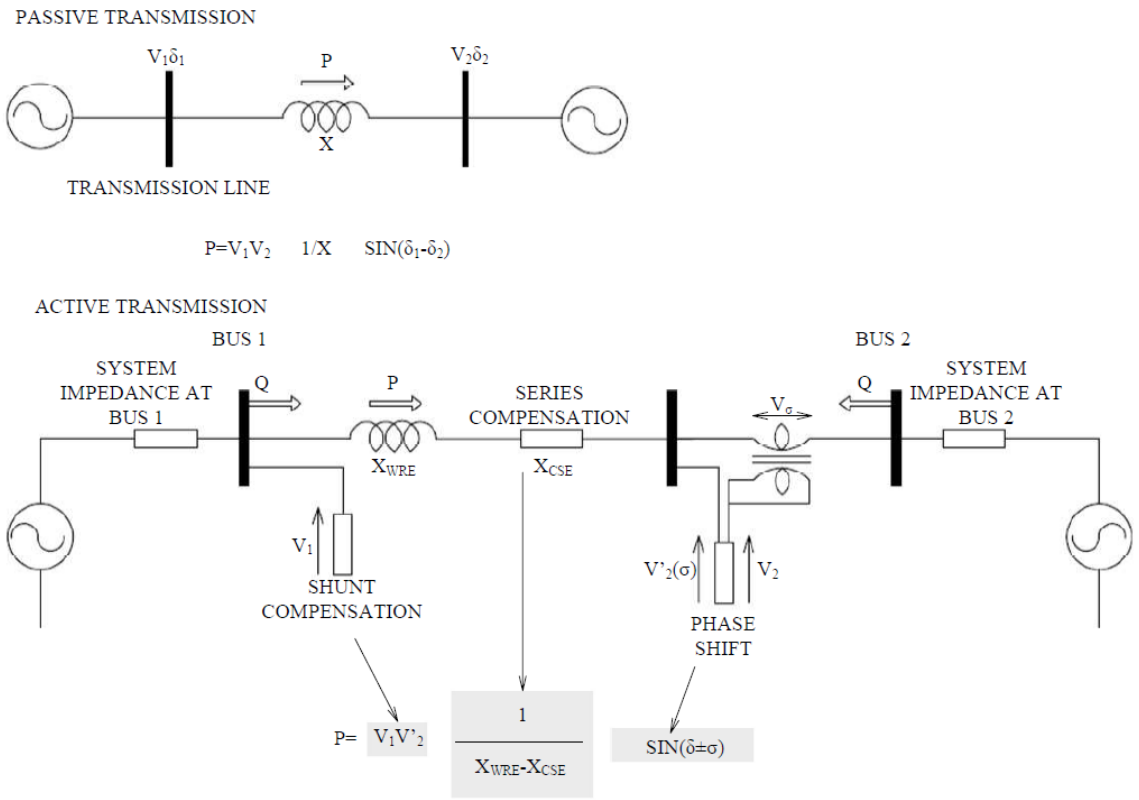

Figure 2- 8: Simplified Illustration of FACTS

2.4.1.1 SVC and STATCOM

SVC's have been used since 1970 and are the most common of the FACTS devices. They consist of traditional thyristors and require complex controllers in comparison to mechanically switched devices. SVC is essentially a parallel-connected static Var generator or load capable of producing or consuming reactive power. The SVC's output is regulated to exchange capacitive or inductive current. This helps to maintain or control specific power system variables, generally the SVC bus voltage. SVC's are usually connected to transmission lines and require high voltage ratings. SVC's are installed to improve dynamic voltage control, which helps to increase the systems load ability [60].

An additional improvement is STATCOM devices which incorporate VSC devices and provide power compensation. Although it is similar to a synchronous condenser, it is superior as it is an electrical device with no inertia. The advantages of STATCOM are its low investment cost as well as lower operation and maintenance costs.

Swift voltage and reactive power control are possible with both devices as well as power oscillation damping features. Series compensation is used for reducing the transmission angle, for long AC lines, therefore, improving stability.

SVC and STATCOM differ in their operation. STATCOM works as a controllable voltage source, SVC works as a dynamically controllable reactance connected in parallel.

Using STATCOM the grid is fed with the maximum available reactive current even at low voltage levels. This is due to the ability of the system to inject reactive power which varies linearly with the voltage at the PCC. For SVC a higher nominal capacity device is required as there is a quadratic dependence of the reactive power to the voltage.

Table 2-1 summarizes the advantages and disadvantages of SVC and STATCOM. The major developments in the STATCOM devices make them an attractive choice for improving an AC power system's performance.

Table 2- 1: Advantages and Disadvantages of SVC and STATCOM

STATCOM	**SVC**
Higher Compensation Accurateness	Lower accuracy than STATCOM
Faster than SVC	Slower than STATCOM
Lower Costs	Higher Costs
Lower Losses	Higher Losses
Better Characteristics	Characteristics are not as good
Constant current	Capacitive reactive current drops linearly
Interfaced with power sources	Cannot be interfaced with power sources
Smaller size	Larger Size
Controllable voltage source	Dynamically controlled reactance
Lower Harmonics	Very High Harmonics

2.4.2 HVDC Transmission Systems

The current capacity and efficiency of HV lines are dependent on the converter used to transform this current from AC to DC and from DC back to AC. A well-configured converter can reduce problems such as harmonics and reliability against faults and can increase power capacity. The two dominant types of HVDC converters used today are the voltage source converter (HVDC-VSC) and the line commutated converter (HVDC-

LCC) also known as Current Source Converters (HVDC-CSC). As they are both DC, they require converters to change AC to DC at the transmitting end and DC back to AC at the receiving end. Performance and operational requirements are considered when HVDC interconnections are configured. For incorporating multiple generation sources multi-terminal HVDC would be considered the best method, which allows two or more sets of converters to operate autonomously as a rectifier or inverter [61].

2.4.2.1 Arrangements of HVDC systems

For efficient operation, HVDC converter bridges and lines can be arranged into numerous configurations. Figure 2-9 shows the arrangement of the converter bridges in monopolar and bipolar configuration and are described as follow:

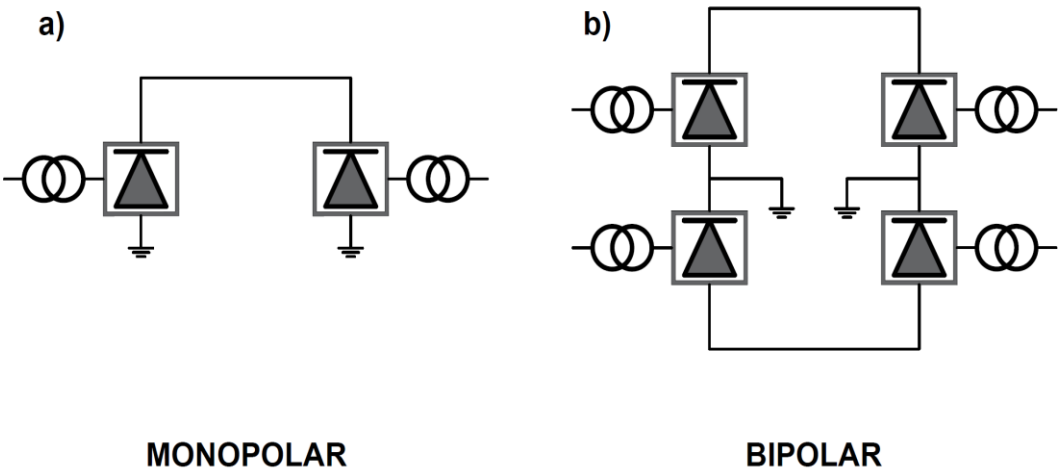

Figure 2- 9: Monopolar and Bipolar Arrangements

a. Monopolar HVDC system

Monopolar configurations connect one terminal of the rectifier to the ground and one to the transmission line. Long-distance transmission using an earth return system is much cheaper than using a neutral conductor, however, this can be problematic. Installation of a return conductor can negate these issues. A system using a ground return is shown in Figure 2-9(a).

b. Bipolar HVDC system

There are two conductors required for bipolar transmission. This system costs more than monopole systems with a return conductor as both conductors are required to be rated for the full system voltage. However, it can be an attractive option, due to its numerous advantages such as minimal earth-current and continuous operation during fault. This is a common configuration for the transmission of HVDC power [38]. Figure 2-9(b) shows the bipolar circuit link.

2.4.2.2 HVDC Configurations

Many configurations can be used with HVDC systems. Selecting the correct configuration is mainly based on the converter station function and location.

1. Back-to-back HVDC

Back-to-back configuration can be in either monopole or bipolar configuration and does not require a transmission line between the two converter stations. These converter stations are usually located in the same building.

2. Point to Point HVDC

Point-to-point configurations are used to transmit DC power between geographical locations. A rectifier is used to convert the AC power DC and is then converted back to AC after being transmitted. A major advantage is this configuration can interconnect asynchronous substations.

3. Multi-terminal HVDC transmission system.

The most common configuration of an HVDC link is the connection of two converter stations. Multi-terminal HVDC links, that connect multiple points, are increasing in importance but are rare. The multi-terminal configuration can be in series, parallel, or hybrid (a mixture of series and parallel). Figure 2-10(b) shows parallel multi-terminal DC configurations. Converter bridges added in series, create a series multi-terminal DC shown in Figure 2-10(a). Multi-terminal DC systems are extremely expensive as a result of the additional substations.

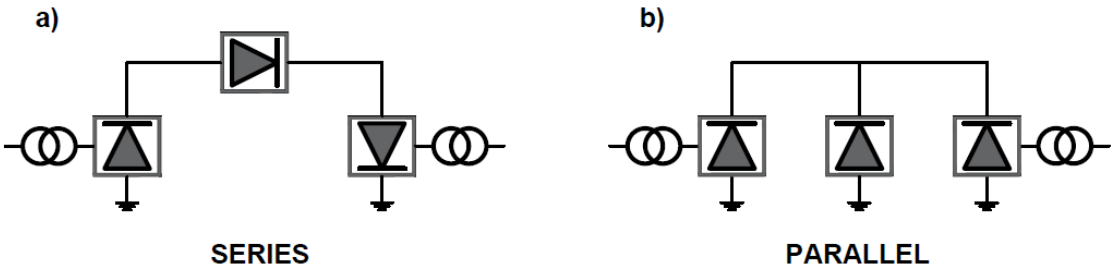

Figure 2- 10: MTDC Connections

2.4.3 Advantages and disadvantages of HVDC

HVDC transmission has many advantages over HVAC, such as:

a. Smaller Tower Size

Alternating Current (AC) is generally considered in Root Mean Square (R.M.S). This means that the insulation for a 500kV conductor is required to be $\sqrt{2} \times 500 = 707.11kV$.

Therefore, the insulation will have to be able to handle approximately $708kV$. In Direct Current (DC), however, this problem does not exist and a DC line only requires two conductors whereas in AC three conductors, if not more, are required for the same reliability. Therefore, both electrical and mechanical requirements allow for the use of a smaller tower size.

b. Asynchronous interconnection possible

In AC, asynchronous systems cannot be interconnected, as they must have the same frequency. These systems can be easily interconnected through DC links. Power authorities must maintain different tolerances on their supply voltages even though technically at the same frequency. This option is not practical with AC while in DC systems there is no such problem.

c. Lower short circuit fault levels

The fault levels for an AC system increase when the system is extended. This leads to the replacement of circuit breakers and other protection equipment which is extremely expensive. DC does not contribute current to the AC short circuit beyond its rated current. In the event of a fault, automatic grid control limits the current after a momentary discharge of the line capacitance.

2.4.3.1 Disadvantages of HVDC

Although there are many advantages for HVDC over HVAC, HVDC transmission systems also have their downfalls.

a. Expensive converters

Ac systems only require a power transformer, while to allow for DC transmission, expensive converter stations are required on the DC transmission link. These converter stations lead to high initial costs.

b. Reactive power requirement

Converters for both rectifications as well as inversion require high reactive power. Each converter can consume reactive power up to 50% of the active power rating of the DC link. Static capacitors and filter capacitance supply the reactive power required.

c. Generation of harmonics

A large number of harmonics are created in DC systems due to the switching of the converters. These harmonics affect both the AC and DC side of the system. Harmonic filters are connected on the AC side to reduce the number of harmonics transferred to the system while smoothing reactors are used for DC systems. These components add to the cost of an already expensive converter.

2.4.4 Comparison of HVAC and HVDC transmission

There are two main factors of a high voltage transmission line, current limits and voltage limits. Due to the skin effect, the AC resistance of a conductor is higher than its DC resistance, which in turn results in a higher loss for transmission of AC. For high voltage transmission lines switching surges are a serious concern, for AC the peak values are 200 to 300% of the nominal voltage, whilst for DC transmission it is 170% the system voltage [62]. Corona and radio interference is significantly lower in HVDC transmission lines compared to HVAC transmission lines [63]. Corona losses for an 895 km, 450 kV HVDC transmission line is less than 5 MW [64]. A serious problem in long HVAC transmission lines is the production and consumption of reactive power. This increases the power loss. Equation (2-9) shows the reactive power produced by the line, where: (L) is the series

inductance (C) is the shunt capacitance per unit of length, (V) is the operating voltage, and (I) is the system current.

$$Q_C = \omega C V^2 \tag{2-9}$$

The consumers' per unit length reactive power is given by Equation (2-10):

$$Q_L = \omega L I^2 \tag{2-10}$$

If $Q_C = Q_L$ then Z_S can be calculated by Equation (2-11).

$$\frac{V}{I} = \left(\frac{L}{C}\right)^{\frac{1}{2}} = Z_S \tag{2-11}$$

where Z_S is surge impedance of the line. The power in the line is given by (2-12) and is called the natural load.

$$P_n = VI = \frac{V^2}{Z_S} \tag{2-12}$$

Therefore the power carried by the transmission line is dependent on the operating voltage and the surge impedance.

Equation (2-13) shows the power transfer in a transmission line and power flow in an AC system.

$$P = \frac{E_1 E_2}{X} \sin\delta \tag{2-13}$$

E_1 and E_2 are the two terminal voltages, δ is the phase difference between these voltages, and X is the series reactance of the line. When δ= 90º maximum power transfer is experienced and is given by Equation (2-14).

$$P_{\max} = \frac{E_1 E_2}{X} \tag{2-14}$$

$P_{\max}$ is the steady-state stability limit. Long-distance transmission lines contributed the most to the system reactance while the two terminal stations only provide a small part.

A single conductor overhead line has an inductive reactance of 0.5 Ω/km, while the inductance in a double conductor is 75% greater. The reactance and length of the line are

directly proportional, and thus power per circuit of an operating voltage is limited by stability during steady-state, which is inversely proportional to the line length [65].

2.4.5 Comparison between HVAC and HVDC cable systems

For long-distance transmission of power, either underground or submarine, it is more difficult to employ HVAC. A cylindrical shunt capacitor can be used to model an AC cable [66]. A reactive charging current is caused due to this capacitive nature of the cable shown in Equation (2-15). The charging current of the cable is directly proportional to the frequency, conductor length, and nominal voltage.

$$I = \frac{V_n}{-jX_C} = j\omega C_n V_n \tag{2-15}$$

Due to Ohms law, the high voltages used for long-distance transmission as well as the charging current make the reactive power significant, and reactive compensation is required. This can be installed at various points of the cable depending on the length. The investment and installation costs of compensation equipment are high, making HVAC transmission more expensive over long transmission distances [67].

As HVDC does not have a frequency, they do not experience a steady state charging current. Furthermore, HVDC cables can be installed in a pair rather than in a three-phase configuration as HVAC. This reduction in the number of cables reduces the investment costs per unit length for HVDC systems [68].

As HVDC requires a converter for each substation, costs and losses are generally higher than HVAC systems. However, true cable losses are higher for HVAC systems. HVAC cable losses consist of four components [66]: -

- I^2R conductor losses, which are increased by skin effect and proximity effect.
- I^2R metallic shield losses, a current is induced into the cable armouring due to magnetic flux
- I^2R losses in the steel wire armour, a current is induced in the armour by the current in the conductors
- Dielectric losses, which are relatively small.

As there are no armour or shield currents induced in HVDC, the absence of skin and proximity effect lessen conductor losses. Charging currents are non-existent in HVDC cables and do not increase the cable current as is the case for HVAC cables [46].

One of the important factors in economic comparison between HVAC and HVDC is the choice between HVDC VSC and HVDC LCC. This influences the result of the comparison significantly. Power and voltage ratings also play an important role in the outcome of the comparison of transmission systems.

2.5 Economics

2.5.1 System Description

2.5.1.1 HVAC Systems

HVAC transmission systems use cross-linked polyethylene (XLPE) cables to interconnect two substations. These substations include switchgear, protection devices, power transformers, and reactive compensation. HVAC transmission systems commonly use single-core or three-core XLPE cables for submarine transmission. Three-core cables, however, have the advantage due to reduced power losses and installation costs [69].

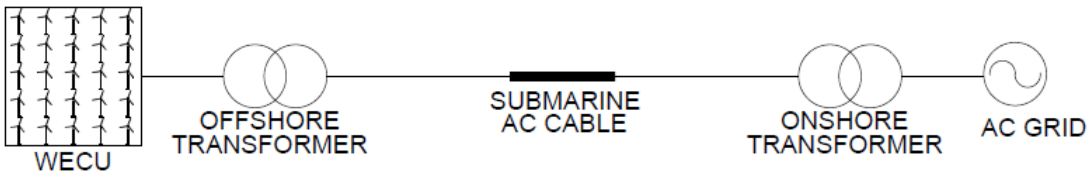

Figure 2- 11: HVAC Configuration

The AC collector grid operates between 33-66kV, this requires the system voltage produced by the wind farm to be stepped up for transmission. An onshore transformer may also be required if the operating voltages differ.

To allow for higher power capacity and improved reliability of the substations, two transformers are commonly connected in parallel and are rated at 60 % of the wind farms' nominal power [70]. As the cable length increases a resulting increase is caused in the reactive power. This, in turn, reduces the delivered active power as well as the offshore transmission link cable length [71]. The use of reactive power compensation aids in reducing power losses and assists with voltage control [72]. Figure 2-11 shows an HVAC offshore transmission system.

2.5.1.2 HVDC Systems

Although both HVDC-LCC and HVDC-VSC converters are used for DC-AC conversion, LCC has no black start capability and high commutation failure. These make HVDC LCC unsuited for offshore wind farms systems. Currently, transmission systems that utilise VSC technology are deemed to be a highly suitable solution for this application.

HVDC-VSC systems are constructed from two system elements; converter stations and cables. The offshore and onshore converter stations are connected via a pair of polymeric extruded cables. VSC converters use IGBT technology, which, due to the switching frequency (1.3-2.0 kHz), produces a lower amount of harmonic distortion. Active and reactive power control is done independently in VSC systems, allowing greater voltage and frequency stability, and the use of advanced PWM technology enables bidirectional power transmission [73]. Figure 2-12 shows a basic HVDC-VSC system configuration for offshore wind farms.

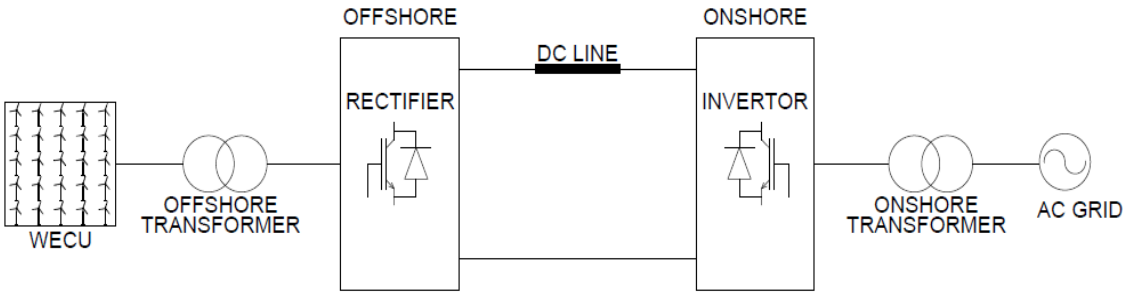

Figure 2- 12: HVDC Configuration

2.5.2 Cost Modelling

The cost modelling for HVAC and HVDC systems is detailed in this section. For each system, the investment costs, as well as the system components costs, are shown.

2.5.2.1 HVAC Cost

2.5.2.1.1 System Variables

South African standard frequency f_{HVAC} is 50Hz [3]. The standard voltage levels U_{rms} for submarine transmission vary between 110-400 kV. I_{rated} is the rated current and is chosen based on the calculated current passing through the cables, this calculation is shown in Equation 2-16 [74]:

$$I = \frac{k \times P_{wf}}{\sqrt{3} \times U_{rms}} \tag{2-16}$$

where k is the coefficient for current tolerance of +10%, therefore $k = 1.1$ and P_{wf} is the rated power of wind farm. Using the supplier technical data, the cross-section S, and the number of three core cables n_{cb} can be determined.

2.5.2.1.2 Cable

Due to rapidly developing cable technology, including all factors in cost modelling has become increasingly difficult, thus resulting in the overall cost being affected. The modelling of a three-core cable was done by Lundberg using an exponential equation with an offset constant [75]. The cables rated current and voltage are the two most important factors affecting the cost. The amount of copper is based on the rated current, while the insulation material is based on the voltage rating.

The equation for the cost of a 132kV cable $C_{cb(132)}$ is presented in Equation 2-17.

$$C_{cb(132)} = 249.72 + 26.48e^{\frac{379.5I_n}{10^5}} \times l \tag{2-17}$$

Where l is the transmission distance and S_n is the rated apparent power of the cable in MW. I_n can be calculated using Equation 2-18.

$$I_n = \frac{S_{rated}}{\sqrt{3} \times U_{rms}} \tag{2-18}$$

2.5.2.1.3 Switchgear

Based on the data in Table 2-2, Equation 2-19 was formed. Therefore the cost of the switchgear can be obtained by:

$$C_{sg} = 0.0007 \times U_{rms} + 0.036 \tag{2-19}$$

To protect vital components of the offshore and onshore substations, switchgear is required at both the sending and receiving ends. Therefore, two HV switchgear devices are required per cable.

Table 2- 2: Switchgear Sizing and Cost

Switchgear rated voltage (kV)	**33**	**132**	**220**	**400**
Cost (M€)	0.058	0.124	0.183	0.303

2.5.2.1.4 Transformer

Based on the information in [76], the following graph in Figure 2-13 was developed. Each point represents a real case transformer cost for its specific power rating.

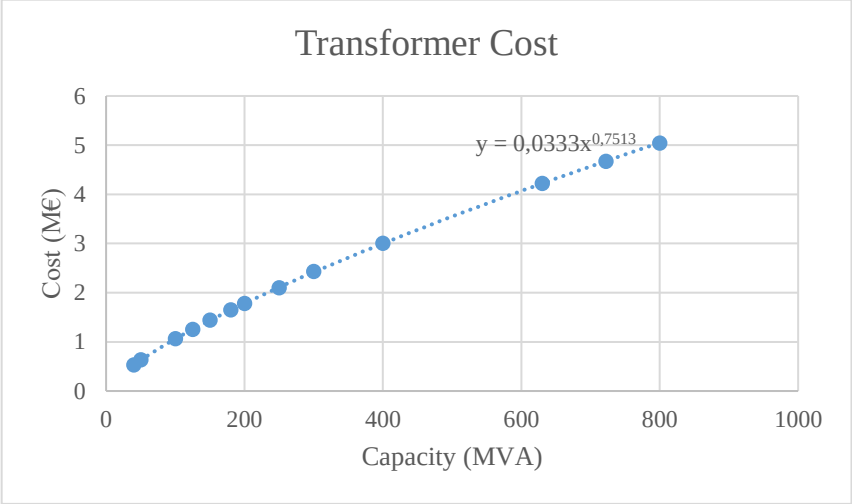

Figure 2- 13: Transformer Rated Power vs Cost

The rated power of a transformer, (S_{TR}), determines the cost associated with it. The number of the transformers required is determined by the number of substations. Two transformers are required for each substation. Based on Figure 2-13 the cost Equation 2-20 was developed.

$$C_{TR} = 0.0333 \times S_{TR}^{0.7513} \tag{2-20}$$

2.5.2.1.5 Substation

The size and cost of an offshore substation are directly proportional. The electrical infrastructure and the presence of required services such as; accommodation, helipads, and fuel tanks determine the dimensions of the platform. Equation (2-21) shows the cost of a substation [75, 77]

$$C_{ss} = 2.534 + 0.0887 + n_{wt} \times P_{wf} \quad (2\text{-}21)$$

where P_{wf} is the rated power of the offshore wind farm and n_{wt} is the number of turbines.

2.5.2.1.6 Reactive Power Compensation

Reactive power compensation is essential for HVAC transmission systems. The amount of compensation required is dependent on the voltage level and the transmission distance. The linear equation 2-22 is derived from the graph seen in Figure 2-14 [17, 71, 78]:

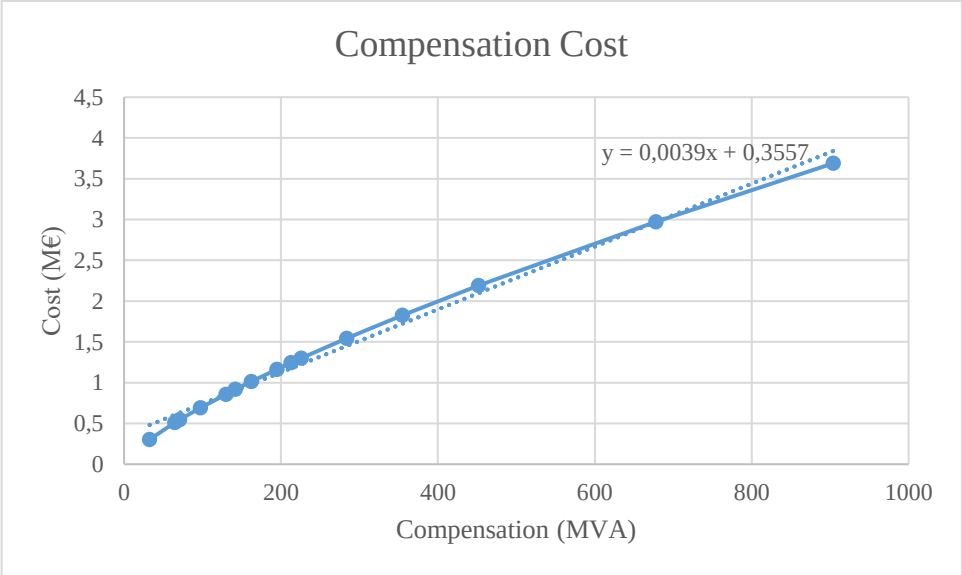

Figure 2- 14: Reactive compensation costing

$$C_{re} = 0.0039Q_l + 0.3557 \quad (2\text{-}22)$$

Q_l is the compensated reactive power. The required reactive power can be determined by Table 2-3.

Table 2- 3: Required compensation for transmission distance and voltage level

MVA	**DISTANCE (km)**					
TRANSMISSION VOLTAGE	50	100	150	200	250	300
132KV	32,5	65	97,5	130	162,5	195
220KV	71	142	213	284	355	
400KV	226	452	678	904		

2.5.2.2 HVDC Cost

2.5.2.2.1 Base variables

A set of variables are used to determine the cost of an HVDC system. System voltages U_{HVDC} vary between 80-320 kV. As the system is bipolar, the number of cable pairs n_{cb} is by default equal to 1. Each cross-section S_{HVDC} and cable rated current I_{rated} is estimated from the values given by supplier datasheets.

2.5.2.2.2 Cable

The cost of HVDC cables can be calculated by using the linear Equation 2-23. This equation is developed based on the cost and MW capacity of the cables installed in previous HVDC projects found in [79-81]. Table 2-4 shows these values.

Table 2- 4: Cable Costing vs Capacity

Cable Capacity (MW)	**Project**	**Price in 2004 (M€/km)**	**Price in 2020 (M€/km)**
600	Swe-Pol Link	0.9	1.148
550	Iceland Link	0.811	1.034
500	Ital-Gre Link	0.7	0.893
440	Skagerrak 3 Link	0.616	0.786

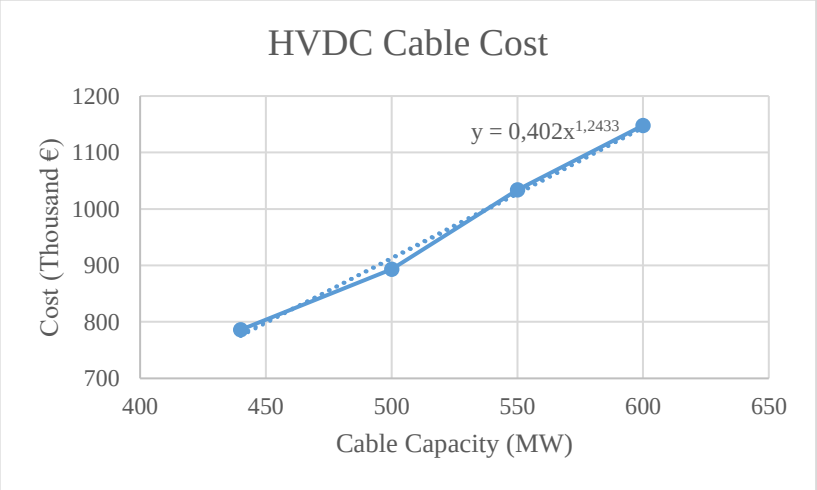

Figure 2- 15: HVDC Cable Costing Graph

Figure 2-15 is developed from Table 2-4 and an equation can be developed to determine the cable cost C_{cb} for HVDC systems. C_{cb} is presented in Equation 2-23:

$$C_{cb} = \left(0.402 * P^{1.2433}\right) \times l \tag{2-23}$$

where P is the rated power capacity.

The rated power of the cable pair can be calculated using Equation 2-24:

$$P_{rated} = 2 \times U_{HVDC} \times I_{rated} \tag{2-24}$$

2.5.2.2.3 Transformer

Transformers are also required for HVDC systems, these are used to step up the voltage from the collection grid to the transmission cables and further on to the grid. The same optimal configuration with two transformers at each substation is assumed and the cost equation shown in Equation 2-20 is used.

2.5.2.2.4 Substation

HVDC substations require expensive AC-DC converters, which causes the substation cost to be higher for HVDC than HVAC. Components such as power electronics, phase reactors, filters, transformers, enclosed valves, are also required. From literature, [82, 83], it is determined that the cost for HVDC substations is approximately 57.9% to 115.4% higher than an HVAC substation for the same power rating. Taking this into account a 90% average is taken into account and the cost equation, Equation 2-25 is determined.

$$C_{ss} = 1.85 \times (2.534 + 0.0887 + \frac{P_{wf}}{1000}) \tag{2-25}$$

where P_{wf} is the rated power of the offshore wind farm in MW.

2.5.2.2.5 HVDC Converter Station

As a result of an offshore platform, onshore converter stations are much cheaper than offshore systems. The difference between offshore and onshore converter stations is quite

substantial due to the offshore installation. VSC converter offshore and onshore is defined by Equation 2-26 and 2-27 respectively [68, 76, 84].

$$C_{dc,off} = 42 + 27 \times \frac{P_{N,conv}}{300} \tag{2-26}$$

$$C_{dc,on} = 18 + 27 \times \frac{P_{N,conv}}{300} \tag{2-27}$$

where $P_{N,conv}$ is the converters rated power.

2.5.2.2.6 HVDC Converters

LCC and VSC technologies are based on different converter technology. The difference in their costs may play a factor in the use of either. Based on the data found in [83], tables 2-5 and 2-6 show system costs for HVDC VSC and LCC respectively.

Table 2- 5: HVDC VSC System Costs

Capacity (MW)	500	850	1250	2000
Cost (M€)	75-92	98-105	121-150	144-196

Table 2- 6: HVDC LCC System Costs

Capacity (MW)	1000	2000	3000
Cost (M€)	81-104	150-184	196-230

An average of the cost range was taken and the respective cost graphs were determined.

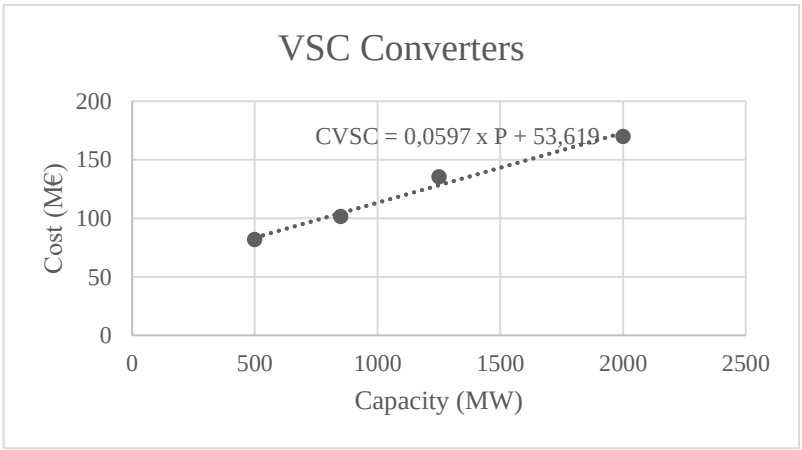

Figure 2- 16: VSC Converter Cost Graph

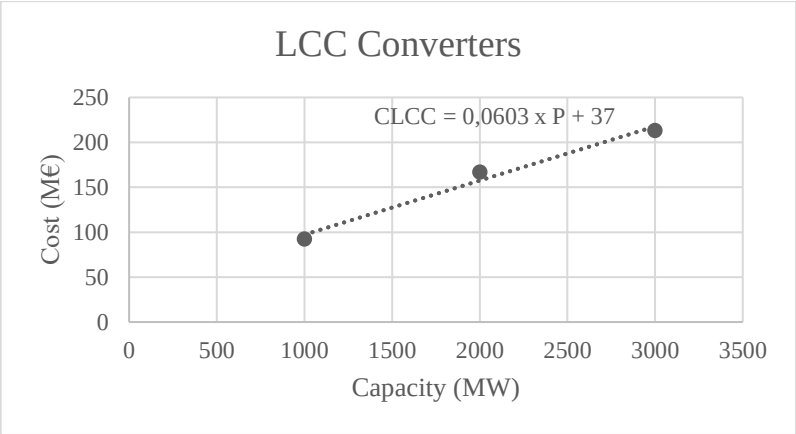

Figure 2- 17: LCC Converter Cost Graph

From the figures, 2-16 and 2-17 equations can be determined for the converter cost. Equations 2-28 and 2-29 show the converter costs for VSC and LCC converters respectively.

$$C_{VSC} = 0.0597 \times P + 53.619 \tag{2-28}$$

$$C_{LCC} = 0.0603 \times P + 37 \tag{2-29}$$

Where P is the power capacity required for the converter.

2.6 Conclusion

This chapter has looked at the current literature on wind farms, turbines, and the differences in HVAC and HVDC systems. Including the types of topologies used and the economic aspects of both systems. In summary, HVAC systems work well for shorter distances, while, HVDC systems are more cost-effective and efficient over long distances due to the lower losses they experience and the absence of line compensation reactors. The following chapter will provide a more detailed look into HVAC collection systems and where they are used.

CHAPTER 3: THEORETICAL BACKGROUND OF HVAC AND HVDC WIND FARMS COLLECTION GRIDS

3.1 Introduction

As previously mentioned, this dissertation aims to provide a comparative evaluation between HVAC and HVDC collection grids. This chapter provides an in-depth look into wind farms that use HVAC and HVDC collection systems. Case studies that use these collection grids have been presented based on previous research. Collection grid topologies are explained to determine the best-suited topology for the application. Wind energy conversion units and wind farm components have also been detailed in this chapter. This will provide a theoretical base to allow for a comparison of each system and will help to answer the research question "What is the efficiency of the AC and DC collection grid systems?" presented above.

3.2 Previous Case Studies for HVAC Collection Grids

Nearly all existing offshore wind farms use HVAC transmission systems for the transmission of electrical energy between the onshore grid and offshore substations [23]. HVAC is a deep-rooted technology that has been tried and tested over many years.

Lazaridis studied the economic comparison of HVAC and HVDC solutions for large offshore wind farms under special consideration of reliability. The paper presented an evaluation of existing HVAC-HVDC transmission systems from large offshore wind farms. The transmission cost of the transmission system was calculated taking into consideration the rated powers, transmission distances, and average wind speed. The larger wind farms are located mainly offshore where the wind potential is significant to provide the desired outputs. The design of transmission systems for long-distance applications plays an important aspect in the overall performance of the system. Low-cost systems which can transmit maximum energy are considered a good design. The results of the research showed that HVAC systems are only economical over short distances while HVDC VSC provided the lowest transmission cost.

Williams studied HVDC vs HVAC cables for an offshore wind farm. The paper focused on the cost of cabling of both HVDC and HVAC systems pre and post-installation. HVDC cables were found to be cheaper with limited losses and more suitable for energy

transmission over long distances. However, HVDC transmission is a new and developing technology compared to HVAC systems. The decision on whether to use HVAC or HVDC for offshore wind farm installations is highly dependent on the distance of a project from shore. When looking at the cost of operation and maintenance post-installation, the maintenance of DC converters may be more intensive than AC transformers.

Rebled Lluch studied power transmission systems for offshore wind farms: Technical economic analysis. The paper provided a technical-economic analysis to estimate the optimal transmission system to transmit the generated energy at the offshore wind farm. The work aimed to determine the most suitable power transmission technology for a set of offshore wind farm characteristics. From case studies, it was that the losses in the HVDC system were lower compared to the HVAC system during distribution. The losses found in the HVAC system were mostly situated in the cables, whereas for HVDC the biggest share of the losses were in the converters. It is important to note that the losses experienced from the HVDC converters decreased from 3 % down to 1 % in the last decade, whereas not much improvement is to be expected for HVAC cable losses.

Kling, Bresesti, Canever, Valadè, and Hendriks studied, offshore wind farm transmission systems in the Netherlands. The paper details the technical-economic analysis carried out for three different sizes of wind farms. The results showed that for a distance of 60 Km the HVDC solution was more expensive due to its energy losses and investment costs. It was also found through static short-circuit analysis that the risk of disconnection due to voltage dips poses an increased risk when considering large scale offshore power generation

Chaithanya, Reddy, and Kiranmayi studied, a state-of-the-art review of offshore wind power transmission using a low-frequency AC system. At present, the majority of offshore wind farms are integrated into the offshore grid with HVAC transmission. Due to the cable charging current experienced in HVAC, long-distance transmission systems use HVDC with offshore wind farms. While HVDC transmission is an excellent choice for long-distance transmission, a major drawback of the system is the maintenance required for the VSC substation. The paper reviewed the use of low-frequency AC transmission (LFAC) for offshore wind farm integration. Not requiring an offshore converter station is a major advantage of LFAC, while the main disadvantage of the

lowering of the frequency increases the size of the cable conductors. This makes the solution to be more expensive and therefore more research has to be conducted for the development of LFAC transmission.

3.3 HVAC collection grid topologies

3.3.1 AC collection systems

In wind farms with HVAC collection grids, AC power lines are used to transmit the wind turbines generated power to the collection point or the offshore substation. Even though different transmission options exist, current offshore wind farms utilize AC collection systems with AC transmission systems to the onshore utility grid [11].

AC collection systems are divided into three connection types, which are the ring, the radial, and the star connections.

3.3.2 Radial topology

The most common topology used today is the radial topology. This is due to its simplistic control and reduced cost by having a mutual feeder that collects the power from each turbine and transfers it to the offshore substation. A radial collection system links multiple wind turbines within a series to a single feeder cable. Figure 3-1 shows a diagram of radial topology. The maximum number of wind turbines per string is based on the generator capacity and cable rating. Even with the ease of control and cost-efficiency, there are still drawbacks with this topology when it comes to reliability. A component failure at the end of the system will cause a break in power transmission [11].

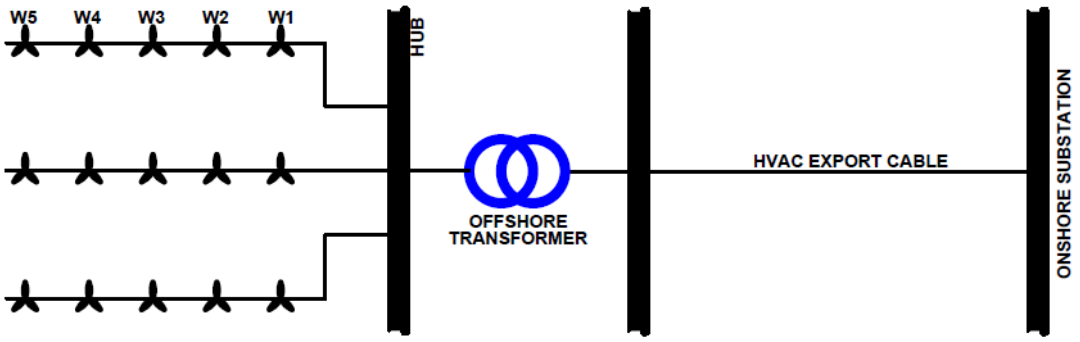

Figure 3- 1 : Radial Design System

3.3.3 Ring topology

Ring collection systems are divided into two types; single-sided ring and double-sided ring. These topologies are more developed and costly than the radial collection systems.

3.3.3.1 Single-sided ring design

A single-sided ring system connects the last wind turbine back to the collection system with an additional cable, as seen in Figure 3-2, this allows for high reliability during a fault as power can still be transmitted. The additional cable does increase the cost, but this is outweighed by the reliability improvement from the redundancy [11].

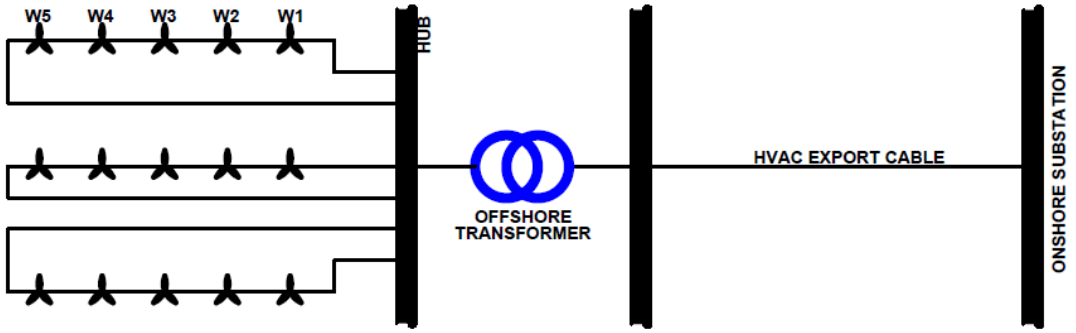

Figure 3- 2: Single-Sided Ring Design System

3.3.3.2 Double-sided ring design

Figure 3-3 shows a double-sided ring design. In this collection system, the last turbines of the strings are joined and the cable of the next string is used as the redundant circuit, reducing the cost disadvantages as seen in a single-sided ring. Due to this redundancy, the collect bus is designed to double power capacity to allow for the failure of a string, in turn diverting through the redundant string.

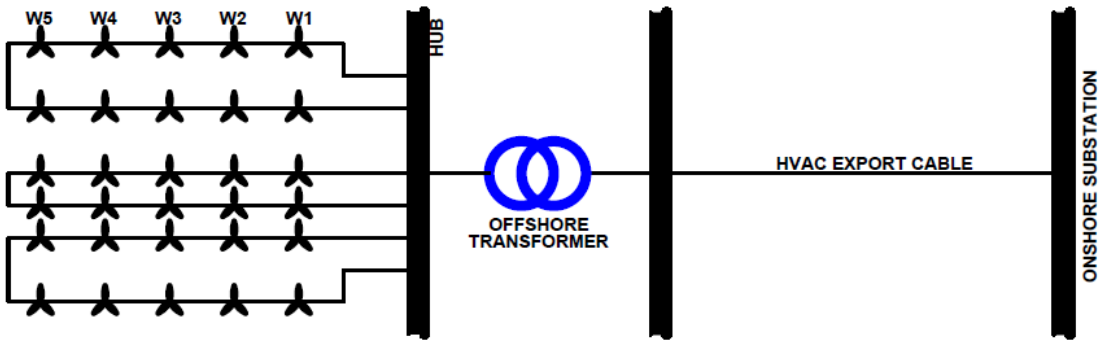

Figure 3- 3: Double-Sided Ring System

3.3.4 Star topology

Star-connected systems aim to lessen cable ratings of the turbine and PCC connection. A shared point of connection, located in the centre of the wind turbines is used. This topology increases the reliability of the system, as only one machine is lost in the event of a cable failure. There are also many drawbacks with this system, such as higher losses and costs than other systems caused by long cable lengths and lower voltage ratings. Star-connected systems have lower cable ratings for wind turbines to collector bus connections. It does, however, have the highest reliability and superior voltage regulation [85]. Figure 3-4 shows a star-connected system.

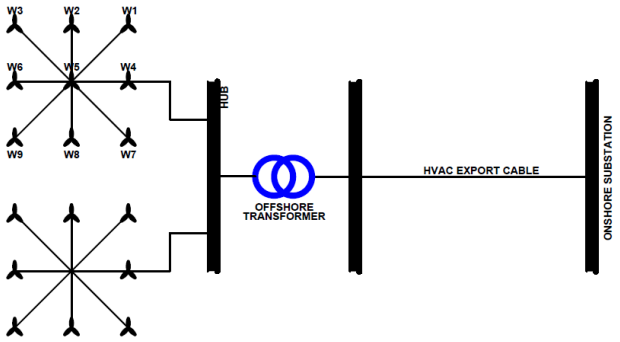

Figure 3- 4: Star Design System

3.4 Typical HVAC wind conversion unit models

A wind turbine or WECS comprises of a generator and power converter as the two main electrical components. Three groups can be derived from various combinations and designs of these components[13]:

- Fixed-speed WECS without power converter interface

- WECS using reduced-capacity converters
- Full-capacity converter operated WECS.

Any type of three-phase generator can be connected to a wind turbine, they are divided into two groups, namely Synchronous and Asynchronous generators.

3.4.1 Asynchronous generators

Asynchronous generators, also known as induction generators, use a rotating magnetic field between a stator and a rotor to induce a current in the windings of the rotor. These generators can be self-excited or excited by the power grid. The slip rate of the generator allows the output power to increase or decrease.

- Squirrel cage induction generator (SCIG)
- Wound rotor induction generator (WRIG)
- Doubly Fed induction generator (DFIG)

3.4.2 Synchronous generators

Synchronous generators comprise of a rotor, turning at the same speed as the stator magnetic field. The generator can be divided into two types by its structure: a rotating armature and a rotating magnetic field. The most commonly used alternator is a synchronous generator, it is widely used in various types of power generation.

- Wound rotor generator (WRSG)
- Permanent magnet generator (PMSG)

3.4.3 Fixed-Speed WECS without Power Converter Interface

Figure 3-5 shows the configuration of WECS without a power converter interface. This configuration connects the generator to the grid via a transformer and uses only a squirrel cage induction generator. The generator's frequency and the number of poles determine its rotational speed. A four-pole, one-megawatt generator with a 60 Hz supply, operates at slightly higher than 1800 rpm. The generator speed varies within 1% of its rated speed even with varying wind speeds. Due to the very small speed range of the generator, this system is often known as a fixed-speed WECS.

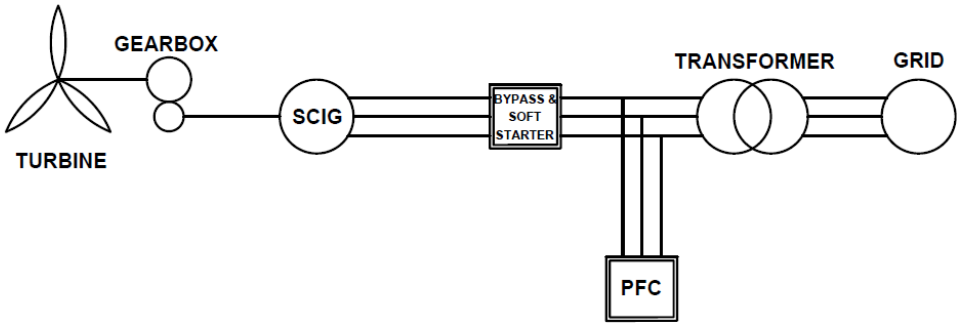

Figure 3- 5: Wind Energy Conversion System Without Power Converter Interface

For the generator to deliver the maximum power at the rated wind speed, a gearbox is required to couple the generator to the turbine blades and match their different speeds. A soft starter is required in this configuration to limit the inrush current produced during start-up. Once the system is started the soft starter is no longer required and is bypassed using an automatic transfer switch.

During normal operation, a capacitor bank is required for reactive power compensation and does not require any power converter unit. Although this method is generally accepted for its simplicity and low costs, it has two major drawbacks. Firstly, the system can only deliver the rated power to the grid at a given wind speed, which causes low efficiency. The second is that the power measured at the point of common coupling fluctuates subject to the wind speed, which causes disruptions to the grid and power quality.

3.4.4 Variable-Speed Systems with Reduced-Capacity Converters

Variable speed systems increase the efficiency of the wind energy conversion unit as compared to fixed-speed wind systems. It also helps to reduce the mechanical stress from fluctuating wind gusts, expanding the life span of the equipment by reducing wear and tear on the gearbox and bearings. This reduction in wear and tear also allows for lower maintenance costs and fewer breakdowns. One of the major disadvantages of this system is the expensive and complex power converter required, used to control the generator speed. The power converter does allow the generator to be decoupled, allowing active and reactive power control of the grid-side [13].

Variable speed systems can be broken down into two categories, depending on the power rating of the converter:

- Reduced-capacity power converter
- Full-capacity power converter

Wound-rotor induction generators (WRIG) control the rotor currents to achieve variable-speed operation. Reduced capacity converters are only feasible in such uses. There are two designs for the WRIG configurations: one with a converter-controlled variable resistance, and the other with a four-quadrant power converter system.

3.4.4.1 Wound Rotor Induction Generator with Variable Rotor Resistance.

Figure 3-6 shows an illustration of a WECU using a WRIG and a variable resistance in the rotor circuit. Variable-speed operation of the turbine can be achieved by changing the rotor resistance, which is adjusted by the power converter allowing a speed adjustment range limited to 10% above the synchronous speed of the generator [86]. Variable speed operation allows higher power generation with the drawback of energy losses caused by the rotor resistance. This configuration also requires reactive power compensation as well as a soft starter.

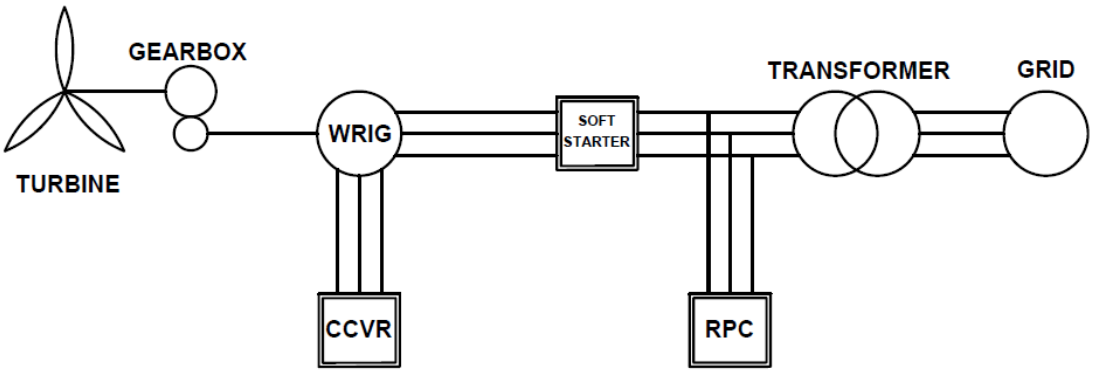

Figure 3- 6: Variable Speed Configuration With Variable Rotor Resistance

3.4.4.2 Doubly Fed Induction Generator with Rotor Converter.

The DFIG system's configuration is very similar to that of the WRIG system. The systems differ in two ways, the soft starter and reactive compensation are not required and the

variable resistance is replaced by a power converter. These power converters allow for adjustments of the system power factor. The main advantage of this system is that the converters required are rated approximately 30% of the generators' rated power. This makes the converters cheaper than other full-power capacity converters [13].

The DFIG is widely utilized in the industry as it is superior to the fixed speed WECS as it has improved efficiency in power conversion, high speed ranges for the generator, and enhanced dynamic performance.

Figure 3-7 illustrates a doubly fed induction generator (DFIG) wind energy system.

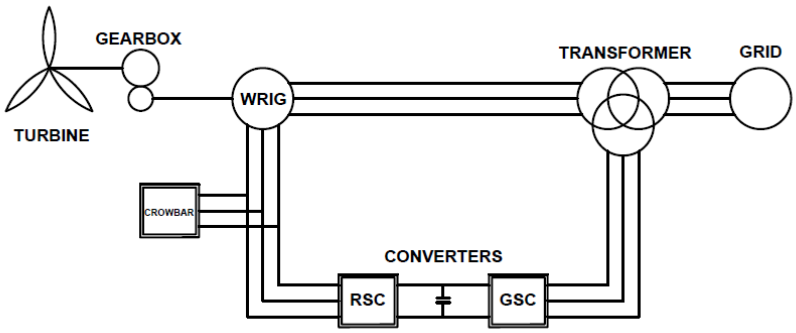

Figure 3- 7: Doubly Fed Induction Generator Wind Turbine

3.4.5 Variable-Speed Systems with Full-Capacity Power Converters

Full capacity power converters can enhance the performance of wind energy systems. A generator using a full capacity converter system to connect to the grid is shown in Figure 3-8 [87]. SCIG's, WRSG's, and PMSG's can all be used with full capacity power converters with a power rating of up to several megawatts. Generally, the generator and converter will both require the same power rating. The power converter allows the generator to be completely decoupled from the grid and operate at its full speed range. The converter also allows reactive power compensation and smooth grid connection.

The cost and complexity of the system is the main drawback. If a low-speed synchronous generator is used a gearbox is not required. Although this may improve the system efficiency and the initial cost, the low-speed generator is substantially larger which may lead to an increase in generator and installation costs.

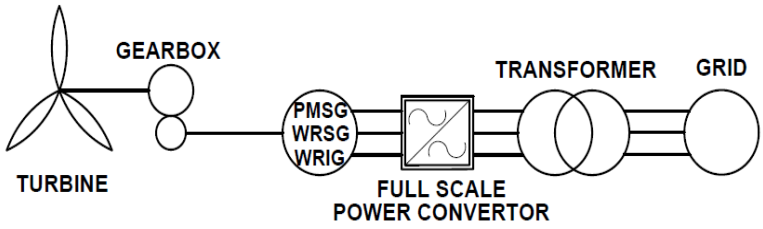

Figure 3- 8: Full-Scale Power Converter System

3.5 Previous Case Studies for HVDC Collection Grids

Offshore wind resources are only now becoming widely used, with factors such as data access and transmission costs being its main stumbling block. Nowadays, research data is widely available to allow the production of electrical energy using wind power [35].

Kirby and Xu studied HVDC transmission for large offshore wind farms. With an increase in demand for wind energy, limited space, and lower wind speeds onshore, wind farms are being forced to offshore locations. Therefore the generated power is required to be transmitted over long distances to shore for it to be distributed to customers. Lower power and shorter distances allow for HVAC transmission to be utilized whilst high power and long-distance enforces the use of HVDC transmission. The paper established that an HVDC system would be a good solution when the offshore distance is greater than 100 km and the wind farm size is greater than 350 MW.

Ryndzionek and Sienkiewicz studied the development of the HVDC link used for an onshore grid to offshore wind farm connection. The paper presented the development of the HVDC link for grid connection. The trend has shown that the offshore energy market promoted innovations of HVDC technology over the years. It is believed that a DC super grid can be created with the continuous development of offshore wind power plants. The paper showed the technical progress over the past 10 years to enable deeper waters and longer transmission lengths to the onshore grid. To make the HVDC technology economically viable, cheaper transistor modules e.g. (SiC) have been used to reduce the cost of power electronic terminals. This new advancement shifts the balance in favour of DC transmission.

Ackermann, Negra, and Todorovic studied losses in HVAC and HVDC transmission large offshore wind farms. The paper compared losses for the different transmission topologies for offshore wind farms. Wind farms with various power ratings and distances were compared. The evaluation of the different systems proved that HVAC solutions comprised of the lowest losses for short distances, while HVDC LCC proved efficient over longer distances. Factors such as system reliability, number of cables, life cycle, and cost influence the final choice of the design. Therefore further investigations are required to determine the best transmission system design.

Torres, Garces, and Diaz investigated HVDC transmission for offshore wind farms. Offshore wind farms have gained popularity due to their limited visual impact from shore and the constant wind velocity found offshore. The paper presents different types of configurations for offshore wind farm grid integration. Although HVAC is commonly chosen for short distances, offshore wind farms are at longer distances than HVAC can handle. HVDC has become a more attractive option for distances further away from shore. Between HVDC-LCC and HVDC-VSC, HVDC-LCC has the highest efficiency and is the most cost-effective solution for HVDC systems.

3.6 HVDC Design model

HVDC collection systems link DC output turbines with a transmission link to the onshore grid. The DC grid consists of several series or parallel clusters [12]-[30]. Due to the large difference in the turbine output power and the total grid power, several DC/DC converters are required for the voltage steps [30]. DC collections systems that can be utilized for offshore wind farms are examined below.

3.6.1 One-stage collection system

Figure 3-9 shows a simple block diagram of a one-stage concept collection system. In this concept, the generator AC output voltage is converted to a DC voltage and is directly connected to the offshore collection grid. The DC voltage is then stepped up by a DC-DC converter for transmission to the onshore grid.

As this system has a lower number of converters, losses are reduced and less maintenance is required. As the generators' output voltage affects collection grids efficiency, the wind turbines are designed based on high voltage generation and converters, [88].

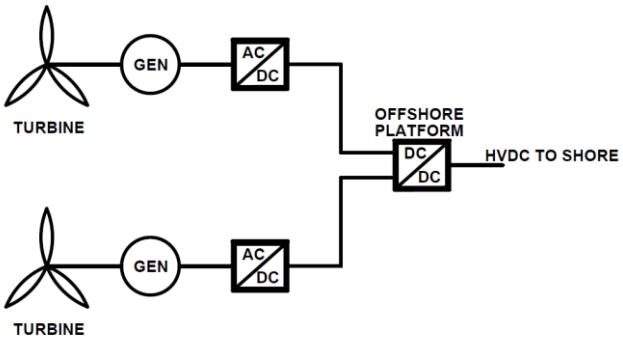

Figure 3- 9: One-Stage Concept Connection

3.6.2 Dispersed two-stage collection system

Figure 3-10 shows that this collection system consists of two voltage converters to the offshore platform. There is also a DC/DC converter on the output of the turbine to allow for the output voltage to be stepped to the required level. This results in a lower current and in turn lower losses.

The main advantage of this system is the output voltage of generators remains undisturbed by the losses experienced in the collection grid. This allows the use of low voltage generators and power converters [88].

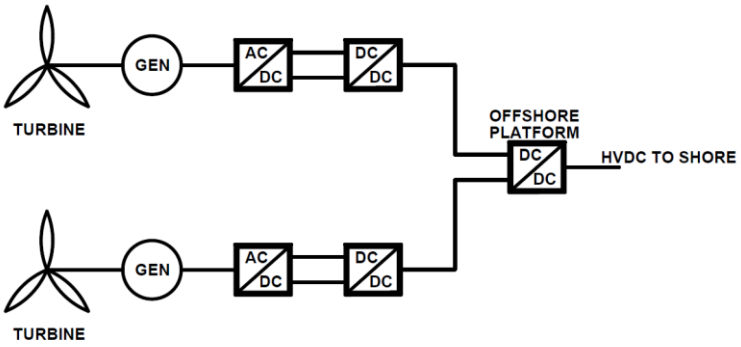

Figure 3- 10: General Connection Of Dispersed Two-Stage Concept

3.6.3 Series two-stage collection system

This system allows for multiple turbines to be connected in series and increases the output voltage level of the wind farm. The number of wind turbines required for the system depends on the voltage level required. The required number of converters is reduced by this series connection of the wind turbines.

A serious drawback of this system is that for the wind farm to transfer power, each of the turbines is required to operate. This means that the series arrangement that is shown in Figure 3-11, only generates energy once each of the wind turbines is operating. Based on the layout of the turbines not being uniform and the wake effect experienced, high voltage variations are experienced between the turbines [88]. Future more, if any turbine fails, a lower voltage must be accepted or the remaining turbines must compensate for the loss.

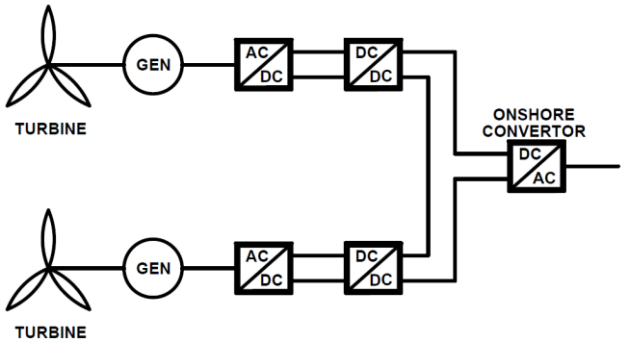

Figure 3- 11: Series Two-Stage Concept

3.6.4 Centralized two-stage collection system

An illustration of a centralized two-stage system is shown in Figure 3-12. This arrangement is similar to that of the single-stage as wind turbines with single AC/DC converters are connected to DC/DC converters to step-up voltages. Higher cables efficiency and lower cable costs are experienced with this system. The system also requires less power electronic converters which reduces travel and maintenance costs. A drawback of the system, however, is the extra offshore platform required for the DC/DC power converter.

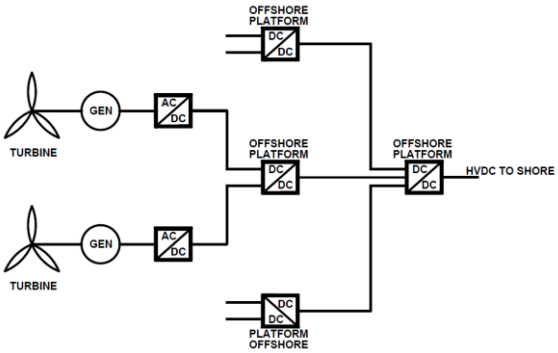

Figure 3- 12: Centralized Two-Stage Concept

A comparison of each HVDC collector system is shown in Table 3-1, which shows the advantages and disadvantages of each HVDC collector system.

Table 3- 1: Comparison of HVDC collection systems

HVDC Collector	Advantage	Disadvantage
One stage	• Fewer power converters. • Lower maintenance, repair, and travel costs. • Lower weight.	• High power cable losses • High cable size.
Two-stage dispersed	• Higher voltage level. • Low conduction losses.	• High Investment cost. • Increased repair, maintenance, and travel cost.
Two-stage series	• Low conduction losses. • No platform offshore	• Difficult commissioning. • Voltage variations. • Higher Failure. • High insulation cost.
Two-stage centralized	• Low collector losses • Cable losses and cost is low • Fewer converters • Lower maintenance and repair costs	• Extra offshore platform

3.7 Typical topology of HVDC wind farm collection grid

3.7.1 Offshore Wind Farm Collector System

A wind farm collector system has the main purpose of collecting the power generated from each wind turbine and maximizing the total generated energy. There are many wind

farm collector system arrangements, either in operation or suggested as a theoretical design [24]. Different layouts can be used to employ these collection systems, based on the size of the wind farm and required reliability. Configurations for this are discussed below:

3.7.2 Radial Layout

Figure 3-13 shows a radial layout, which is straightforward and can be used for large wind power plants. Low cable costs, as well as the simple control systems, are the main advantages of this layout. However, a major drawback of the system is its low reliability. A cable or switchgear fault on the radial clusters hub end may block all turbines downstream from transmitting during the fault [89].

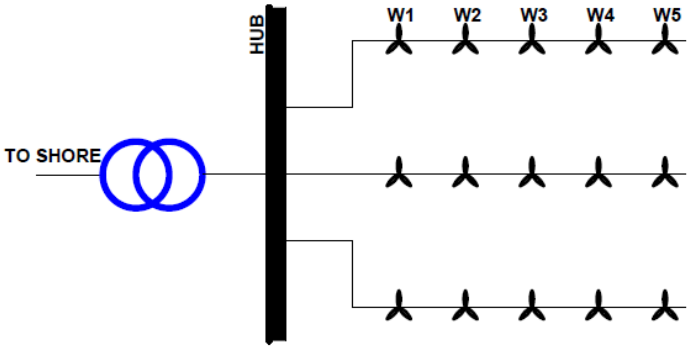

Figure 3- 13: Radial Network

3.7.3 Single-Return Layout

A single return layout is shown in Figure 3-14 and provides alternate paths of power flow during fault conditions. Although the reliability is higher than the radial layout, cable costs are for a specified number of wind turbines [28].

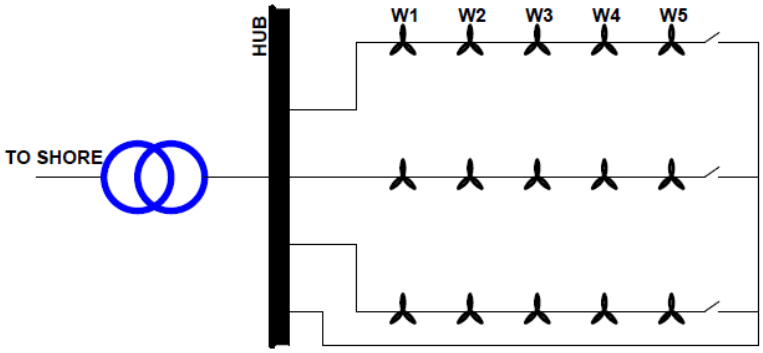

Figure 3- 14: Single Return Network

3.7.4 Ringed Layout

Figure 3-15 shows a single-sided ring layout. This system provides an alternate route for each line of turbines. Similar to the single-return layout, the reliability of the system is increased with an additional cost of cables. Figure 3-16 is a double-sided ring layout, which connects the last wind turbine of each series to the next. Figure 3-17 shows a multiple-ring layout that interconnects all the last turbines together. Although no redundant cables are required, high-rated cables are required to allow for the flow of power in cases of fault conditions [29]. Cable costs for various voltage ratings are the disadvantage along with the cost of additional offshore hubs. The additional costs require an in-depth consideration of the benefits versus the cost for the application [28].

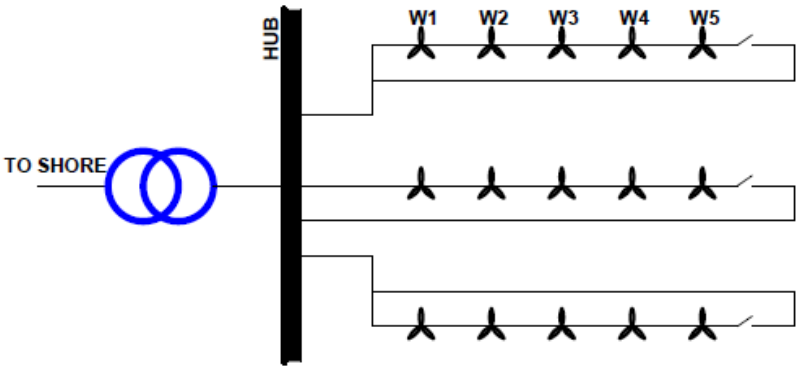

Figure 3- 15: Single-Sided Ring Network

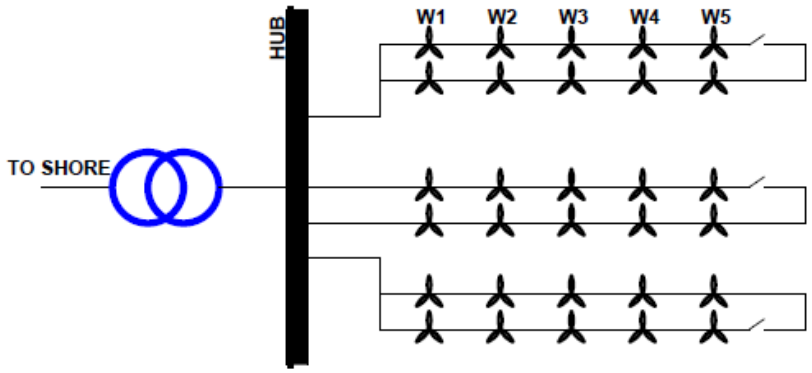

Figure 3- 16: Double-Sided Ring Network

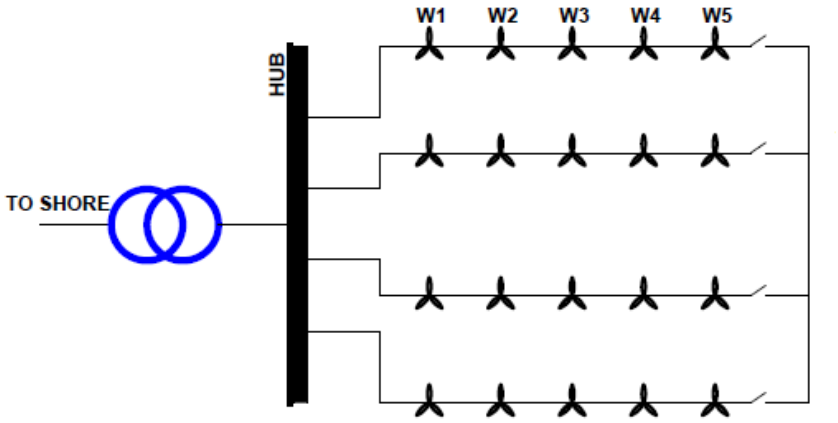

Figure 3- 17: Multiple Ring Network

3.7.5 Star Layout

The star design Figure 3-18 reduces cable ratings and allows high reliability of the wind farm. Better voltage regulation is expected between the wind turbines, however, additional cable expenses are expected. The cable costs experienced are insignificant especially when compared to the cost implications of more complex switchgear [28].

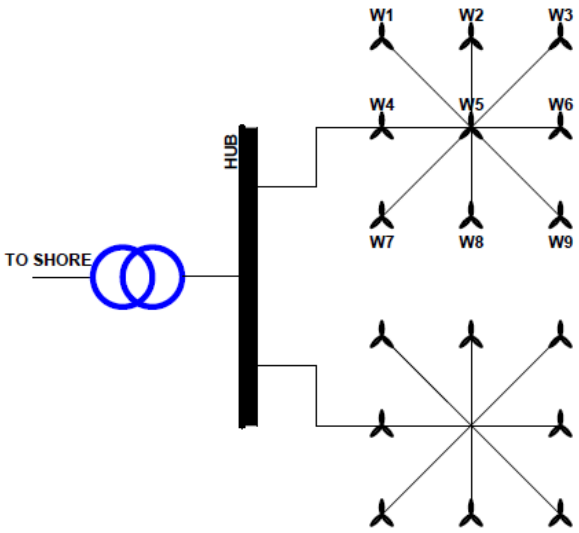

Figure 3- 18: Star Network

3.7.6 Network with Multi-Hub Ring Layout

A multi-hub ring is shown in Figure 3-19 and provides low losses using high voltage collection. Higher reliability is provided by the use of several hubs, however, expensive HV cables are required.

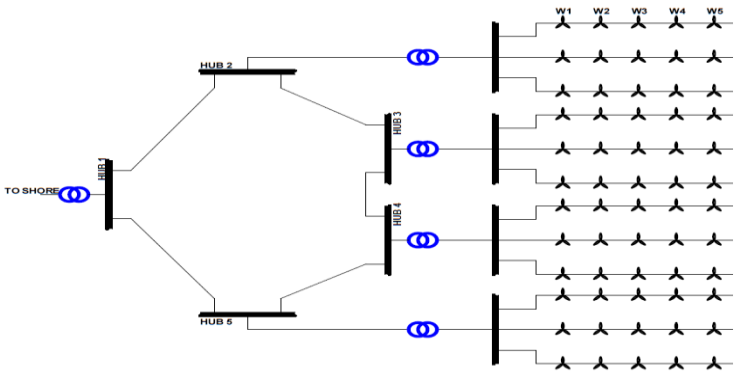

Figure 3- 19: Network With Multi-Hub Ring

3.8 Delivery System Topologies

Various delivery system arrangements exist, the main systems are:

- Radial connection
- Split connection
- Backbones
- Grids

3.8.1 Radial Connections

A single line to shore is known as a radial connection. Individual direct connections from the wind farm or a central hub can be utilized where many wind farms feed into a single line to shore.

3.8.2 Split Connections

A split connection is a connection of an individual wind farm or a hub of multiple wind farms to multiple onshore connections. Power in AC systems will flow based on the electrical impedance of the network while in DC systems, the power flow is controlled by the converter stations.

3.8.3 Backbone

A backbone connection is the link of various offshore platforms. The output link at each platform forms the “ribs” of the system, while the offshore connections form the “spine.” Backbone topology increases reliability and is likely to be used where multiple radial systems are built along a section of shoreline. It will require careful coordination of the technologies used at each wind farm to ensure the capability to make the interconnection.

3.8.4 Offshore Grid

An offshore grid connection involves the interconnection of multiple offshore wind farms and provides multiple connections onshore. Although a backbone connection is considered as a form of an offshore grid, complex interconnections are required. The optimal connection at any given site or area will depend on various factors. Plans for further wind farms, distance to shore and the electricity demand are some of these factors. Hub connections will be more economically attractive for wind farms that are planned to be in close proximity and far from shore.

Offshore hubs are expected to alleviate the ecological impacts and societal objections to laying the higher number of cables as required for stand-alone wind farms. The use of offshore grids can benefit various regions. They can provide large-scale wind energy and avoids onshore transmission system bottlenecks. This connection will increase connections between regions and alleviate stress on onshore systems.

Although offshore grids could be developed using either AC or DC technology, long-distance cable connections are required as they are expected to cross multiple regions. HVDC systems then become the probable technology. More precisely, multi-terminal HVDC systems are necessary to realize an offshore grid. HVDC technologies could be used for these grids, and although no multi-terminal systems have been built using the technologies best suited for offshore grids, manufacturers are confident that such systems can be built within the next few years.

At least two different types of HVDC grids can be identified:

• Regional HVDC grid—this is a multi-terminal HVDC system that consists of one protection zone for DC ground faults. It is fully possible to build a regional HVDC grid today using proven technology. HVDC breakers are not needed for regional HVDC grids. A fault on the DC side would be cleared using the AC breakers on the AC side to trip the whole HVDC system, and the portions of the DC system that are free from faults could then be rapidly restarted. The temporary loss of the entire regional HVDC system would have a limited impact on the overall power system. This type of HVDC grid is normally in radial or star network configurations, and the power rating of the grid is limited.

• Interregional HVDC grids—this is a multi-terminal HVDC system that needs multiple protection zones for DC ground faults. Interregional HVDC grids will require the use of HVDC breakers, fast protection and control schemes, and HV DC-DC converters for connecting different regional systems. Although some manufacturers may be able to provide HVDC breakers today, continuing development is needed along with proper standards among the manufacturers to support the technology developments and encourage the confidence to invest in multi-terminal HVDC systems. Regulatory issues, such as how to coordinate the operation of the new grids among different regions, also need to be solved.

3.9 Wind farm components

3.9.1 HVAC

3.9.1.1 Wind probability

Based on literature by Holttinne and Norgaard in [90], the best way to model the output of a wind farm is to use an aggregated model. Further analyses of losses and reliability can be determined using this methodology. These parameters will be the input data for the simulation models.

Wind speed is a continuous random variable, it differs based on time and season. Using the probability distribution function, it can be modelled using the common Weibull distribution. A forecast of the expected wind speed can be determined using the equation shown in Equation (3-1).

$$f(w_s) = \frac{k}{c}\left(\frac{w_s}{c}\right)^{k-1} e^{-\left(\frac{w_s}{c}\right)^k} \tag{3-1}$$

Where f (w_s) is the probability density for wind speed, w_s is the wind speed, c is the Weibull scale factor, and K is the empirical Weibull shape factor. Figure 3-20 shows different average wind speeds for an area.

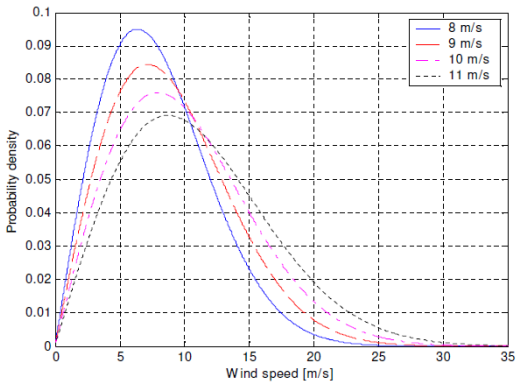

Figure 3- 20: Wind Probability

3.9.1.2 Wind turbine

Equation (3-2) allows the modelling of a wind turbine during steady-state. Simulation of the wind turbine can be accomplished by determining the torque exerted on the mechanical shaft.

$$T_{turbine} = \frac{P_M}{\Omega_t} \tag{3-2}$$

Where $T_{turbine}$ is the turbines' produced torque, P_M is the output power of the turbine and Ω_t is the mechanical speed of the turbine. The power output of the wind turbine is represented in Equation (3-3).

$$P_M = \frac{1}{2}\rho A V_w^3 C_p \tag{3-3}$$

Where A is the swept area, ρ is the density of the air, v is the speed of the wind and Cp is the power coefficient of the turbine, which depends on the tip speed ratio, λ and pitch angle, β. The tip speed ratio (λ) can be represented by Equation (3-4).

$$\lambda = \frac{\omega_r R}{V} \tag{3-4}$$

In which ω_r is the angular velocity of the rotor, $\omega_r = \frac{2\pi n}{60}$, and n is the revs/min.

3.9.1.3 Generator

The DFIG is commonly used for wind power conversion. The stator is directly connected to the load, while a power converter is used to connect the rotor to the load. A two-level IGBT VSC is normally used and in a back-to-back configuration. The operation of DFIG can easily be explained in two axes, d-q coordinate frame. The conversion from ABC to dq is done using the park transformation in Equation (3-5).

$$\begin{pmatrix} d \\ q \\ 0 \end{pmatrix} = \frac{2}{3}\begin{bmatrix} \cos\theta & \cos(\theta - \frac{2\pi}{3}) & \cos(\theta + \frac{2\pi}{3}) \\ -\sin\theta & -\sin(\theta - \frac{2\pi}{3}) & -\sin(\theta + \frac{2\pi}{3}) \\ \frac{1}{2} & \frac{1}{2} & \frac{1}{2} \end{bmatrix}\begin{bmatrix} A \\ B \\ C \end{bmatrix} \tag{3-5}$$

$$V_{sd} = R_s I_{sd} + \frac{d\varphi_{sd}}{dt} - \omega_s \varphi_{sq} \tag{3-6}$$

$$V_{sq} = R_s I_{sq} + \frac{d\varphi_{sq}}{dt} - \omega_s \varphi_{sd} \tag{3-7}$$

$$V_{rd} = R_r I_{rd} + \frac{d\varphi_{rd}}{dt} - \omega_r \varphi_{rq} \tag{3-8}$$

$$V_{rq} = R_r I_{rq} + \frac{d\varphi_{rq}}{dt} - \omega_r \varphi_{rq} \tag{3-9}$$

$$\varphi_{sd} = L_s I_{sd} + L_m I_{rd} \tag{3-10}$$

$$\varphi_{sq} = L_s I_{sq} + L_m I_{rq} \tag{3-11}$$

$$\varphi_{rd} = L_r I_{rd} + L_m I_{sd} \tag{3-12}$$

$$\varphi_{rq} = L_r I_{rq} + L_m I_{sq} \tag{3-13}$$

$$L_s = L_{is} + L_m \tag{3-14}$$

$$L_r = L_{ir} + L_m \tag{3-15}$$

Where V_{sd}, V_{sq}, V_{rd}, V_{rd} are the stator and rotor voltages in the d and q axis respectively. R_s, R_r are the stator and rotor resistances respectively, L_s, L_r are the stator and rotor inductances respectively; L_{is}, L_{ir} are the stator and rotor self-inductance respectively, L_m is the mutual inductance; I_{sd}, I_{sq} are the stator currents in the d and q axis respectively; I_{rd}, I_{rq} are the rotor currents in the d and q axis respectively; φ_{sd}, φ_{sq} are the stator fluxes in the d and q axis respectively, and φ_{rd}, φ_{rq} are the rotor fluxes in the d and q axis respectively.

The torque, active and reactive power generated by the generator can be obtained using Equations (3-16), (3-17), and (3-18):

$$T_e = 1.5 N_p \frac{L_m}{L_s}\left(I_{sq}\varphi_{sd} - I_{sd}\varphi_{sq}\right) \tag{3-16}$$

Where N_p is the number of poles of the generator.

$$P_s = \frac{3}{2}\left(V_{sq} I_{sq} + V_{sd} I_{sd}\right) \tag{3-17}$$

$$Q_s = \frac{3}{2}\left(V_{sq} I_{sd} + V_{sd} I_{sq}\right) \tag{3-18}$$

3.9.1.4 Wind turbine transformer

Each wind turbine is equipped with a step-up transformer that is rated 0.69/33 kV, 5 MVA. This transformer allows transmission within the local grid to the main transformers for transmission to the onshore substation.

3.9.1.5 Converters and control

Figure 3-21 shows the DFIG is connected with a back-to-back converter and comprises of the rectifier or rotor-side converter (RSC) and inverter or grid-side converter (GSC). The RSC is used to control the output power delivered by the stator in order to achieve the required speed characteristic. While the GSC is used to control the power delivered to the grid by regulating the voltage at the DC bus [91].

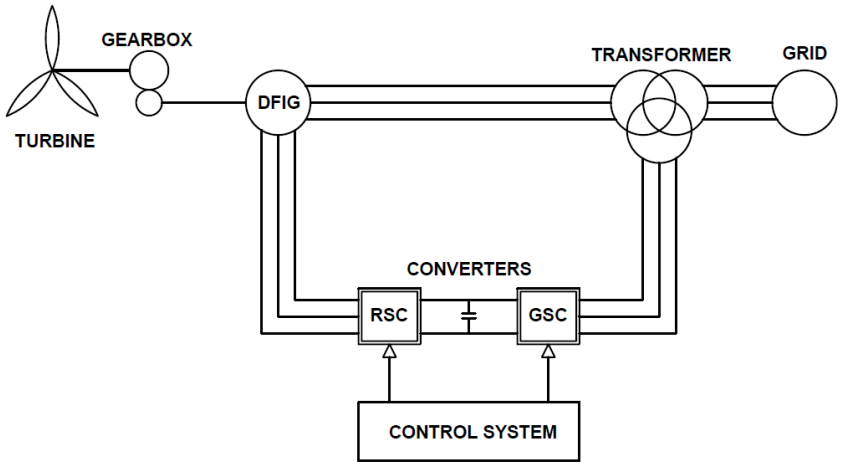

Figure 3- 21: DFIG Schematic

3.9.1.6 Rotor side control (RSC)

The active and reactive powers produced by the stator are controlled by the RSC. The control block diagram is composed of two controller stages.

The first stage determines the direct and quadrature components of the rotor current references by using Equations (3-19) and (3-20). L_s and L_m are the stator self-inductance and inductance fluctuation respectively. P_s and Q_s are the stators' active and reactive power.

$$i_{qr_{ref}} = \frac{2}{3}\left(\frac{L_s}{L_m}\right)\frac{P_s}{V_{qs}} \tag{3-19}$$

$$i_{dr_{ref}} = \frac{\varphi_{ds}}{L_m} - \frac{\left(\frac{2}{3}\right)\frac{L_s}{L_m}Q_s}{V_{qs}} \tag{3-20}$$

The second stage is devoted to the rotor current controller. The rotor currents of the DFIG are sensed and transformed to the d-q reference frame by using Park transformation. The q-axis component of the rotor current controls the active power while the d-axis component controls the reactive power.

$$V_{dr} = R_r.i_{dr} + L.\left(\frac{d\left(i_{dr}\right)}{dt}\right) - s.L.i_{qr} \tag{3-21}$$

$$V_{qr} = R_r.i_{qr} + L.\left(\frac{d\left(i_{qr}\right)}{dt}\right) + s.L.i_{dr} + s\left(\frac{L_m V_s}{\omega_s L_s}\right) \tag{3-22}$$

$$L = L_r - \frac{L_m^2}{L_s} \tag{3-23}$$

$$s = 1 - \frac{\omega_r}{\omega_s} \tag{3-24}$$

3.9.1.7 Grid side control (GSC)

Voltage regulation of the DC-link and power factor is controlled by the grid side converter. A vector control approach is used with a reference frame oriented along the grid voltage vector, enabling independent control of the DC link voltage and reactive power flowing between the grid and the GSC.

In the first stage, the DC reference voltage is compared with the sensed DC voltage across the DC link capacitor V_{dc}.

$$i_{gd\_ref} = \frac{Q_{g\_ref}}{V_{ga}} \tag{3-25}$$

The direct axis current is used to regulate the GSC reactive power and the quadrature axis current is used to regulate the DC bus voltage. This method also gives the possibility to control independently the active and reactive power between the GSC and electrical grid.

$$V_{gq\_ref} = V_{gq} + \omega_s L_g i_{gd} + V_{gq} \tag{3-26}$$

$$V_{gd\_ref} = V_{gd} + \omega_s L_g i_{gq} \tag{3-27}$$

3.9.2 HVDC

For DC collection grids, all of the wind farm components are identical to the system model for the AC grid in the previous chapter. The difference between the systems will be the converters used for AC/DC and DC/AC conversion as well as the transmission line.

3.9.2.1 Turbine DC converter

Figure 3-22 shows the DFIG generator output connected to a 33 kV AC/DC converter. The produced AC voltage is converted to DC and then utilized.

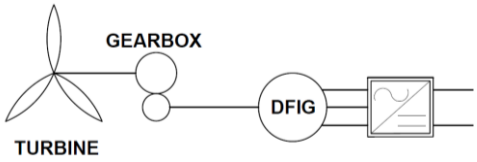

Figure 3- 22: Turbine with DFIG and AC/DC converter

3.9.2.2 DC/DC boost converter

The boost or the step-up converter is common for moderate input/output voltage ratios. Figure 3-23 shows a schematic of the boost converter, which contains a few very simple components. The converter can only be used in conditions where the input voltage V_{in} is lower than the output voltage V_{out}.

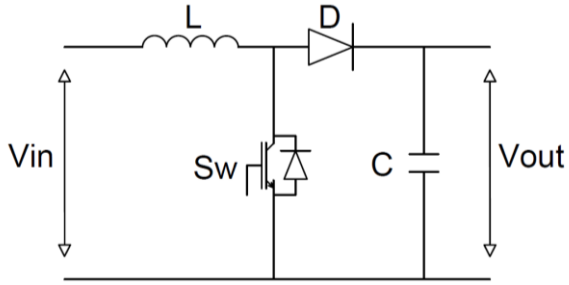

Figure 3- 23: Boost converter schematic

The boost converter stores and releases energy based on the cycle. While the switch Sw is on, energy is stored in the inductor L, and energy is released to the load while the switch is off. The voltage output Vout can be regulated by varying stored energy.

The current in the inductor increases linearly to the voltage while the switch is active and the capacitor C energy to the load. Therefore, the capacitor voltage is decreased. During the off state, the load is supplied via the diode D. Equation 5-28 can be used to determine the output voltage if the diode and transistor voltage drop is neglected.

$$V_{out} = \frac{V_{in}}{1 - D} \tag{3-28}$$

Where D is the duty cycle.

3.9.2.3 HVDC transmission line

A submarine HVDC cable consists of various complex layers. Based on the project specification the cable may be copper or aluminium. The conductor and the metallic screen are protected by an insulation layer. XLPE cables are generally used in HVDC-VSC schemes as it is cost-effective and robust [3]. For this study, the wind farm output is transferred to the AC grid through an HVDC cable. A 150 kV DC cable is used, which is 120 km long. A lumped parameter model cable's resistance, capacitance, and inductance, together typically form one or more PI sections. The study uses 2 sections of 60 km each.

3.9.2.4 DC/AC converter

The output of the HVDC transmission line is converted back to AC by the onshore DC/AC VSC converter. Figure 3-24 shows a VSC system converter station schematic. The VSC unit is the most vital as it allows DC/AC conversion. Due to the developments in IGBT technology, the converter can reach high levels of power conversion. The converter switching frequency determines the harmonics produced, filters required, power losses, and the inefficiency of the system. Therefore great care has to be taken when the switching frequency is determined.

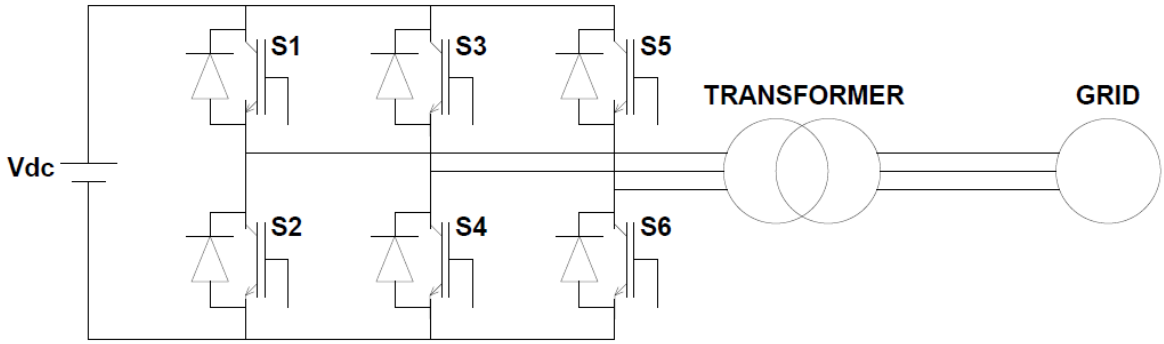

Figure 3- 24: DC/AC converter schematic

To allow for AC grid connection, the voltage is stepped down by the transformer. The interface transformer provides reactance between the AC and VSC system and prevents zero frequency currents from flowing between the AC system and the converter.

3.10 System description

3.10.1 HVAC

A traditional offshore wind farm consists of wind turbines, generators, converters, transformers, transmission lines, and grid connections. The wind farm discussed as seen in Figure 3-25 consists of 8 wind turbines rated at 5 MW each. The wind farm is connected to a local AC hub, which is then connected via a transformer to the transmission cables. The transmission length is determined by the offshore and onshore distances to the grid.

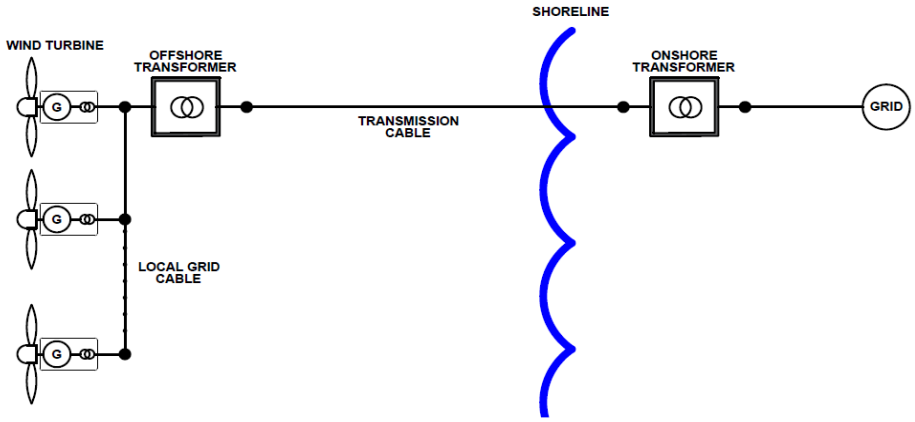

Figure 3- 25: HVAC Wind farm Schematic

For this system, an output voltage of 33 kV AC is seen for each WECU and is connected to the local AC grid. Figure 3-26 shows the main transformer, 33/150 kV AC, that connects the wind farm from the collecting point to the PCC.

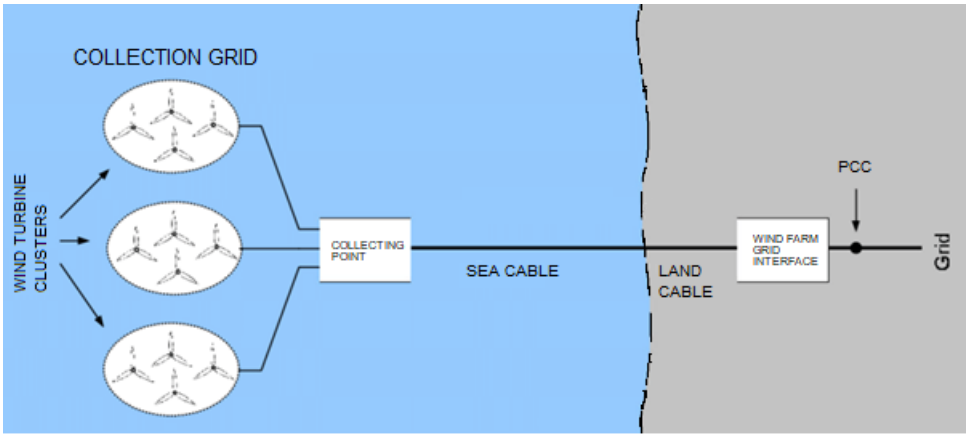

Figure 3- 26: HVAC Wind farm Layout

A 120 km, 150 kV cable connects the offshore transformer of the wind farm to the onshore distribution transformer for the AC grid. The wind farm grid consists of 33 kV AC cables and WECUs with 33 kV transformers connected to the generator. The offshore transformer is a 33/150 kV AC transformer. There is also a reactive power compensation, to allow for a unity power factor.

3.10.2 HVDC

There are various designs for an offshore wind farm with a DC collection grid. It can be designed similarly to that of an AC grid, where the turbines are connected to a mutual DC/DC converter as seen in Figure 3-27. DC grid wind farms differ from traditional wind farms as the AC cables are replaced with DC cables, and the transformers are replaced by DC/DC converters.

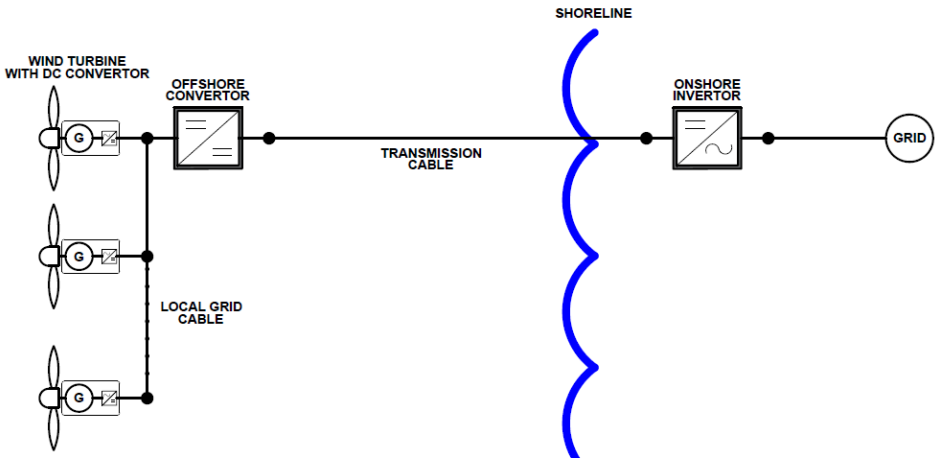

Figure 3- 27: Wind farm with DC collection grid layout

As in the traditional wind farm, several wind turbines are connected together. A DC/DC boost converter connects the wind farm to the transmission line and steps up the voltage to allow for transmission. The generator is connected to a full-power converter. To allow for power flow and voltage level control, a DC/DC converter connects the internal DC link to the DC collection grid. This results in two DC/DC converters between the turbine and the HVDC transmission system. The HVDC transmission level is increased by the second converter for transmission purposes as shown in Figure 3-28.

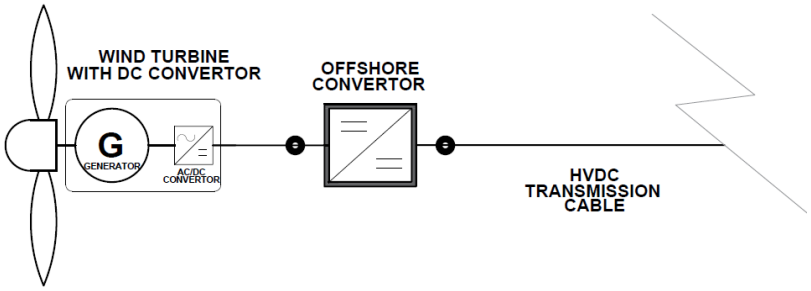

Figure 3- 28: HVDC Wind farm turbine and transmission line converters

An output voltage of 33 kV DC is seen by all eight turbines connected to the DC sub-grid. The subgrid is fed into a 33/150 kV DC/DC converter. A 120 km, 150 kV DC cable is used for transmission to the onshore grid via the DC/AC converter to allow for connection onshore. Each wind turbine has a 33 kV AC/DC converter and there is a total of 8 turbines.

3.11 Conclusion

There are many different types of topologies, configurations, and uses for HVAC and HVDC collection grids. HVDC grids are useful for long-distance transmission and allow an efficient cost-effective solution for long-distance transmission of wind energy. HVAC collection grids are useful for low-cost, short-distance systems.

CHAPTER 4: SYSTEM MODELLING AND SIMULATION

4.1 Introduction

The purpose of this chapter is to assess and compare HVAC and HVDC collection grids systems for offshore wind farms. Parameters such as component cost, system losses, and fault characteristics will be considered. The systems' power, the output power generated from the wind farm, will be kept constant in both, the AC and DC, systems. However, wind farms differ from power generation plants and do not allow an increase with an increase in consumption. This chapter defines the output power of the wind farm, the system modelling, and the simulated outputs under normal and fault conditions. These simulations will be used to determine which system has the best performance by looking at the system efficiency and fault currents. Both systems will be kept identical in terms of wind farm size, wind speeds, system power ratings, and transmission distances to provide a more accurate comparison. Matlab/Simulink software was used to analyse these systems. The best-performing system should be considered as an option in wind farm design as it could improve the efficiency and costs of future systems.

4.2 System modelling

4.2.1 HVAC

In this study, Matlab/Simulink software has been used to model the wind energy system. This was chosen as it is user-friendly and contains many of the required components in pre-set blocks to design the model of a wind system. The wind farm is rated at 40 MW with 8, 5 MW rated wind turbines. Each turbine uses a Doubly Fed Induction Generator (DFIG) rated at 690 V. A transmission distance of 120 km and a transmission voltage of 150 kV are used for both systems. All these parameters will be kept constant for both systems, to ensure more accurate results.

4.2.1.1 AC wind farm simulation model

Figure 4-1 shows a Matlab/Simulink model of the AC collection grid system with a DFIG turbine. The wind farm block was created as a mask to declutter the simulation and contains all the wind farm components, such as the wind turbine, drive train, DFIG, converters, and transformer.

As the Matlab software provides most of the components as in its library, only certain system components needed to be modelled. Modelling of the DFIG turbine and generator, the converters and their control, and the three-phase, three winding transformers were required.

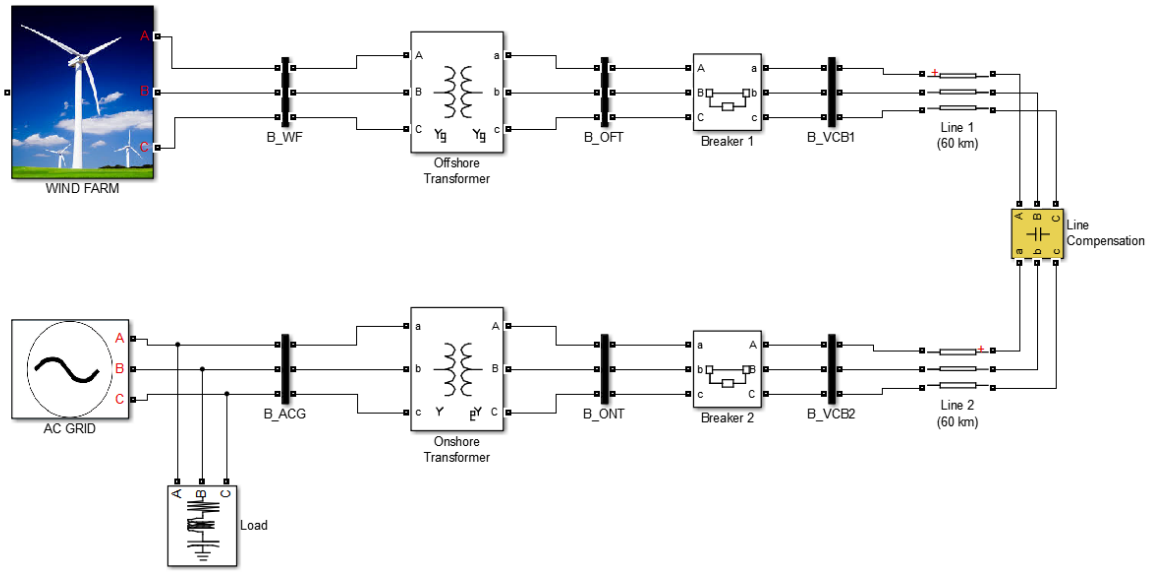

Figure 4- 1: HVAC Simulation Model

4.2.1.2 Wind speed and turbine

After calculations using Equation (3-1) and (3-2) and the graph in Figure 5-3, a wind speed of 10m/s was determined for the model. The maximum C_p was determined by Equation (3-3) modelled using a wind turbine characteristic curve $C_p(\lambda, \beta)$ from supplier data.

4.2.1.3 Drive train

The input to the drive train was entered from the output of the wind turbine. The low rpm of the wind turbine is then converted through the drive train gearbox by the use of Equation (4-1) to provide a torque output.

$$r_{gb} = \frac{(1-s).60.f_s}{P.n_M} \tag{4-1}$$

Where P is the number of pole pairs of the generator, s is the rated slip, n_M is the turbine rated rpm and f_s is the frequency of the stator.

The output torque is entered into the shaft of the generator, as were the mechanical elements of the turbine, such that the stiffness of the drive train is infinite, with the friction and inertia of the turbine being modelled using the single-mass model.

4.2.1.4 Wind turbine transformer

The transformer was modelled using the pre-set transformer block which consisted of three phases and two windings. Table 4-1 shows the parameters for the primary and secondary winding. A nonlinear characteristic curve was used for core saturation.

Table 4- 1: Wind Turbine Transformer Parameters

Parameters	**Primary**	**Secondary**
Vector group	D	Y
R (Ω)	0.002	0.42
L (Ω)	0.0327	13.41

4.2.1.5 Doubly fed induction generator (DFIG)

A Simulink predefined asynchronous machine block was used to model the generator. The machine could be defined as either a motor or generator, based on the polarity of the torque, T_m. T_m was entered into this block from the drive train, while the resistance and inductance for the rotor and stator were added as seen in Table 4-2.

Table 4- 2: DFIG Parameters

Parameters	**Value**
L-L Voltage (V)	690
Stator Resistance (p.u)	0.023
Stator Inductance (p.u)	0.18
Nominal Power (MVA)	5

4.2.1.6 Converters

The RSC and GSC converters, as shown in Figure 4-2, were modelled using the provided universal bridge blocks and IGBT in Simulink. The converter control was implemented using the Math operation blocks. The input parameters for the converter are shown in Table 4-3.

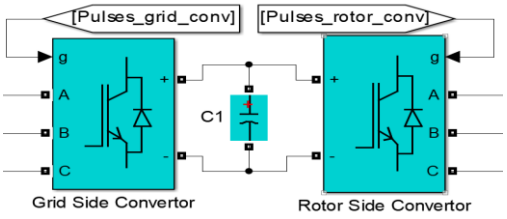

Figure 4- 2: Rotor and Grid Sid Converter

Table 4- 3: Converter Control Parameters

Parameters	**Value**
Grid Side PWM freq (Hz)	2700
Rotor Side PWM freq (Hz)	1620
Max Pitch Angle (Deg)	27
Max rate of change (Deg/s)	10

4.2.1.7 Offshore transformer

The transformer in an offshore AC substation steps up the wind farm output voltage to between 150 kV for further transmission. The stepping up of voltage is important to reduce the current flow through the cables, which results in a decrease in the cable requirements and a reduction in the power losses. The parameters of the transformer are shown in Table 4-4.

Table 4- 4: Offshore Transformer Parameters

Parameters	**Primary**	**Secondary**
Vector group	Y	Y
V (kV)	33	150
R (Ω)	0.002	0.002
L (Ω)	0.08	0.08
Power (MVa)	100	

4.2.1.8 Transmission line

For transmission to the onshore grid, a 120km AC cable is used. This cable is modelled using an XLPE cable. The parameters are shown in Table 4-5. The transmission cable is

isolated from the grid and wind farm by two circuit breakers which protect in the event of a fault.

Table 4- 5: HVAC Transmission Line Parameters

Parameters	Value
R (Ω/km)	0.015
L (H/km)	0.792e-3
C (F/km)	14.4e-9

4.2.1.9 AC Grid

To allow for the generated power to be useful, it has to be interconnected with the national grid. The wind farm is linked to the 400 V AC grid via the onshore transformer which steps down the voltage from 150 kV to a useable 400 V.

4.2.2 HVDC

For the DC wind farm, the same parameters and simulation system are used. The transmission length, system voltages, and currents are kept constant. This will allow accurate comparison between the two systems.

4.2.2.1 DC simulation model

Figure 4-3 shows the model of a wind farm utilizing a DC collection grid and DFIG turbines. Matlab/Simulink software was used to model the system and the same wind farm block was used in the HVAC simulation with the addition of a DC converter to each wind turbine output.

As the Matlab software provides most of the components as in its library, only certain system components needed to be modelled. Modelling of the DFIG wind turbine and generator, the converters, and their control were required.

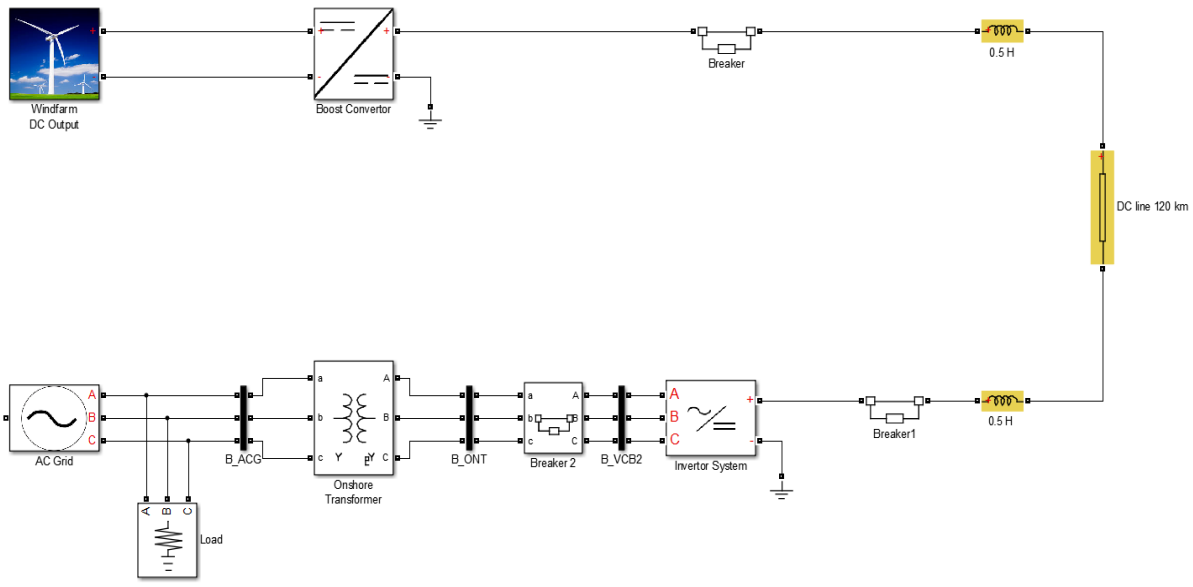

Figure 4- 3: HVDC Simulation Model

4.2.2.2 DC/DC boost converter

The DC boost converter is modelled as seen in Figure 4-4. The parameters used are shown in Table 4-6.

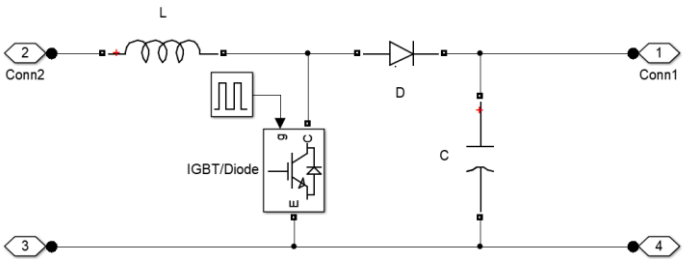

Figure 4- 4: DC-DC boost converter simulation

Table 4- 6: Boost Converter Parameters

Parameters	Value
Duty Cycle	0.78
L (mH)	5
C (F)	15

4.2.2.3 Transmission line

For transmission from the offshore wind farm to the onshore grid, a 120 km DC cable is used. This cable is modelled using an XLPE cable. The cable is rated at 150 kV. The

parameters are shown in Table 4-7. The transmission cable is isolated from the grid and wind farm by two circuit breakers which protect in the event of a fault.

Table 4- 7: HVDC Transmission line parameters

Parameters	Value
R (Ω/km)	0.015
L (H/km)	0.792e-3
C (F/km)	14.4e-9

4.3 Simulation

4.3.1 HVAC

4.3.1.1 Wind farm

A time step of 50 µs and a sample time of 1 s were chosen to run the simulation. The output voltage and current of the wind farm during normal operation are shown in figures 4-5 and 4-6 respectively. The output voltage and current show the wind farm producing a voltage of 33 kV with a current of 800 A. This can be used to calculate the wind farm power output.

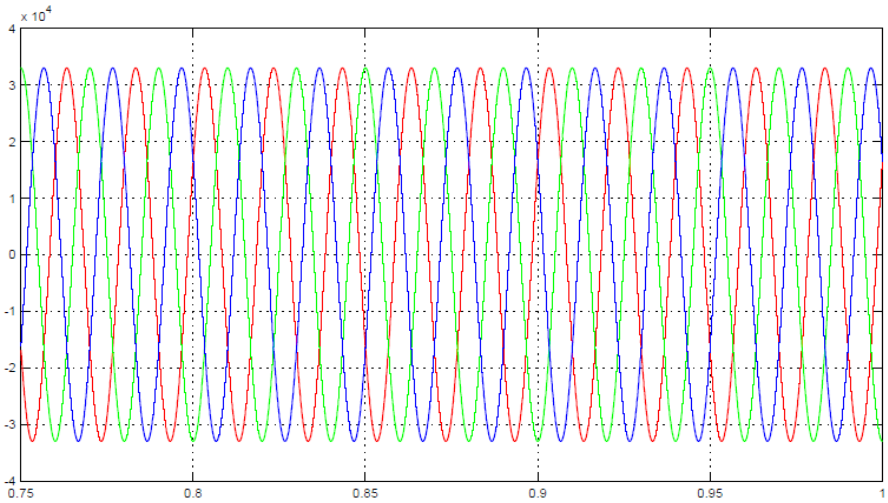

Figure 4- 5: HVAC Wind farm Output Voltage

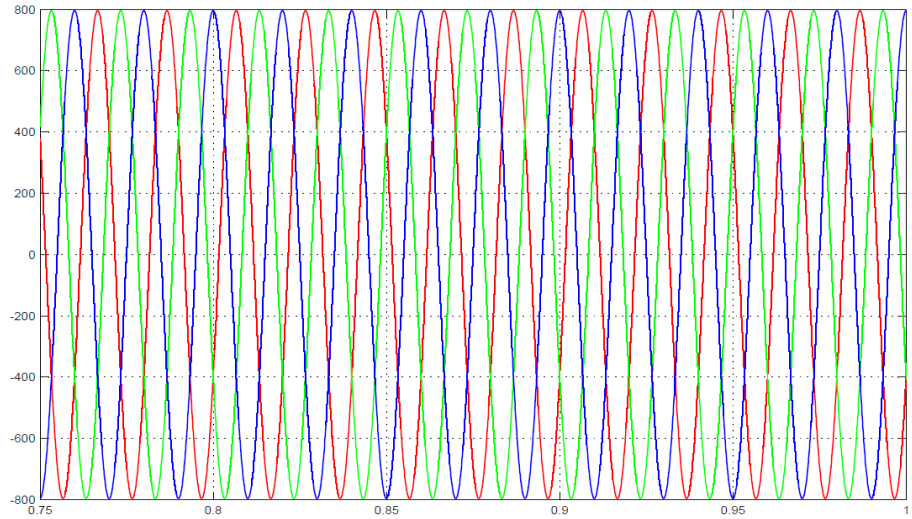

Figure 4- 6: HVAC Wind farm Output Current

4.3.1.2 Transformer

The output of the wind farm is connected to the offshore transformer. The output voltage of the transformer is shown in Figure 4-7. The output voltage is 150 kV and the transformer is used to step up the voltage from 33 kV to 150 kV.

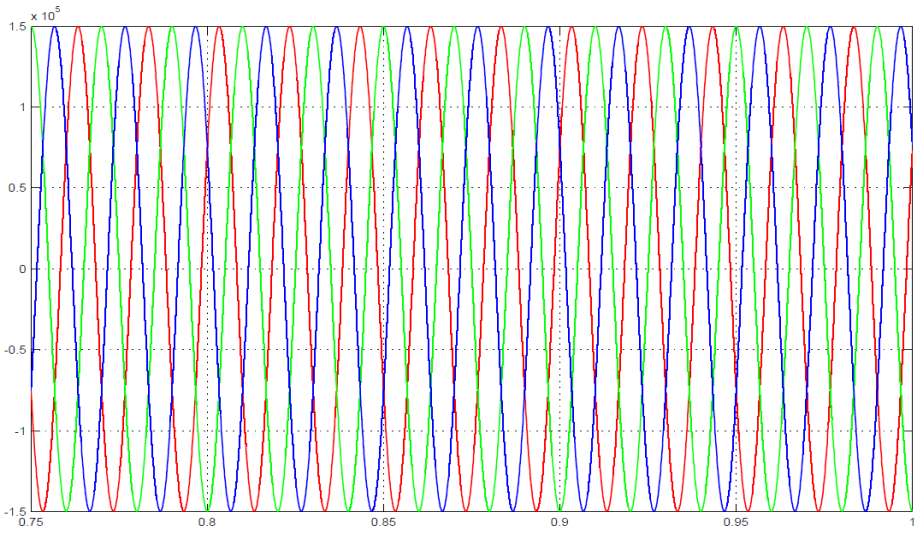

Figure 4- 7: Offshore Transformer Output Voltage

4.3.1.3 Line output

The transmission line receiving end voltage, 130 kV is shown in Figure 4-8. The voltage drop of the line is calculated by subtracting the transformer output and the line output voltages. The voltage drop of the line is 20 kV.

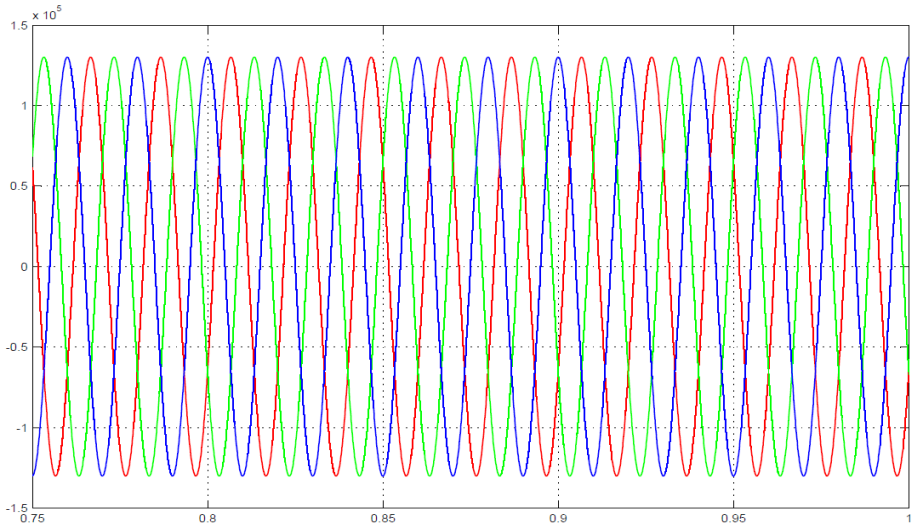

Figure 4- 8: HVAC Transmission Line Receiving End Voltage

4.3.1.4 Onshore transformer

The voltage and current of the onshore transformer output are shown in Figure 4-9 and Figure 4-10. The final output voltage and current are 400 V and 468 kA respectively. The output power of the system is 35.77 MW.

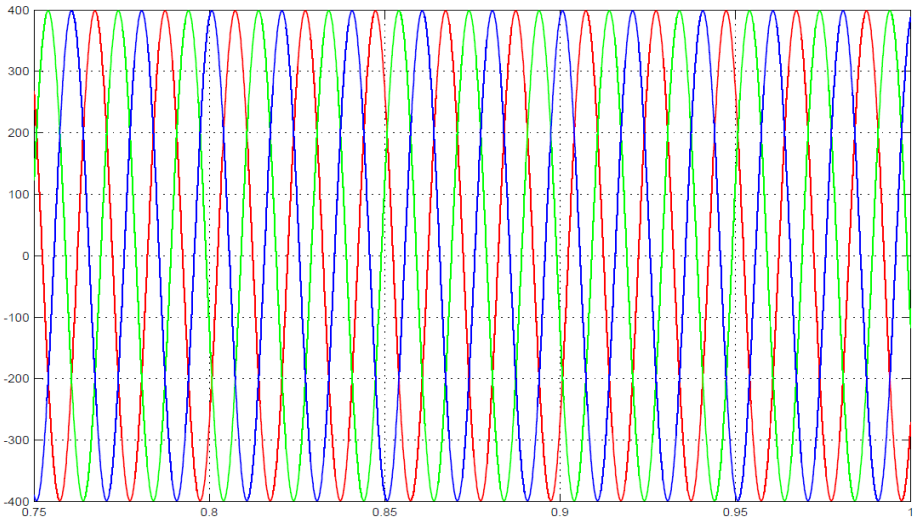

Figure 4- 9: HVAC Onshore Transformer Voltage

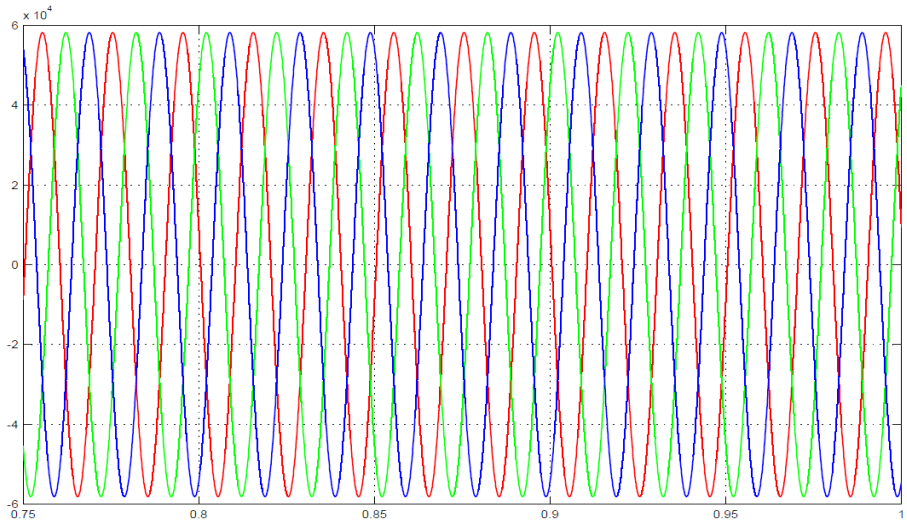

Figure 4- 10: HVAC Onshore Transformer Current

The efficiency of the system can be calculated by Equation (4-2) below. The output power of the system is 35.77 MW and the system input is 40 MW. The system efficiency is 89.425%.

$$\%\eta = \frac{P_{in}}{P_{out}}.100 \tag{4-2}$$

4.3.2 HVDC

4.3.2.1 Wind farm

The same step time and sample time were chosen as in the AC simulation. The output voltage and current of the wind farm during normal operation are shown in figures 4-11 and 4-12 respectively. The output voltage and current show the wind farm producing a voltage of 33 kV with a current of 1700 A. This can be used to calculate the wind farm power output.

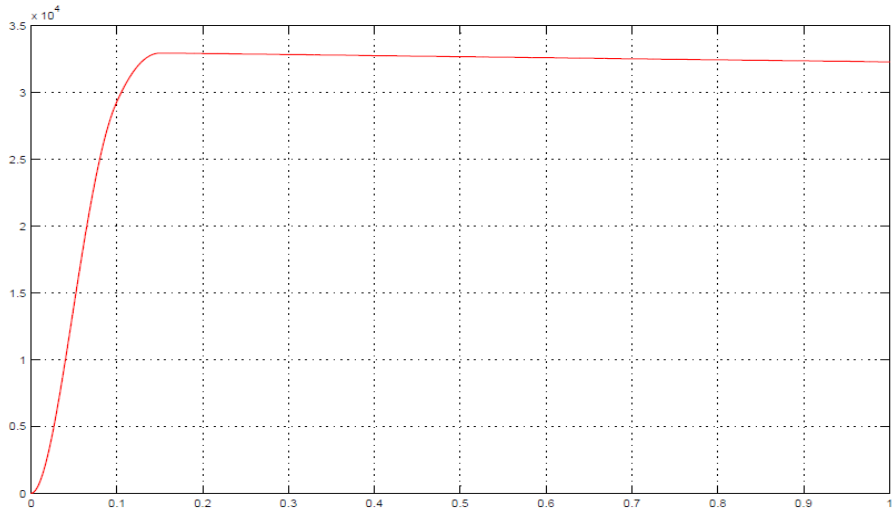

Figure 4- 11: HVDC Wind farm Output Voltage

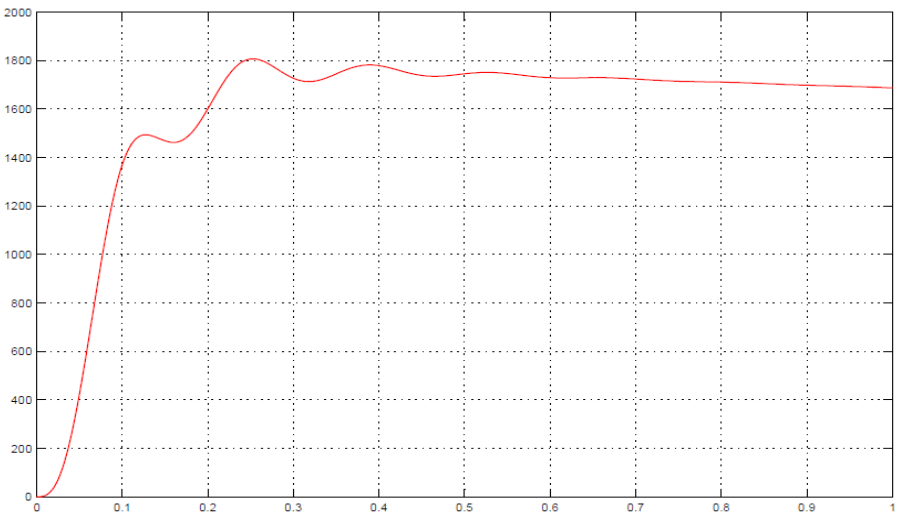

Figure 4- 12: HVDC Wind farm Output Current

4.3.2.2 DC-DC Boost converter

The output of the wind farm is connected to a boost converter. This will allow the voltage to be stepped up for transmission to the onshore converter. The output voltage of the boost converter is shown in Figure 4-13. The output voltage is 150kV as the boost converter is used to step up the voltage from 33kV to 150kV. The boost converter current output is shown in Figure 4-14. This voltage and current are the input to the HVDC transmission line.

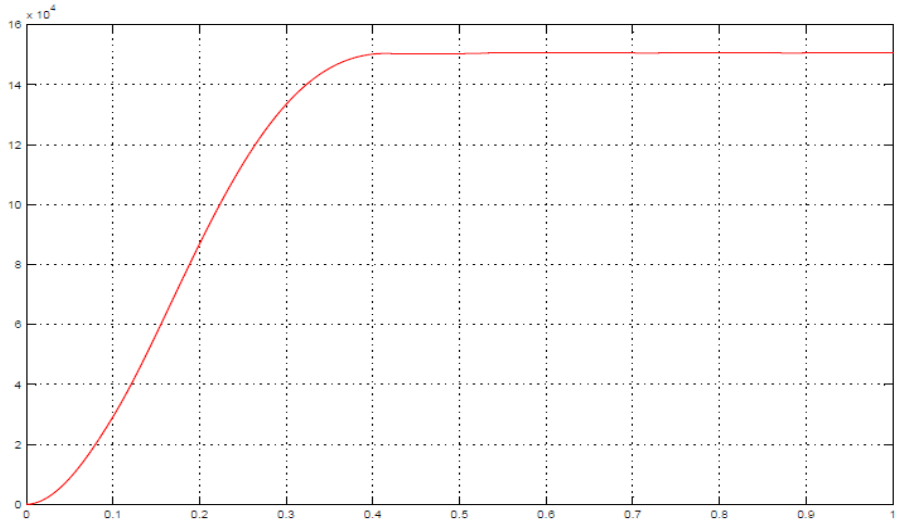

Figure 4- 13: Boost Converter Output Voltage

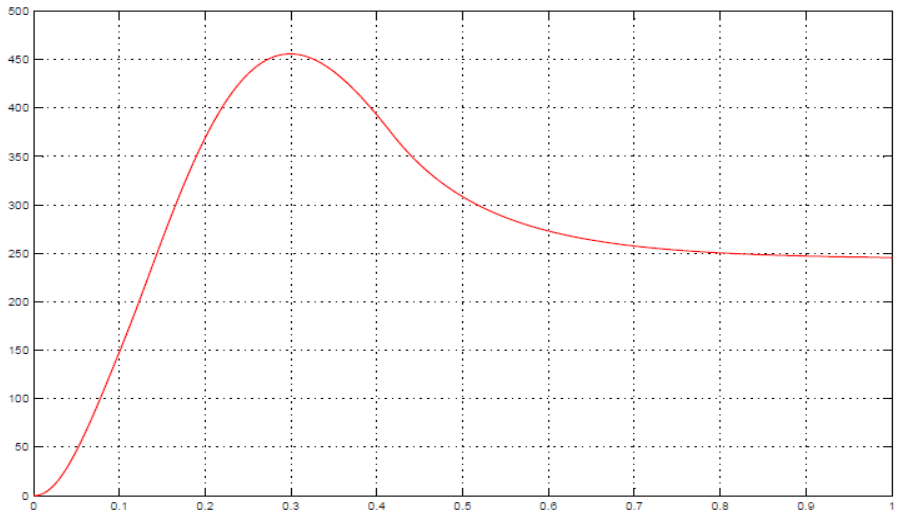

Figure 4- 14: Boost Converter Output Current

4.3.2.3 Line output parameters

The voltage at the receiving end of the transmission line is shown in Figure 4-15. The voltage drop of the line is calculated by subtracting the output of the boost converter and the line output voltages. The voltage at the output of the line is 138 kV, resulting in a voltage drop of the line is 12 kV.

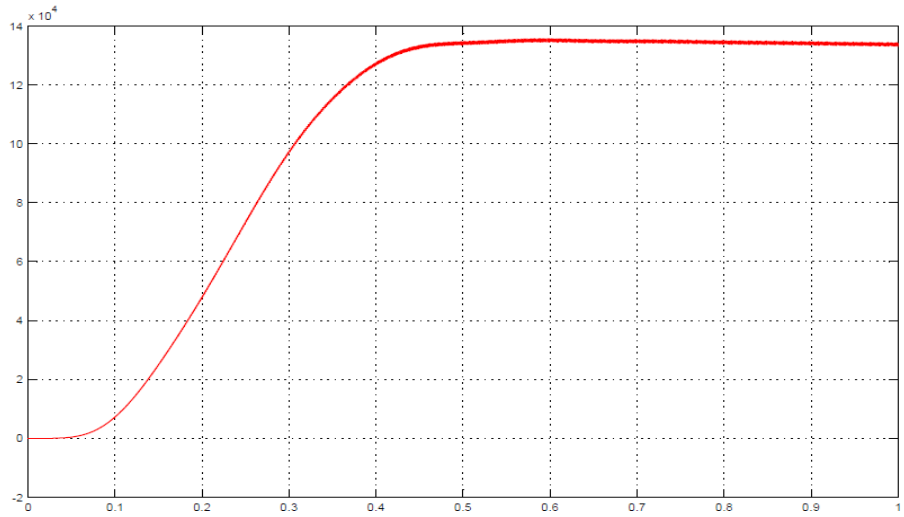

Figure 4- 15: HVDC Transmission Line Receiving End Voltage

4.3.2.4 Onshore inverter

The voltage of the inverter is shown in Figure 4-16. The voltage needs to be converted to AC to allow for use in the national grid. The inverted voltage is then fed to the onshore transformer and stepped down back to a useable voltage level.

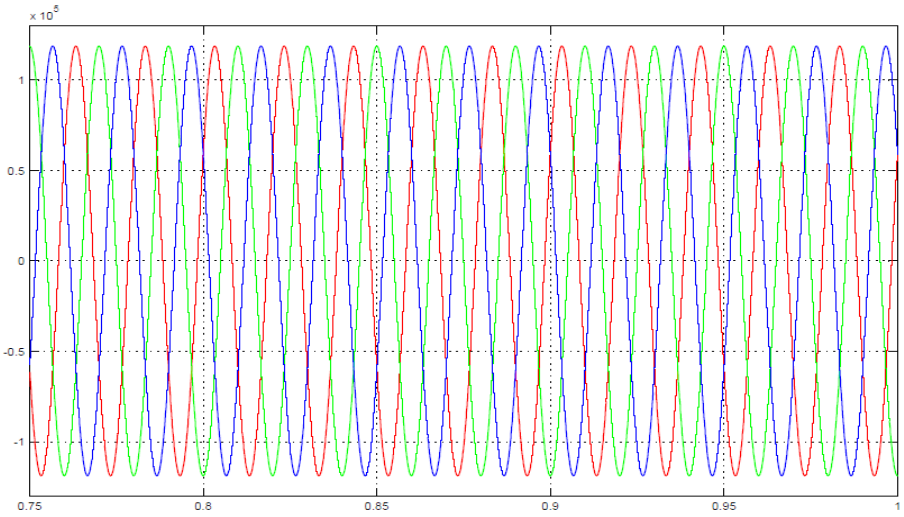

Figure 4- 16: Inverter Output Voltage

4.3.2.5 Onshore transformer

The voltage and current of the onshore transformer output are shown in Figure 4-17 and Figure 4-18. The final output voltage and current are 400V and 55.7 kA respectively. The output power of the system is 38.59 MW.

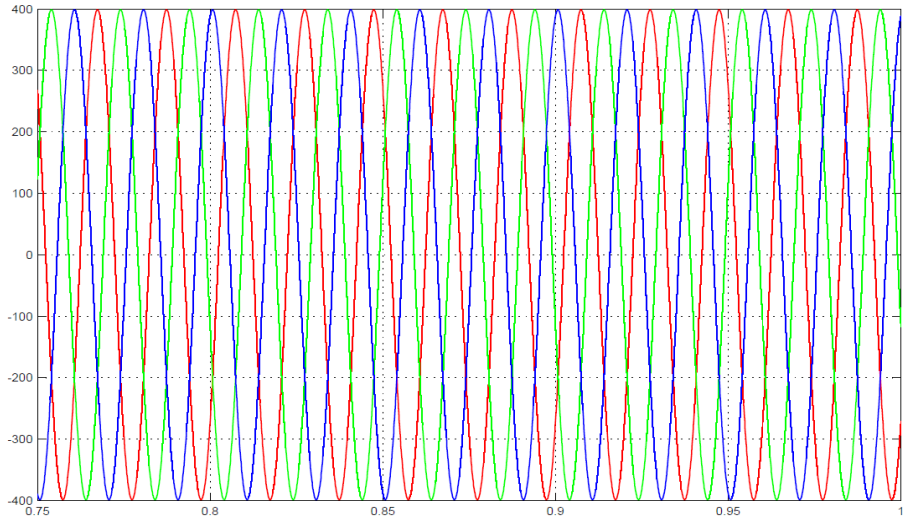

Figure 4- 17: Onshore Transformer Voltage

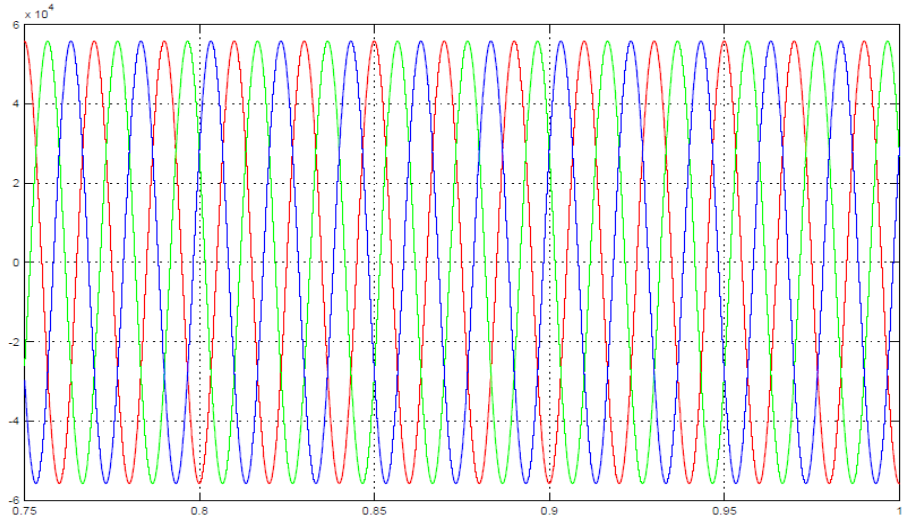

Figure 4- 18: Onshore Transformer Current

The efficiency of the system can be calculated by Equation (4-2) as shown previously. The output power of the system is 38.59 MW and the system input is 40 MW. The system efficiency is 96.475%.

4.4 Fault scenario

4.4.1 HVAC collection grid system

Faults on a power system are quite common and can occur at any time and without any warning. Faults are categorised into symmetrical and asymmetrical faults. Symmetrical faults are less common, with asymmetric faults being prevalent.

There are three common types of asymmetric faults, namely:

- Line to line fault
- Line to ground fault
- Double line to ground fault

A short circuit between two lines is referred to as a line-to-line fault. This fault is caused by physical contact between the lines. Physical damage of a line due to factors such as lighting or heavy winds can result in a line to ground fault. If the same occurs and two lines are disrupted, a double line to ground fault occurs.

4.4.1.1 Simulation

For this study, a single line to ground fault was simulated to determine the fault current as well as the effect of the fault on the wind farm, and the receiving end of the system.

Figure 4-19 shows the system with the fault location. The fault is located midway on the transmission line. The fault occurs at 0.3s and is kept constant for both systems.

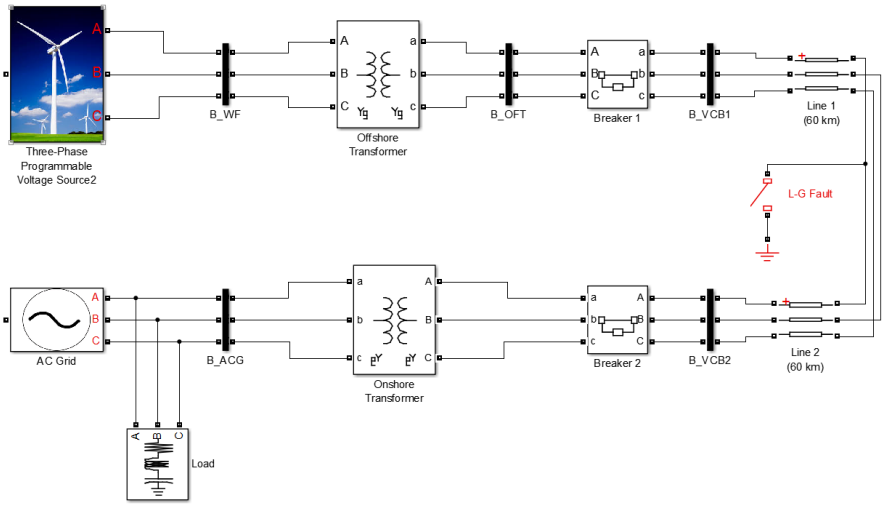

Figure 4- 19: Traditional HVAC Wind Farm System With Fault

For the AC collection grid system, the fault current peaks to a value of 12000 A as seen in Figure 4-20. This value is significantly high and will have a major impact on the system components.

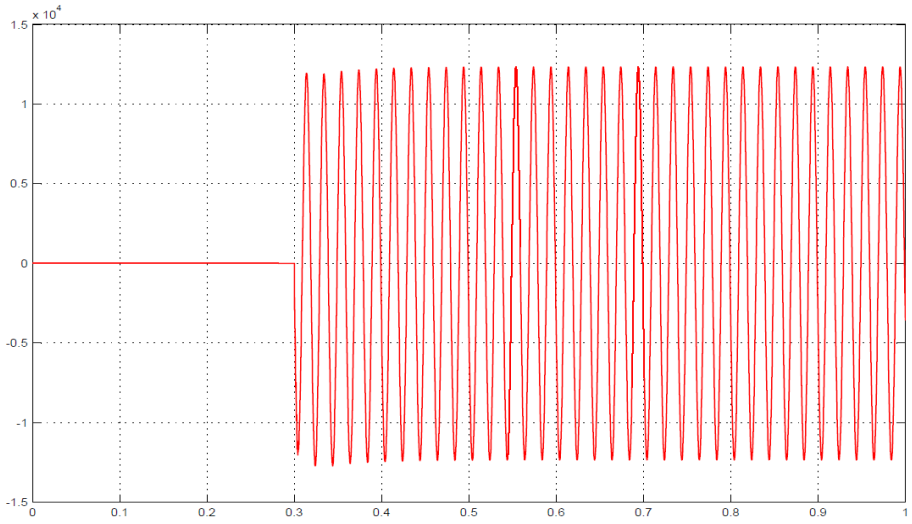

Figure 4- 20: Fault Current For HVAC System

The effects of the fault current on the wind farm can be observed from the Figure below. Figure 4-21 shows that, due to line to line fault, the sending end voltage waveform. The voltage spikes at the moment of the fault. The voltages for each phase are no longer symmetrical sine waves, even though the fault occurs over 60 km away from the wind farm. The voltage surges from 33 kV to a maximum of 50 kV.

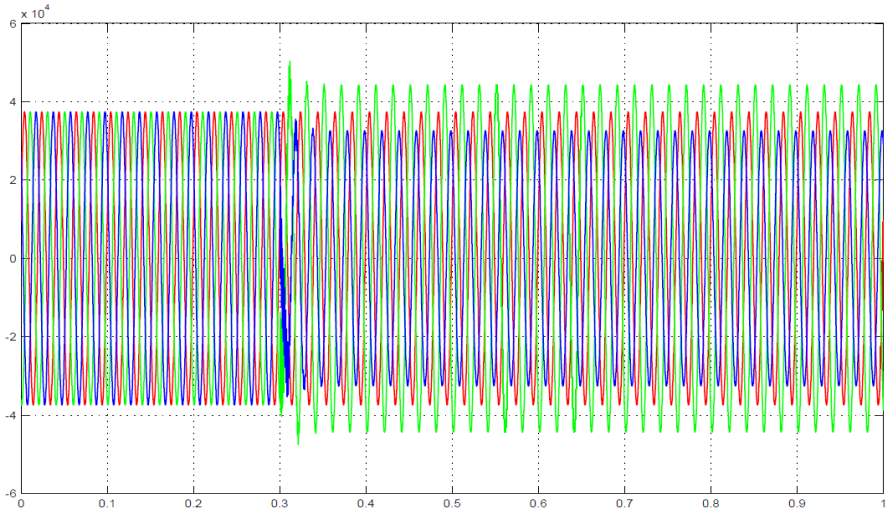

Figure 4- 21: HVAC System Wind Farm Voltage During Fault

Figure 4-22, shows the current waveform during the fault. It is clear that the sending end current is greatly increased. This current surges to a maximum of approximately 600 A, as opposed to the running current of 220 A.

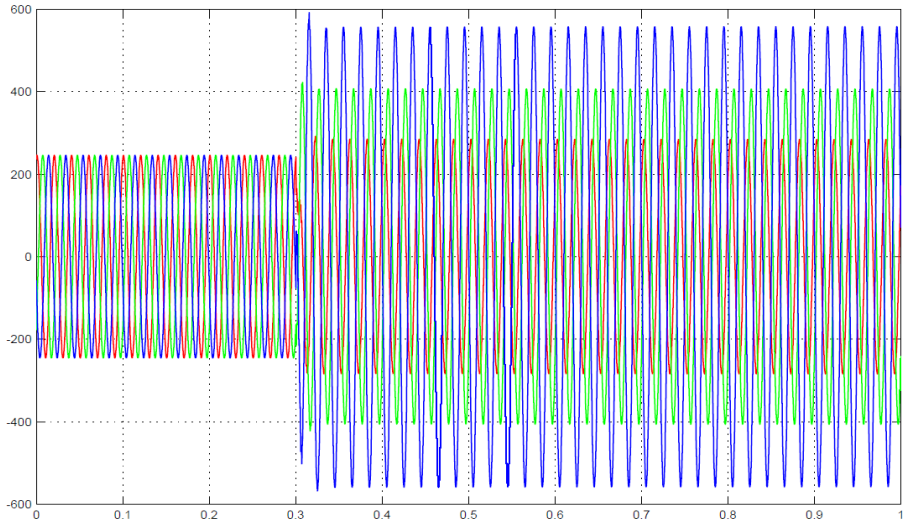

Figure 4- 22: HVAC System Wind Farm Current During Fault

The receiving end voltage and current are shown below. Figure 4-23 shows the voltage peaking at 650 V at the receiving end of the system. Figure 4-24 shows the current for the receiving end. The effects of the fault are visible with both the voltage and current distorted.

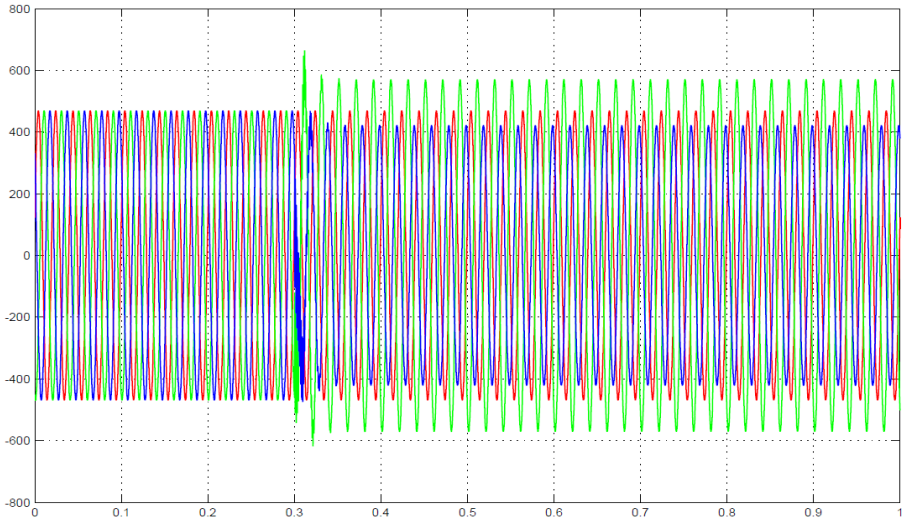

Figure 4- 23: HVAC Receiving End Voltage During Fault

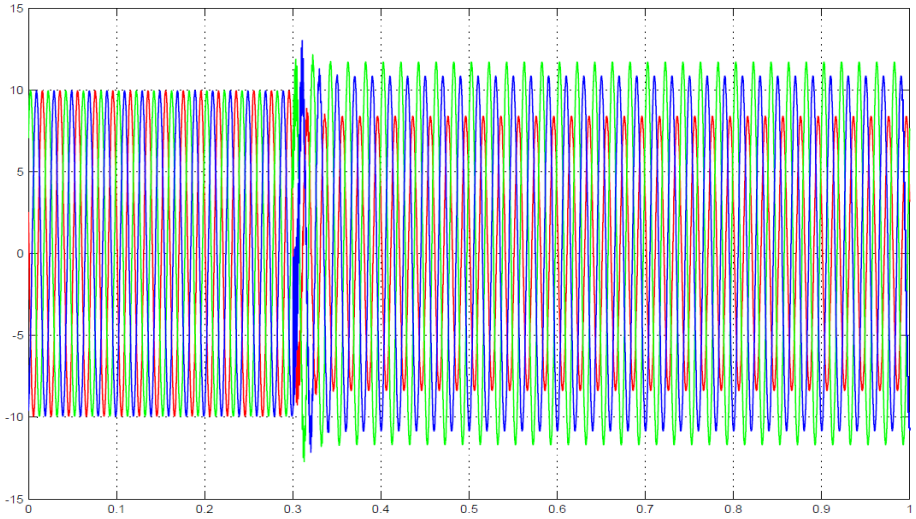

Figure 4- 24: HVAC Receiving End Current During Fault

From the fault simulation above, it is clear that the traditional wind farm system is highly affected by a transmission line fault. The fault affects all parts of the system including the wind farm, transmission line, and the systems' receiving end.

4.4.2 HVDC collection grid system

The same fault was simulated as in the HVAC system to allow for an accurate comparison between the systems. To provide accurate results, the fault is simulated in the same location. The line is faulted to ground at 60 km into the transmission line. Figure 4-25 shows the system with the fault location. The fault occurs at 0.3s and is kept constant for both systems.

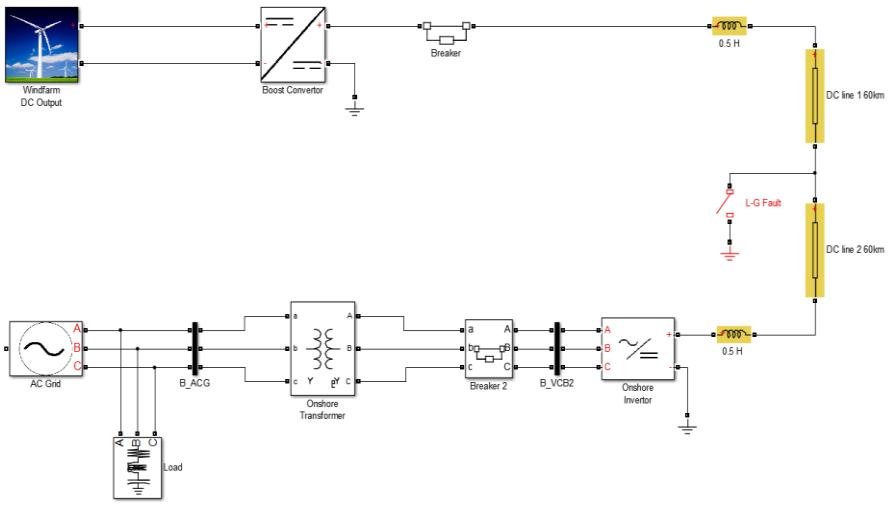

Figure 4- 25: HVDC Collection Grid System With Fault

Figure 4-26 shows the fault current for the DC collection grid wind farm system. The fault current peaks at a current of 620 A. This value is significantly low and will allow for cheaper protection equipment based on the fault current rating.

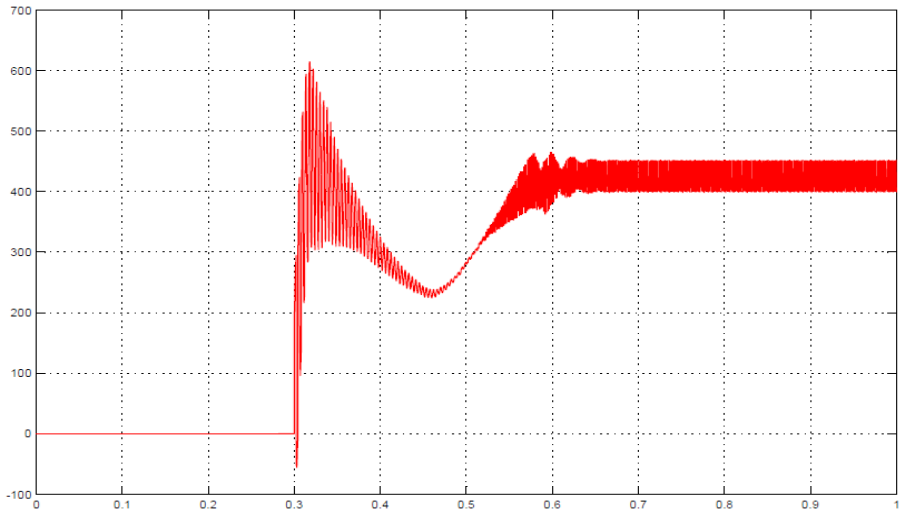

Figure 4- 26: HVDC Collection Grid System Fault Current

The effects of the fault current are shown in the figures below. Figure 4-27 and Figure 4-28 show the wind farms voltage and current output respectively, during the fault. The simulation shows that fault has no effect on the wind farm and produces a constant voltage and current output.

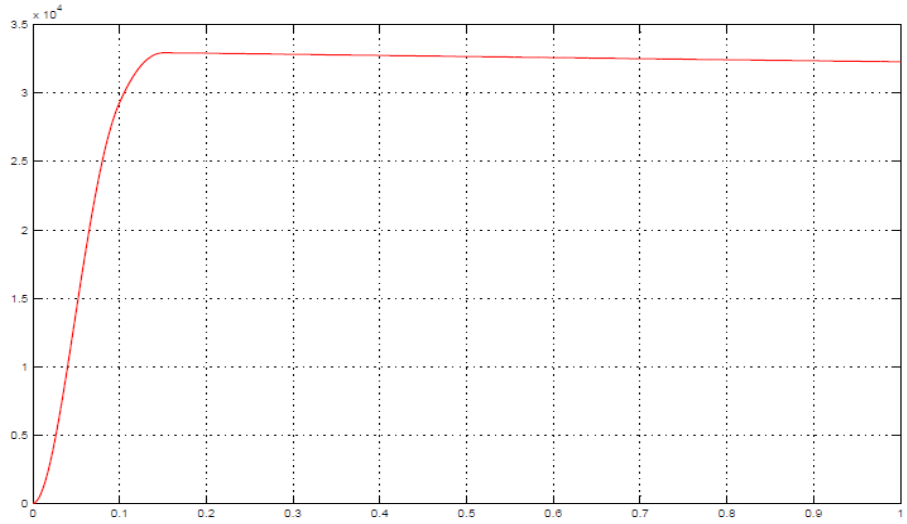

Figure 4- 27: HVDC Wind farm Output Voltage During Fault

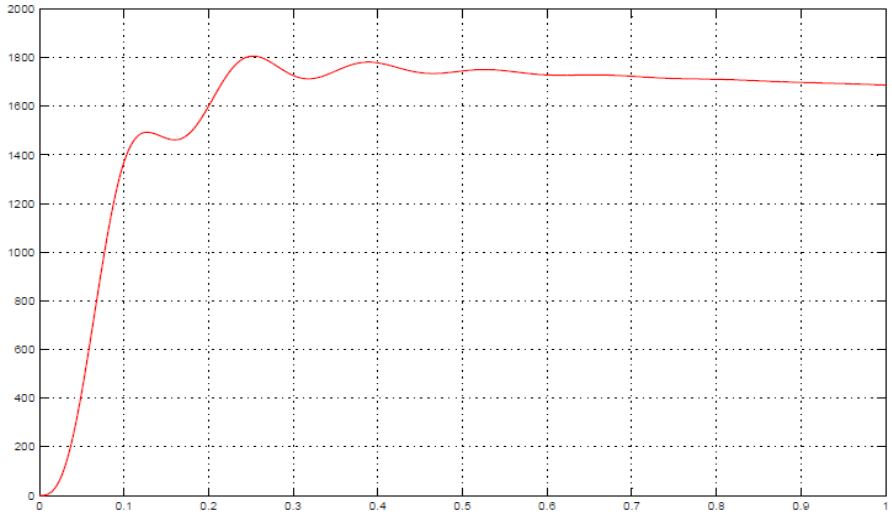

Figure 4- 28: HVDC Wind farm Output Current During Fault

Figure 4-29 and Figure 4-30 show the receiving end voltage and current for the system respectively. The fault in the DC system only affects the related area. As the fault occurs on the transmission line, the line is grounded and the voltage to the inverter is affected. The converter receives a lower input voltage and produces a smaller AC output wave. As seen in the Figures below, the voltage and current waveforms are reduced at the time the fault is experienced. The fault occurs at 0.3s, as the converter voltage and current were rising to steady-state, the fault occurs and causes them to be reduced due to the lower input to the converter.

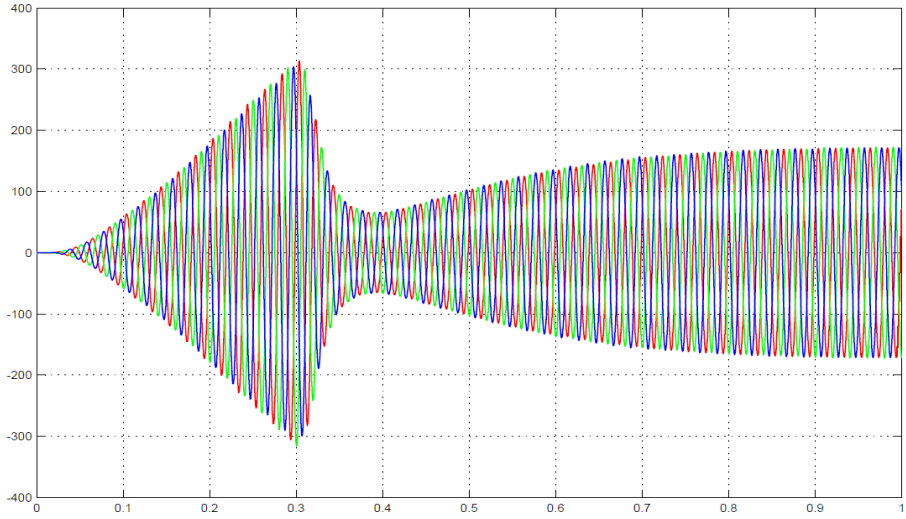

Figure 4- 29: HVDC System Receiving End Voltage During Fault

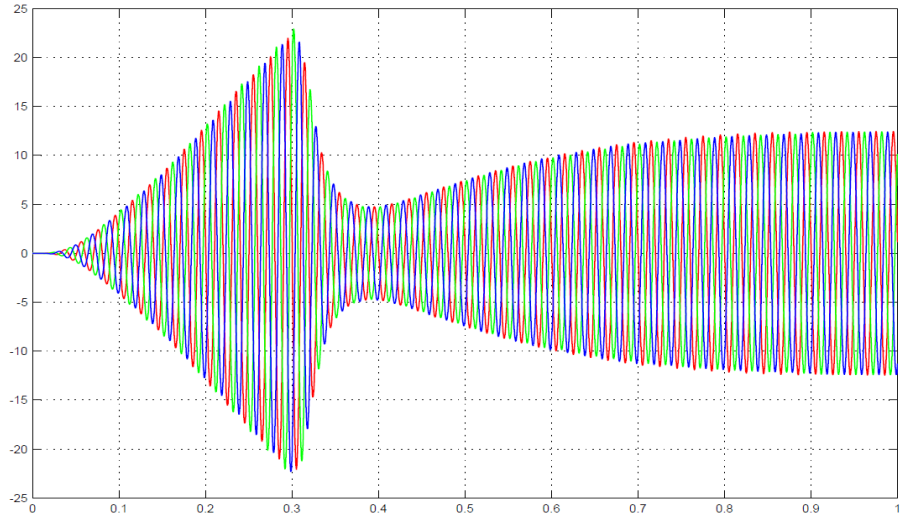

Figure 4- 30: HVDC System Receiving End Current During Fault

From the fault simulation above, it is clear that the DC collection grid system is not very affected by a fault on the transmission line. The fault only affects the transmission line. This will allow for lower costs due to protection devices for the system.

4.5 Conclusion

Simulation models for both HVAC and HVDC systems were developed and their performances during normal and fault conditions were studied. These systems were kept

identical to allow for an accurate comparison. The HVDC system had much higher efficiency than the HVAC system and also performed better during a fault. The following chapter will look at the results obtained from the simulations and analyse these to show a clearer indication of the performance of both systems.

CHAPTER 5: RESULT ANALYSIS AND DISCUSSION

5.1 Introduction

This chapter explains the results obtained from the simulations in chapter 4. The results are compared and the effectiveness of each collection grid is shown. The results from the normal operation and fault simulation are discussed and it is found that HVDC collection grids outperform HVAC systems. An economic comparison of both systems is conducted and costs for distances over the break-even distance are seen to be much higher in HVAC systems. The results found in this chapter have also been explained based on previous research conducted in this area.

5.2 Normal Operation

5.2.1 Line loss

Using the results gathered during the simulation in chapter 4 it can be seen in Figure 5-1, that the AC system collection grid has a voltage drop of 20 kV while the DC system, sees a loss of only 12 kV. The results experienced are corroborated by T.W. May and B. Albannai in [92] and [93] respectively. In transmission systems that use HVAC, a high percentage of the system losses are related to the transmission line while HVDC systems are not limited by transmission distances due to the absence of reactive power loss [92]. The DC system does not have to deal with losses such as skin effect and charging current. With DC voltage being constant during operation and AC periodically alternating, HVDC conductors are rated to carry higher power than HVAC conductors of the same size. Insulation size and spacing in AC conductors are not rated on the RMS voltage but rather based on the peak voltage. DC systems on the other hand are constant and allow the conductor to carry 100% of the rated power. [93].

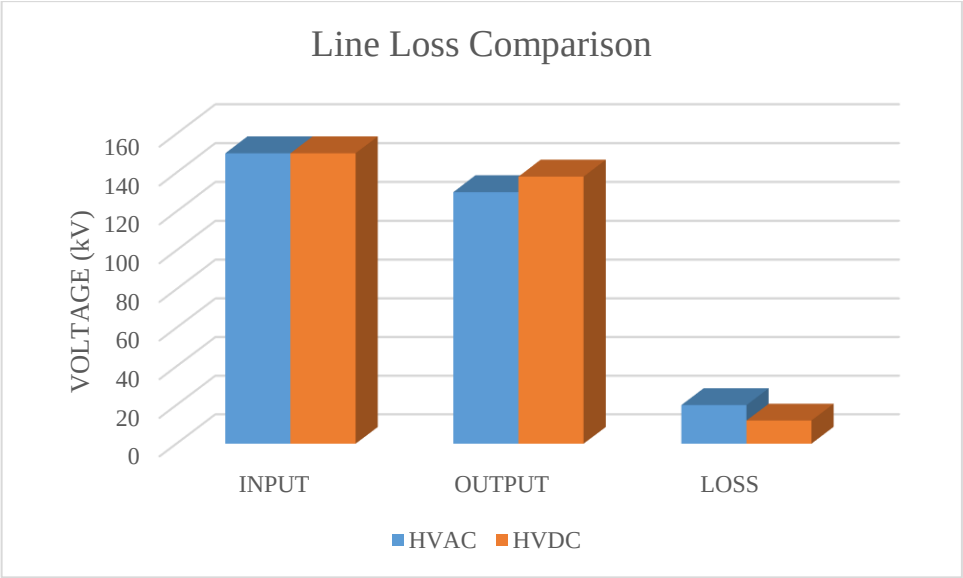

Figure 5- 1: Line Loss Comparison Graph

5.2.2 Overall system efficiency

By looking at the overall system efficiency we can determine the best-suited system to allow for maximum use of the wind energy with minimal wastage. Using the standard efficiency formula, the efficiency of both systems was calculated in the previous chapter. These results can are graphed and compared as seen in Figure 5-2. Each system has an equal power input of 40 MW, fed from their individual wind farms. The AC system shows an output power of 35.77 MW, while the DC system has a total output power of 38.59 MW. These results can be shown as a percentage efficiency of 89.425% for the AC system and 96.475% for the DC system. Although the converters in the HVDC system do reduce the efficiency, it is still more efficient than the HVAC system. The efficiency results of the systems are satisfied by literature seen by Behravesh [94] and Pillay [95]. HVDC collection and transmission grids can be used for long distances as the efficiency of the systems is increased and the losses are reduced as compared to HVAC [95]. For the distance simulated, the HVAC system does not match the HVDC systems efficiency.

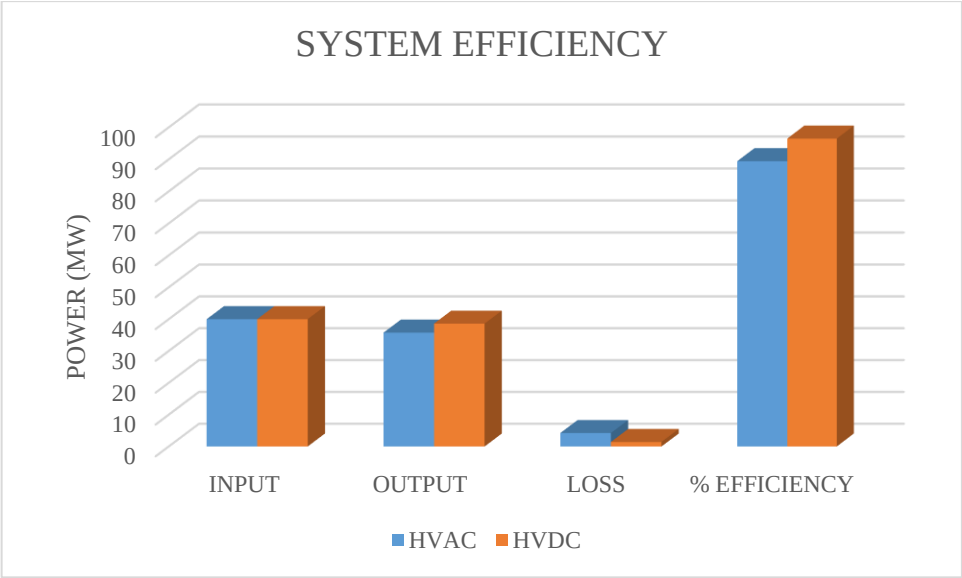

Figure 5- 2: System Efficiency Comparison

5.3 Fault Operation

5.3.1 Fault currents

Figure 5-3 shows the fault current results obtained during the simulation of a single line to ground fault for each system. For the AC collection grid system, a fault current of 12 kA is experienced with a line to ground fault. The DC system experiences a fault current of just 620 A. This difference in the fault current affects the pricing of each system as the protective equipment required will be much higher priced for larger fault currents.

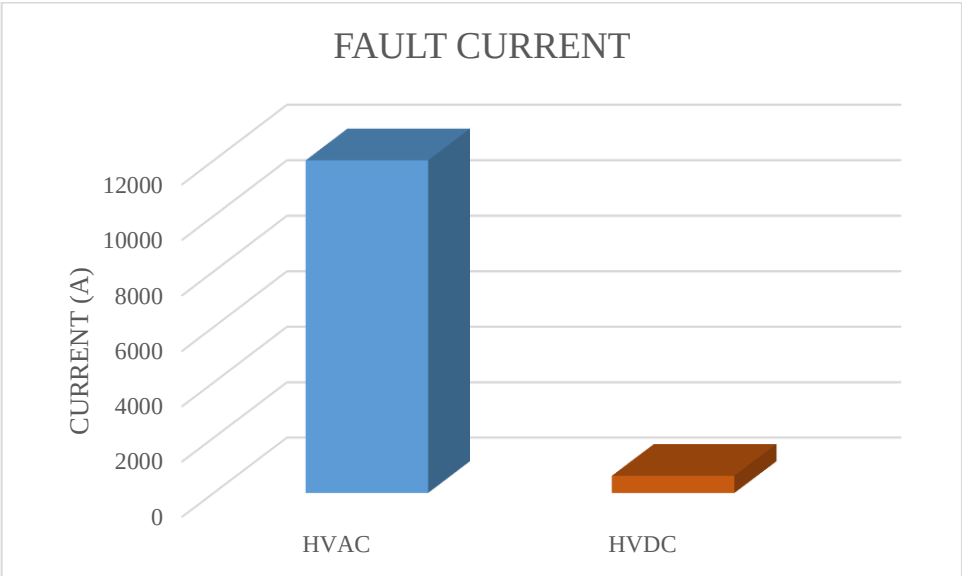

Figure 5- 3: Fault Current Comparison

5.3.2 Fault effect on wind farm output

When the fault occurs on the transmission line, the effects of this fault can flow back to the wind farm. The graph in Figure 5-4 shows the effects of this fault on each wind farm system. A high overvoltage is experienced in the AC wind farm, yet the DC wind farm does not see any increase in voltage. This overvoltage spike of 51% in the AC system is twice the system voltage, this high voltage can be detrimental to the equipment in the system. This result is also seen in the literature. Only the immediate section is affected when a fault occurs on a system using HVDC [96]. Due to a line-to-ground fault on the transmission line, the faulted phase is grounded. HVAC and HVDC both experience distorted waveforms during the fault, however, in the HVDC system only the transmission line section is highly affected. Therefore the wind farm is not affected by this fault as much as seen in the AC system.

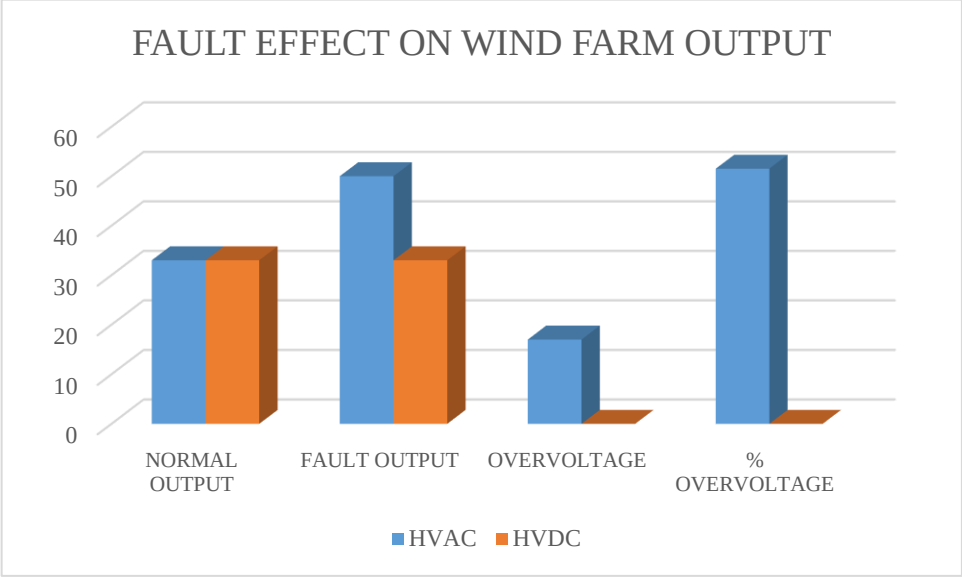

Figure 5- 4: Fault Effect on Wind farm Output

5.4 Cost Comparison

The cost modelling for each system is seen in Chapter 2. For transmission distances of 70 km and lower, HVAC is seen as the most cost-effective solution. In distances above 70 km, HVAC system costs rapidly increase and make HVDC systems the cost-effective solution. In the case of a 120 km line, DC is seen to be the cheaper alternative.

From the graphs and equations shown in Chapter 2, an approximate costing can be determined for each system. The wind energy system is composed of several components that allow wind energy to be connected to the grid. Cables, substations, both onshore and offshore, transformers, reactive power compensation, and converters all add to the cost of the systems. The cost of each component can be added to determine the total system cost. The cost of each system is given by Equation (5-1) and Equation (5-2) for HVAC and HVDC systems respectively.

$$C_{T-HVAC} = C_{WT} + C_{C-AC} + C_{SG} + C_{SS} + C_{TR} + C_{RE} + C_{AC-PF} \tag{5-1}$$

$$C_{T-HVDC} = C_{WT} + C_{C-DC} + C_{SG} + C_{SS} + C_{TR} + C_{CON} + C_{DC-PF} \tag{5-2}$$

Where, C_{T-HVAC} and C_{T-HVDC} are the total costs of the HVAC and HVDC collection system respectively, C_C is the cable cost, C_{SG} is the cost of switchgear, C_{TR} is the cost of a transformer, C_{SS} is the cost of a substation, C_{RE} is the cost of a reactive compensator, C_{CS} is the cost of a converter station, C_{CON} is the cost of a converter and C_{PF} is the cost of platforms required. These equations can be used to determine the cost for each system.

5.4.1.1 HVAC Cost

By using the cost equation, Equation (5-1), for the HVAC system and substituting the individual component equations, Equation (5-3) is derived. This equation can then be used to determine the system cost, using the parameters of a 40MW wind farm at 120 km offshore. These values can be inputted into Equation (5-3) and the cost is determined as seen in Equation (5-4).

$$\begin{aligned} C_{HVAC-TOTAL} = & \left[1.1\left(2.95\times10^{3}\ln\times P - 375.2\right)\right] + \left[42.688\times S_{TR}{}^{0.7513}\right] + \ldots \\ & \left[\left(249.72 + 26.48\times e^{\frac{379.5\times I_n}{10^5}}\right)\times l\right] + \left[\left(0.0007\times U_{rms} + 0.036\right)\right] + \ldots \\ & \left[\left(2.76 + (0.095\times P)\right)\right] + \left[2.534 + 0.0887 + \frac{P_{wf}}{1000}\right] + \left[0.0039Q_l + 0.3557\right] \end{aligned} \tag{5-3}$$

$$C_{HVAC-TOTAL} = \left[1.1\left(2.95\times10^{3}\ln\times\left(40\right)-375.2\right)\right]+\left[42.688\times\left(40\right)^{0.7513}\right]+\ldots$$
$$\left[\left(249.72+26.48\times e^{\frac{379.5\times(800)}{10^{5}}}\right)\times\left(120\right)\right]+\left[\left(0.0007\times\left(150\right)+0.036\right)\right]+\ldots \quad (5\text{-}4)$$
$$\left[\left(2.76+\left(0.095\times\left(40\right)\right)\right)\right]+\left[2.534+0.0887+\frac{\left(40\right)}{1000}\right]+\left[0.0039\times\left(75\right)+0.3557\right]$$

From Equation (5-4), it can be determined that the cost of a 40 MW, 120 km offshore HVAC system is approximately 137.63M€, which equates to R 2.4 billion. This cost is split into the components as seen in the pie chart shown in Figure 5-5. From this, it is evident that in the HVAC system, the transmission cable is the highest percentage of the overall cost.

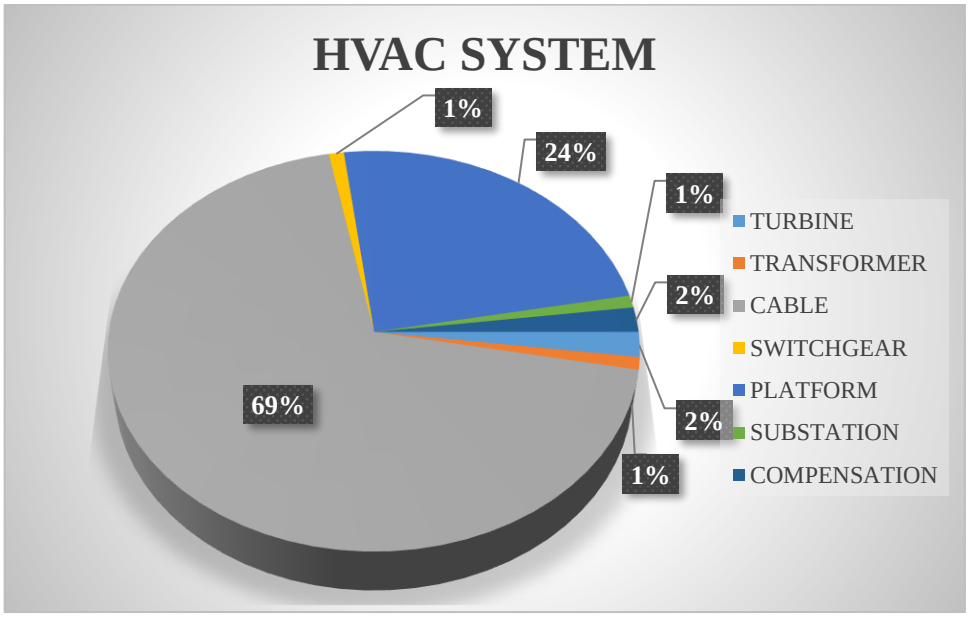

Figure 5- 5: HVAC System Component Pie Chart

5.4.1.2 HVDC Cost

The identical method was used in the process to determine the cost of the DC system. The cost equation for the HVDC system can be broken down into Equation (5-5).

$$C_{HVDC-TOTAL} = \left[1.1\left(2.95\times10^{3}\ln\times P - 375.2\right)\right] + \left[42.688\times S_{TR}{}^{0.7513}\right] + \ldots$$
$$\left[\left(0.0256 + 0.0068\times 2\times P\right)\times l\right] + \left[200\times P\times 2\right] + \left[2\left(0.0007\times U_{rms} + 0.036\right)\right] + \ldots \quad (5\text{-}5)$$
$$\left[0.5\left(2.76 + (0.095\times P)\right)\right] + \left[1.85\left(2.534 + 0.0887 + \frac{P_{wf}}{1000}\right)\right]$$

For the described system, the total costing can be determined by Equation (5-6).

$$C_{HVDC-TOTAL} = \left[1.1\left(2.95\times10^{3}\ln\times(40) - 375.2\right)\right] + \left[42.688\times(40)^{0.7513}\right] + \ldots$$
$$\left[\left(0.0256 + 0.0068\times 2\times(40)\right)\times(120)\right] + \left[200\times(40)\times 2\right] + \ldots$$
$$\left[2\left(0.0007\times(150) + 0.036\right)\right] + \left[0.5\left(2.76 + \left(0.095\times(40)\right)\right)\right] + \ldots \quad (5\text{-}6)$$
$$\left[1.85\left(2.534 + 0.0887 + \frac{(40)}{1000}\right)\right]$$

The total cost of the system equates to 93.52M€ which converted is R 1.7 billion. The cost of the individual components was used to determine the graph seen in Figure 6-6. From this, it is evident that the converter system comprises of 50% of the total system cost, while the cables only account for 33%.

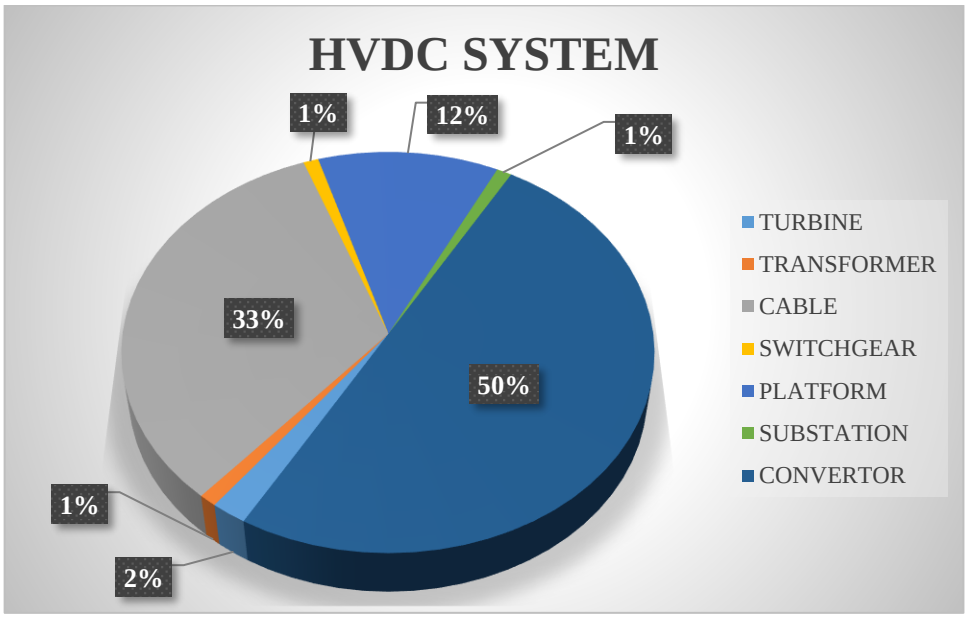

Figure 5- 6: HVDC System Component Pie Chart

From the costing evaluation of both systems, it can be seen that the HVAC system has a higher cost for the given system. This is mainly due to the cable and platform costs.

5.4.1.3 Comparative Cost

From the information above, the costs of both systems can be compared. An analysis was done to determine the system costs at different transmission distances. This information is shown in Figure 5-7. From this graph we can see the break-even distance, and that after this point, the cost of HVAC systems surges past the HVDC system costs. After a distance of 70 km, HVDC transmission systems are more economical than HVAC.

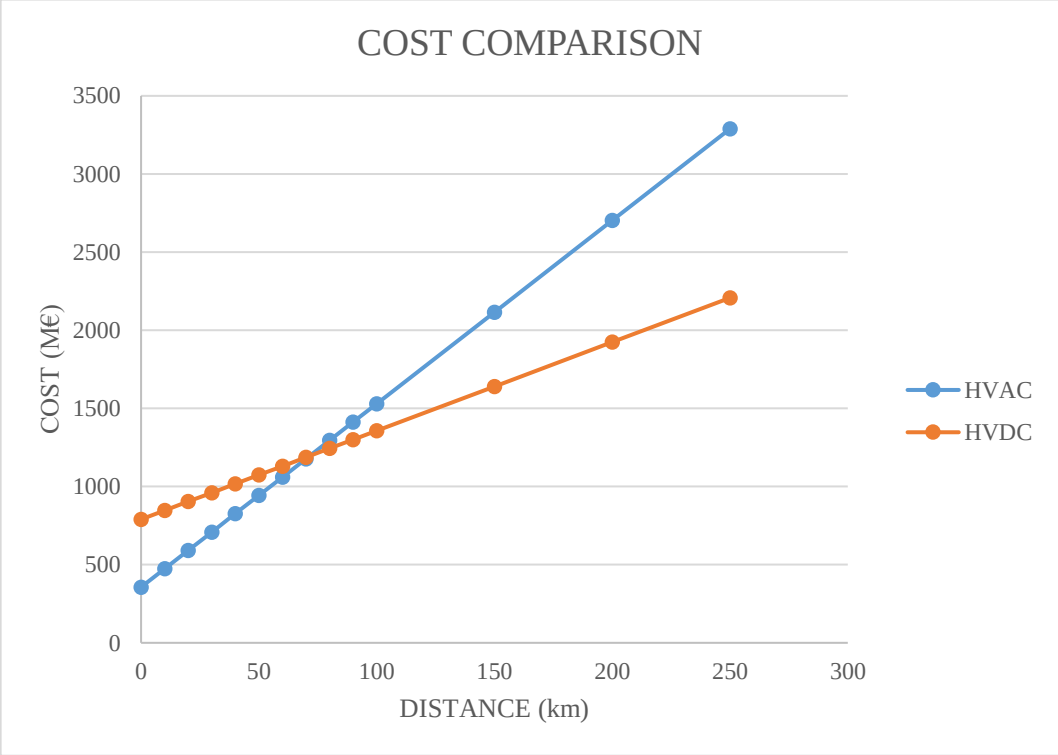

Figure 5- 7: Cost vs Distance Graph

Figure 5-8 shows a side-by-side comparison of the cost of both systems at 40 MW and 120 km.

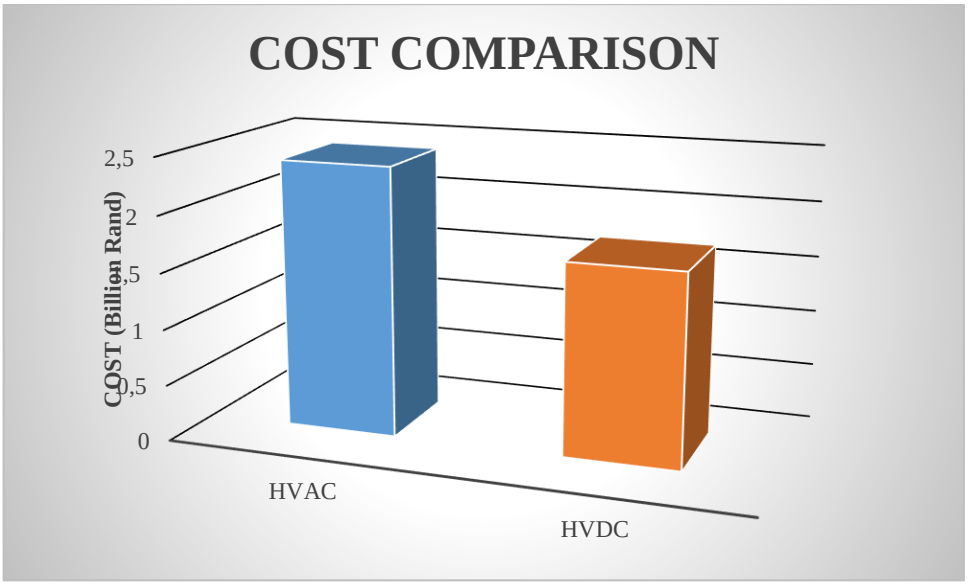

Figure 5- 8: HVAC and HVDC Cost Comparison

From the information above it is clear that for any distance over 70 km an HVDC collection system will be far cheaper than an HVAC system. This can be used to help determine wind farm system design when considering new wind farm systems at great offshore distances.

5.5 Summary

The results found during the simulations were expected as there is literature to support each one. Table 5-1 summarises the results for each system side by side to show a full comparison of the systems.

AC and DC collection grids have been studied and compared. The losses, fault handling, and cost have been discussed. From the results obtained, it is clear that losses in AC collection systems are comparatively higher than DC for longer distances. The high losses experienced in AC systems are a result of the transmission line effects not experienced by DC transmission systems. The fault current experienced by the AC system was extremely high as compared to the DC systems. Although the fault current is lower, the protection systems for DC collection grids are expensive and add to the cost of the system making it much more expensive than standard AC systems. DC-DC converters required for the HVDC systems to operate are also extremely expensive and add additional costs to the system [22].

A costing comparison was conducted on both systems and shows that the HVDC system is the economical choice. This information along with the performance and fault comparisons makes it evident that HVDC systems are much more efficient and economical when transmission distances are high.

Table 5- 1: Overall Summary

Description	Traditional Wind farm	DC collection Grid Wind farm
Wind farm Output Voltage	33 kV	33 kV
Transmission Distance	120 km	120 km
System Power	40 MW	40 MW
System Efficiency	89,425 %	96,475 %
Line Losses	20 kV	12 kV
Fault Location on Transmission Line	Phase A 60 km	60 km
Fault Current	12 000 A	620 A
Wind farm Voltage and Current	Affected	Unaffected
Transmission Line Voltage and Current	Affected	Affected
Receiving End Voltage and Current	Affected	Affected
Costing	R 2.4 Billion	R 1.7 Billion

CHAPTER 6: CONCLUSION AND RECOMMENDATIONS

6.1 Conclusion

This study has focused on the use of HVAC and HVDC collection grids for offshore wind farms. The losses experienced and system costs, as well as their operation and behaviour during normal operation and fault conditions, were simulated. It is clear that for offshore wind farms, HVDC collection grids with HVDC transmission have proven to be the most efficient and cost-effective solution in the long run. Both the HVAC and HVDC systems were simulated with a line to ground fault. HVDC has proven to be a more viable option than HVAC as lower fault currents are experienced and only the faulted section is affected by the fault. As the fault was on the transmission line, the sending and receiving ends of the system were unaffected as the fault did not travel through the system but instead only affected the faulted area.

With the ever-growing population and the increasing demand for electrical energy, renewable energy is in high demand. Transmitting this energy to the existing power grid is a difficult task due to the distance and power quality requirements. HVDC is a fast-growing solution to this problem, with its unlimited distance capabilities at high efficiency and low cost. HVDC technology has improved dramatically over the last decade and this has led to the wider use of HVDC technology in modern power transmission.

Present HVDC systems can be rated to megavolts DC and up to tens of Gigawatts in rated power capacity, while also enhancing robustness and reliability. In 2018, developments of new offshore wind power plants had slightly slowed down but are steadily increasing, according to research. New high-power wind farms are currently being developed, such as the 1000MW, Thor-2020 system. Innovations in HVDC technology will be promoted based on market trends. These innovations will provide environmentally friendly wind farms with high reliability and control.

According to researchers as offshore wind farms develop, DC transmission systems will become increasingly available and will allow for a DC super grid in the future. Intense research in this field provides evidence of these claims. This study shows that technological developments will allow for HVDC collection grids to be a reality in the near future.

The benefits of HVDC systems, as opposed to HVAC systems, in relation to the transmission distance, efficiency, and fault handling, are given. A comparison between offshore wind farms with HVAC and HVDC collection grids was shown in this research. The various configurations available for HVDC, as well as topologies used for HVDC converters, were also explained.

In conclusion, during this research, it is clear that HVDC collection grids are comparatively superior to HVAC collection grids and a few developments in this technology will see HVDC collection systems as a standard in offshore wind energy systems.

6.2 Recommendations

This dissertation has focused on the comparative evaluation of HVAC and HVDC collection grids for offshore wind farms. Although HVDC is seen as an improved alternative to HVAC, future research should be conducted to improve this system.

The improvement of protection devices for HVDC systems could in the future reduce the cost of these devices and further lessen costs and improve HVDC systems. Possible alternatives to lessen the costs of converter stations should also be researched and could allow HVDC to become the main topology for offshore wind farm collection grids. With the improvements in modern technology, power electronic switching devices, and protection devices, the cost of HVDC systems is sure to decrease in the near future.

REFERENCES

[1] K. Musasa, N. I. Nwulu, M. N. Gitau, and R. C. Bansal, "Review on DC collection grids for offshore wind farms with high-voltage DC transmission system," *IET Power Electronics,* vol. 10, pp. 2104-2115, 2017.

[2] I. Pretorius, S. Piketh, R. Burger, and H. Neomagus, "A perspective on South African coal fired power station emissions," *Journal of Energy in Southern Africa,* vol. 26, pp. 27-40, 2015.

[3] (2008). *The South African Grid Code*.

[4] M. H. Bollen and F. Hassan, *Integration of distributed generation in the power system* vol. 80: John wiley & sons, 2011.

[5] Y. Zhao, J. Chai, and X. Sun, "Relative voltage control of the wind farms based on the local reactive power regulation," *Energies,* vol. 10, p. 281, 2017.

[6] T. Ackermann, *Wind power in power systems*: John Wiley & Sons, 2005.

[7] K. P. Cruz, "FEASIBILITY STUDY TO IMPLEMENT AN HIGH VOLTAGE DIRECT CURRENT TRANSMISSION LINK," 2017.

[8] A. Lee. (2019) Offshore wind power price plunges by a third in a year. *Recharge-Renewable energy news and articles*.

[9] G. Quinonez-Varela, G. Ault, O. Anaya-Lara, and J. McDonald, "Electrical collector system options for large offshore wind farms," *IET Renewable Power Generation,* vol. 1, pp. 107-114, 2007.

[10] D. Berenguel, M. Prada, and O. Bellmunt, "Electrical interconnection options analysis for offshore wind farms," *Europe's premier wind energy event, EWEA, Vienna, Austria,* 2013.

[11] M. D. P. Gil, J. L. Domínguez-García, F. Díaz-González, M. Aragüés-Peñalba, and O. Gomis-Bellmunt, "Feasibility analysis of offshore wind power plants with DC collection grid," *Renewable Energy,* vol. 78, pp. 467-477, 2015.

[12] A. Mahmud, "Large scale renewable power generation," 2014.

[13] X. Jin, C. Dai, P. Ji, S. Wu, and P. Jing, "Research of fault current limiter for 500kV power grid," in *2010 International Conference on Power System Technology*, 2010, pp. 1-10.

[14] M. K. Zadeh, A. S. Akmal, E. Siavashi, and A. Parvizi, "Impacts of TCSC on Switching Transients of HV transmission lines due to fault clearing," in *2009 2nd International Conference on Power Electronics and Intelligent Transportation System (PEITS)*, 2009, pp. 231-237.

[15] K. De Kerf, K. Srivastava, M. Reza, D. Bekaert, S. Cole, D. Van Hertem, *et al.*, "Wavelet-based protection strategy for DC faults in multi-terminal VSC HVDC systems," *IET Generation, Transmission & Distribution,* vol. 5, pp. 496-503, 2011.

[16] L. Tang and B.-T. Ooi, "Locating and isolating DC faults in multi-terminal DC systems," *IEEE transactions on power delivery,* vol. 22, pp. 1877-1884, 2007.

[17] F. Deng and Z. Chen, "Operation and control of a DC-grid offshore wind farm under DC transmission system faults," *IEEE Transactions on Power Delivery,* vol. 28, pp. 1356-1363, 2013.

[18] B. Silva, C. L. Moreira, H. Leite, and J. P. Lopes, "Control strategies for AC fault ride through in multiterminal HVDC grids," *IEEE Transactions on Power Delivery,* vol. 29, pp. 395-405, 2014.

[19] W. Xiang, Y. Hua, J. Wen, M. Yao, and N. Li, "Research on fast solid state DC breaker based on a natural current zero-crossing point," *Journal of Modern Power Systems and Clean Energy,* vol. 2, pp. 30-38, 2014.

[20] G. Shi, Z. Chen, and X. Cai, "Overview of multi-terminal VSC HVDC transmission for large offshore wind farms," in *2011 International Conference on Advanced Power System Automation and Protection*, 2011, pp. 1324-1329.
[21] J. Yang, J. E. Fletcher, J. O'Reilly, G. Adam, and S. Fan, "Protection scheme design for meshed VSC-HVDC transmission systems of large-scale wind farms," 2010.
[22] P. Lakshmanan, J. Liang, and N. Jenkins, "Assessment of collection systems for HVDC connected offshore wind farms," *Electric Power Systems Research,* vol. 129, pp. 75-82, 2015.
[23] I. Boldea, *The Electric Generators Handbook-2 Volume Set*: CRC Press, 2005.
[24] Y. Zou, "Induction generator in wind power systems," in *Induction Motors-Applications, Control and Fault Diagnostics*, ed: IntechOpen, 2015.
[25] J. Mwaniki, H. Lin, and Z. Dai, "A condensed introduction to the doubly fed induction generator wind energy conversion systems," *Journal of Engineering,* vol. 2017, 2017.
[26] W. Cao, Y. Xie, Z. Tan, and R. Carriveau, "Wind turbine generator technologies," in *Advances in Wind Power*, ed: InTech, 2012, pp. 177-204.
[27] N. Kumar, T. R. Celliah, and S. P. Srivastava, "Analysis of Doubly-Fed Induction Machine operating at motoring mode subjected to symmetrical voltage sag," 2015.
[28] S. Vitanova, V. Stoilkov, and V. Dimcev, "Comparing SCIG and DFIG for wind generating conditions in Macedonia," in *International Conference on Renewable Energies and Power Quality (ICREPQ'11) Las Palmas de Gran Canaria (Spain), 13th to 15th April, 2011*, 2011.
[29] B. Wu, Y. Lang, N. Zargari, and S. Kouro, *Power conversion and control of wind energy systems* vol. 76: John Wiley & Sons, 2011.
[30] A. R. Tiwari, A. J. Shewale, A. Gagangras, and N. M. Lokhande, "Comparison of various wind turbine generators," *Multidiscplinary Journal of Research in Engineering and Technology,* vol. 1, pp. 129-135, 2014.
[31] A. Jain, S. Shankar, and V. Vanitha, "Power Generation Using Permanent Magnet Synchronous Generator (PMSG) Based Variable Speed Wind Energy Conversion System (WECS): An Overview," *Journal of Green Engineering,* vol. 7, pp. 477-504, 2017.
[32] K. Zipp. (2012, Towers 101. *Wind Power Engineering and Development*. Available: https://www.windpowerengineering.com/towers-101/
[33] M. G. Molina and P. E. Mercado, "Modelling and control design of pitch-controlled variable speed wind turbines," in *Wind turbines*, ed: In Tech, 2011.
[34] M. Rycroft. (2017, Concrete towers lift wind turbines to new heights. Available: https://www.ee.co.za/article/concrete-towers-lift-wind-turbines-new-heights.html
[35] G. Jose and R. Chacko, "A review on wind turbine transformers," in *2014 Annual International Conference on Emerging Research Areas: Magnetics, Machines and Drives (AICERA/iCMMD)*, 2014, pp. 1-7.
[36] J. Lebre, P. Portugal, and E. Watanabe, "Hybrid HVDC (H2VDC) System Using Current and Voltage Source Converters," *Energies,* vol. 11, p. 1323, 2018.
[37] J. Vobecky, "The current status of power semiconductors," *Facta Universitatis, Series: Electronics and Energetics,* vol. 28, pp. 193-203, 2015.
[38] O. E. Oni, I. E. Davidson, and K. N. Mbangula, "A review of LCC-HVDC and VSC-HVDC technologies and applications," in *2016 IEEE 16th International Conference on Environment and Electrical Engineering (EEEIC)*, 2016, pp. 1-7.

[39] Y. Jiang-Hafner, H. Duchen, M. Karlsson, L. Ronstrom, and B. Abrahamsson, "HVDC with voltage source converters-a powerful standby black start facility," in *2008 IEEE/PES Transmission and Distribution Conference and Exposition*, 2008, pp. 1-9.

[40] K. Friedrich, "Modern HVDC PLUS application of VSC in modular multilevel converter topology," in *2010 IEEE International Symposium on Industrial Electronics*, 2010, pp. 3807-3810.

[41] J. Luo, J. Yao, D. Wu, C. Wen, S. Yang, and J. Liu, "Application research on VSC-HVDC in urban power network," in *2011 IEEE Power Engineering and Automation Conference*, 2011, pp. 115-119.

[42] V. Gelman, "Insulated-gate bipolar transistor rectifiers: why they are not used in traction power substations," *ieee Vehicular technoloGy maGazine*, vol. 9, pp. 86-93, 2014.

[43] W. Long and S. Nilsson, "HVDC transmission: yesterday and today," *IEEE Power and Energy Magazine*, vol. 5, pp. 22-31, 2007.

[44] G. Asplund, K. Eriksson, and K. Svensson, "DC transmission based on voltage source converters," in *CIGRE SC14 Colloquium, South Africa*, 1997, pp. 1-7.

[45] B. Andersen, "VSC transmission," *Cigré, Workgroup B*, vol. 4, 2005.

[46] T. Ackermann, N. B. Negra, J. Todorovic, and L. Lazaridis, "Evaluation of electrical transmission concepts for large offshore wind farms," in *Copenhagen Offshore Wind Conference and Exhibition, Copenhagen*, 2005, pp. 26-28.

[47] M. Callavik, A. Blomberg, J. Häfner, and B. Jacobson, "The hybrid HVDC breaker," *ABB Grid Systems Technical Paper*, vol. 361, pp. 143-152, 2012.

[48] Y. Xie, J. Ning, Y. Huang, J. Jia, and Z. Jian, "A review of DC micro-grid protection," in *International Conference on Brain Inspired Cognitive Systems*, 2013, pp. 338-347.

[49] R. M. Cuzner and G. Venkataramanan, "The status of DC micro-grid protection," in *2008 IEEE Industry Applications Society Annual Meeting*, 2008, pp. 1-8.

[50] P. Rakhra, P. J. Norman, S. D. Fletcher, S. J. Galloway, and G. M. Burt, "Evaluation of the impact of high-bandwidth energy-storage systems on DC protection," *IEEE Transactions on Power Delivery*, vol. 31, pp. 586-595, 2015.

[51] L. Xu and D. Chen, "Control and operation of a DC microgrid with variable generation and energy storage," *IEEE transactions on power delivery*, vol. 26, pp. 2513-2522, 2011.

[52] G. Stamatiou, K. Srivastava, M. Reza, and P. Zanchetta, "Economics of DC wind collection grid as affected by cost of key components," in *World Renewable Energy Congress-Sweden; 8-13 May; 2011; Linköping; Sweden*, 2011, pp. 4177-4184.

[53] A. L. Figueroa-Acevedo, M. S. Czahor, and D. E. Jahn, "A comparison of the technological, economic, public policy, and environmental factors of HVDC and HVAC interregional transmission," *AIMS Energy*, vol. 3, pp. 1-18, 2015.

[54] L. Zhang, L. Harnefors, and H.-P. Nee, "Interconnection of two very weak AC systems by VSC-HVDC links using power-synchronization control," *IEEE transactions on power systems*, vol. 26, pp. 344-355, 2011.

[55] J. Hafner, "Proactive Hybrid HVDC Breakers-A key innovation for reliable HVDC grids," in *Proc. CIGRE Bologna Symposium*, 2011, pp. 1-8.

[56] S. Jalbrzykowski and T. Citko, "Push-pull resonant DC-DC isolated converter," *Bulletin of the Polish Academy of Sciences: Technical Sciences*, vol. 61, pp. 763-769, 2013.

[57] M. Kheraluwala, R. W. Gascoigne, D. M. Divan, and E. D. Baumann, "Performance characterization of a high-power dual active bridge DC-to-DC converter," *IEEE Transactions on industry applications,* vol. 28, pp. 1294-1301, 1992.
[58] N. G. Hingorani, "Flexible AC transmission," *IEEE spectrum,* vol. 30, pp. 40-45, 1993.
[59] D. Povh and D. Retzmann, "Development of FACTS for transmission systems," in *The IERE Central America Forum*, 2003.
[60] N. Mithulananthan, C. A. Canizares, J. Reeve, and G. J. Rogers, "Comparison of PSS, SVC, and STATCOM controllers for damping power system oscillations," *IEEE transactions on power systems,* vol. 18, pp. 786-792, 2003.
[61] E. Kontos, R. T. Pinto, S. Rodrigues, and P. Bauer, "Impact of HVDC transmission system topology on multiterminal DC network faults," *IEEE Transactions on Power Delivery,* vol. 30, pp. 844-852, 2015.
[62] S. Surges, "Switching surges: Part iv-control and reduction on ac transmission lines," *IEEE Transactions on Power Apparatus and Systems,* pp. 2694-2702, 1982.
[63] J. Arrillaga and J. Arrillaga, *High voltage direct current transmission*: Iet, 1998.
[64] K. Meah and S. Ula, "Comparative evaluation of HVDC and HVAC transmission systems," in *2007 IEEE Power Engineering Society General Meeting*, 2007, pp. 1-5.
[65] G. El-Saady, E.-N. A. Ibrahim, and A. H. Okilly, "Analysis and control of HVDC transmission power system," in *2016 Eighteenth International Middle East Power Systems Conference (MEPCON)*, 2016, pp. 190-198.
[66] T. Antunes, T. A. dos Reis Antunes, P. J. da Costa Santos, and A. J. P. M. Pires, "Limitations of HVAC Offshore Cables in Large Scale Offshore Wind Farm Applications."
[67] D. Larruskain, I. Zamora, A. Mazón, O. Abarrategui, and J. Monasterio, "Transmission and distribution networks: AC versus DC," in *9th Spanish-Portuguese Congress on Electrical Engineering*, 2005, pp. 1-6.
[68] B. Van Eeckhout, D. Van Hertem, M. Reza, K. Srivastava, and R. Belmans, "Economic comparison of VSC HVDC and HVAC as transmission system for a 300 MW offshore wind farm," *European Transactions on Electrical Power,* vol. 20, pp. 661-671, 2010.
[69] D. Van Hertem, O. Gomis-Bellmunt, and J. Liang, *HVDC grids: for offshore and supergrid of the future*: John Wiley & Sons, 2016.
[70] A. R. Henderson, L. Greedy, F. Spinato, and C. A. Morgan, "Optimising redundancy of offshore electrical infrastructure assets by assessment of overall economic cost," in *European Offshore Wind Energy Conference*, 2009, pp. 14-16.
[71] Z. Guiping, D. Xiaowei, and Z. Chen, "Optimisation of reactive power compensation of HVAC cable in off-shore wind power plant," *IET Renewable Power Generation,* vol. 9, pp. 857-863, 2015.
[72] A. Madariaga, J. Martín, I. Zamora, I. M. De Alegria, and S. Ceballos, "Technological trends in electric topologies for offshore wind power plants," *Renewable and Sustainable Energy Reviews,* vol. 24, pp. 32-44, 2013.
[73] E. Spahic and G. Balzer, "Offshore wind farms-VSC-based HVDC connection," in *2005 IEEE Russia Power Tech*, 2005, pp. 1-6.
[74] ABB, "XLPE Submarine Cable Systems Attachment to XLPE Land Cable Systems - User´s Guide," ABB, Ed., 5 ed: ABB, 2020.

[75] S. Lundberg, "Performance comparison of wind park configurations," Chalmers University of Technology 1401-6176, 2003.
[76] L. Lazaridis, "Economic Comparison of HVAC and HVDCSolutions for Large Offshore Wind Farms underSpecial Consideration of Reliability," ed, 2005.
[77] M. Dicorato, G. Forte, M. Pisani, and M. Trovato, "Guidelines for assessment of investment cost for offshore wind generation," *Renewable energy,* vol. 36, pp. 2043-2051, 2011.
[78] X. Xiang, M. Merlin, and T. Green, "Cost analysis and comparison of HVAC, LFAC and HVDC for offshore wind power connection," 2016.
[79] I. Consulting, "Unit Costs of Constructing New Transmission Assets at 380 kV within the European Union, Norway and Switzerland," 2002.
[80] F. S. o. B. Duke University, "The Icelandic Submarine Cable," 2001.
[81] E. Ilstad, "World record HVDC submarine cables," *IEEE Electrical Insulation Magazine,* vol. 10, p. 64, 1994.
[82] W. L. DTU and W. L. N. A. Cutululis, "Innovative Tools for Offshore Wind and DC Grids."
[83] R. G. N. S. F. T. N. N. S. C. O. G. INITIATIVE), "ENTSO-e European Network of Transmission System Operators for Electricity," 2011.
[84] H. Ergun, D. Van Hertem, and R. Belmans, "Transmission system topology optimization for large-scale offshore wind integration," *IEEE Transactions on Sustainable Energy,* vol. 3, pp. 908-917, 2012.
[85] M. d. Prada Gil, "Design, operation and control of novel electrical concepts for offshore wind power plants," 2014.
[86] D. Burnham, S. Santoso, and E. Muljadi, "Variable rotor-resistance control of wind turbine generators," in *2009 IEEE Power & Energy Society General Meeting*, 2009, pp. 1-6.
[87] F. Blaabjerg and Z. Chen, "Power electronics for modern wind turbines," *Synthesis Lectures on Power Electronics,* vol. 1, pp. 1-68, 2005.
[88] M. Stieneker, A. Monti, and R. W. de Doncker, *Analysis of medium-voltage direct-current collector grids in offshore wind parks*: Lehrstuhl für Stromrichtertechnik und Elektrische Antriebe-PGS, 2017.
[89] A. Kumar, "HVDC (High Voltage Direct Current) Transmission System: A Review Paper," *Gyancity Journal of Engineering and Technology,* vol. 4, 2018.
[90] P. Norgaard and H. Holttinen, "A multi-turbine power curve approach," in *Nordic wind power conference*, 2004, pp. 1-2.
[91] K. P. Shree and S. Ram, "Decoupled control of active and reactive powers of DFIG with cascaded SPWM converters," *International Journal of Engineering Science and Technology,* vol. 3, pp. 7538-7544, 2011.
[92] T. W. May, Y. M. Yeap, and A. Ukil, "Comparative evaluation of power loss in HVAC and HVDC transmission systems," in *2016 IEEE Region 10 Conference (TENCON)*, 2016, pp. 637-641.
[93] B. Albannai, "Comparative Study of HVAC and HVDC Transmission Systems With Proposed Machine Learning Algorithms for Fault Location Detectio," Arizona State University, 2019.
[94] V. Behravesh and N. Abbaspour, "New Comparison of HVDC and HVAC Transmission system," *International Journal of Engineering Innovation & Research*, vol. 1, pp. 300-304, 2012.
[95] C. J. Pillay, M. Kabeya, and I. E. Davidson, "Transmission Systems: HVAC vs HVDC."

[96] M. M. Rahman, M. F. Rabbi, M. K. Islam, and F. M. Rahman, "HVDC over HVAC power transmission system: Fault current analysis and effect comparison," in *2014 International Conference on Electrical Engineering and Information & Communication Technology*, 2014, pp. 1-6.
[97] L. Ramírez, D. Fraile, and G. Brindley, "Offshore wind in Europe: Key trends and statistics 2019," 2020.